Investigating the Performance of Solar updraft Tower for power Generation

M.Sc. Thesis

By

Usman Teshita Gurartu

Thermal and Aerospace Engineering Program

School of Mechanical, Chemical and Materials Engineering

Adama Science and Technology University

Adama, Ethiopia

October 2019

Investigating the Performance of *Solar updraft Tower for Power Generation*

M.Sc. Thesis

By

Usman Teshita Gurartu

A Thesis Submitted to Thermal and Aerospace Engineering Program, School of Mechanical, Chemical and Materials Engineering, Adama Science and Technology University in Partial Fulfilment of The Requirement of The Degree of Masters of Science in Thermal Engineering

Advisor:

Dr. Dawit Gudeta

Adama, Ethiopia

October 2019

Declaration

I hereby declare that this project titled "Investigating the Performance of Solar updraft Tower for power generation" submitted in partial fulfilment of the award of Degree of Masters of Science in Thermal Engineering school of Mechanical, Chemical and Materials Engineering at Adama Science and Technology University Ethiopia, is an authentic record of my work carried out under the supervision of Dr. Dawit Gudeta, Adama Sciences and Technology University Ethiopia.

The material rooted in this thesis has not been submitted for the award of a degree or diploma in any other university. All relevant resource information used in this paper has been suitably documented.

Usman Teshita

Student Signature Date

This is to certify that the above statement made by the candidate is correct to the best of my knowledge and authority. This has been submitted for examination with my approval.

Dr. Dawit Gudeta

Advisor Signature Date

Adama Science and Technology University

School of Mechanical, Chemical and Materials Engineering

Thermal and Aerospace Engineering Program

Approval Board of Examiners

We, the undersigned, members of the Board of Examiners of the final open defense by Usman Teshita Gurartu have read and evaluated his thesis entitled "**Investigating the Performance of Solar updraft Tower for power Generation**" and examined the candidate. Therefore, to certify, the thesis has been accepted in partial fulfillment of the requirement of the Degree of Master of science in Thermal Engineering.

___________________	________________	______________
Chair Person	Signature	Date
___________________	________________	______________
Internal Examiner	Signature	Date
___________________	________________	______________
External Examiner	Signature	Date

ACKNOWLEDGEMENT

First and foremost, my unconditional thanks to God Almighty (the highest of all) for providing me with the strength to follow this project from the beginning to a meaningful interpretation. Moreover, I am whole-heartedly thankful to my advisor Dr. Dawit Gudeta, whose consistent encouragement, guidance and support from initial to the final level enabled me to develop a detailed understanding of the project. I owe a great deal of gratitude to the Thermal engineering program for courteously support on what I ask. Lastly, I offer my humble regards and blessings to my spouse, family and all of those who supported me in any aspect during the completion of my work.

ABSTRACT

A solar updraft tower power plant is a solar thermal power plant utilizing a combination of solar air collector and central updraft tube to generate a solar induced convective flow which drives pressure staged turbines to generate electricity. Several technologies exist to convert solar energy into electrical energy. The solar updraft is part of the solar thermal groups of solar conversion technologies. Solar tower power plants use the buoyancy-nature of heated air to harness the Solar energy. The flow is driven by a pressure difference in the tower system, so traditional towers are extremely tall to increase the pressure differential and the air's velocity. Computational fluid dynamics (CFD) was used to model the airflow through a solar updraft tower. Different boundary conditions were studied to find the best model that simulate the operation of a solar updraft tower assumed to be used in Ethiopia. Solar updraft is very suitable for use in remote communities where there is high solar energy capacity as a power source for both residential and industrial use. It can provide a suitable energy source in many areas of Ethiopia, including areas that are not currently supplied by conventional means. At night, the air is heated by the energy that was stored in the ground during the day diffusing into the cooler air. It is necessary to model a solar tower with a layer of thermal storage as a porous material for FLUENT to correctly calculate the heat transfer between the ground and the air. Porous material is permeable (packed-bed) material used to have conductive, radiative and convective boundary conditions to intensify the night-time heat transfer. To correctly calculate the heat transfer in the system, it is necessary to employ the standard $k - \varepsilon$ turbulence model and Discrete Ordinates radiation model. The air flow through the solar updraft tower is studied using Ansys - fluent and contour, streamline and XY plots for flowing air is discussed. Finally, the relation between some properties are displayed and the power generated dependence on structural and geographical factor is studied.

Keywords: Solar updraft tower; CFD; Buoyancy-Driven Flow; Convection; Thermal radiation; solar Energy; Ansys Workbench

CONTENTS **PAGES**

List of figures

List of tables

Acronym

SUPP Solar updraft tower power plant

DO discrete ordinate (radiation model)

PCU power conditioning unit

HTVTS horizontal to vertical transition section

IGV Inlet Guide Veins

OECD Organization for Economic Cooperation and Development

IEA International energy agency

RES Renewable energy sources

EU European Union

Greek symbol

α Absorptance

Δ Differential

ε Emissivity

η Efficiency [%]

μ Dynamic viscosity [$\frac{kg}{m.s}$]

π Pi

ρ Density [$\frac{kg}{m^3}$]

τ Shear stress [$\frac{N}{m^2}$]

φ Angle [radians or degree]

Nomenclature

A_{sc} Area of solar updraft (m^2)

A_c Area of collector (m^2)

C_p Specific heat capacity of air ($\frac{KJ}{Kg\ K}$)

d_{sc} Diameter of solar updraft (m)

H_{sc} Height of solar updraft (m)

F_R Heat removal factor

H_c Height of solar collector (m)

P_d Dynamic pressure (pa)

P_{tot} Total pressure (pa)

T_a Ambient Temperature (k)

T_f Temperature of the fluid (k)

S_1 solar radiation absorbed by the collector cover ($\frac{w}{m^2}$)

S_2 solar radiation absorbed by the ground ($\frac{w}{m^2}$)

H_d Diffused component of solar radiation ($\frac{MJ}{m^2}$)

H Monthly average global horizontal radiation on a surface ($\frac{MJ}{m^2}$)

$\tau\alpha$ transmittance- absorptance product

h_{cf} convective heat exchange between collector cover and the air flow ($\frac{w}{m^2k}$)

h_{gf} convective heat exchange between ground and the air flow ($\frac{w}{m^2k}$)

h_{rs} Radiation heat transfer from cover to ambient (sky radiation) ($\frac{w}{m^2k}$)

h_w wind convection loss coefficient $\frac{w}{(m^2k}$)

U_t Top loss coefficient ($\frac{w}{m^2k}$)

U_b bottom loss coefficient ($\frac{w}{m^2k}$)

U_e collector edge loss coefficient ($\frac{w}{m^2k}$)

U_l over all heat transfer coefficient ($\frac{w}{m^2k}$)

V_{sc} Velocity of air flow through the chimney ($\frac{m}{s}$)

V_{max} maximum air flow rate through the chimney ($\frac{m}{s}$)

η_c Collector efficiency

η_t turbine efficiency

η_{sc} chimney efficiency

η_{scpp} efficiency of solar updraft power plant

ε_c emissivity of collector

ε_g ground emissivity

φ latitude of location (deg)

δ declination (deg)

ν dynamic viscosity ($^{m^2}/_{s}$)

Re Reynolds number

ws sun set hour angle (deg)

β slope (tilt) angle (deg)

ρ_{air} density of air ($\frac{kg}{m^3}$)

α_g ground absorptivity

CHAPTER ONE

INTRODUCTION

1.1 Background

Energy is central to sustainable development and poverty reduction efforts. It affects all aspects of development such as social, economic, and environmental including livelihoods, access to water, agricultural productivity, health, population levels and education related issues. None of any development goals can be met without major improvement in the quality and quantity of energy services in any country. But there are a number of problems related to energy, especially in developing countries.

1.1.1 The world Energy demand

Following IEA (2004), in the absence of new government policies, world primary energy demand is projected to expand by almost 60% between 2002 and 2030 with an average annual growth rate of 1.7%, which is lower than in the past three decades (2% per year; Table: 1.3). Moreover, the transport and power-generation sectors will absorb a growing share of global energy in line with past trends (Table: 1.2). Let us consider each fuel separately. Fossil fuels (oil, natural gas and coal) dominate the global primary energy mix with a share about 80% (Table: 1.3, total fossil fuels). Moreover, according to IEA (2006a), fossil fuels will account for around 83% of the increase in world primary demand over the period 2004-2030. Oil is the largest fuel in global primary energy mix (Table: 1.3), with annual growth rate of its demand about 1.6% per year (Table: 1.1). The share of renewable resources remains very low (0.07% in 1971 and 0.51% in 2004) because they start from a very low level.

- ✓ Summarizing, this section concludes that, regarding energy, there is clear dependence of the world economy on non-renewable resources. Indeed, as it was shown before, non-renewable energy resources represent 86.84% of the world's primary energy demand in 2004, with a share of fossil fuels about 80% (Table 1.3, total non-renewables and total fossil fuels).

Table 1.1: Average annual growth rate of world primary energy demand (%) (IEA,2004)

Energy	1971-2002	2002-2010	2010-2020	2020-2030
Coal	1.70	1.80	1.60	1.50
Oil	1.4	2	1.8	1.6
Natural gas	2.90	2.70	2.60	2.3
nuclear	10.8	1.5	0.6	0.4
Hydro	2.5	2.6	2	1.8
Biomass & waste	1.6	1.5	1.4	1.3
Another renewable [a]	8.5	8	6.2	5.7

[a] Geothermal, solar, wind, tidal and wave energy. Source: World Energy Outlook. IEA (2004)

Table 1.2: Sectoral shares in world primary energy demand (%)

Energy	1971	1990	2002	2004	2010	2020	2030
Power generation	21.88	32.07	36.38	36.89	37.83	39.08	40.21
Industry	27.19	24.44	21.41	22.41	21.14	20.82	20.46
transport	15.46	16.43	17.57	18.29	18.29	19.13	19.85
Own use & losses	9.5	10.05	9.5	9.87	9.87	9.77	9.61
Others	25.98	17.01	13.63	12.87	12.87	11.21	9.86
Total	100	100	100	100	100	100	100

Source: World Energy Outlook. IEA (2004, 2006a)

Table 1.3: World primary energy demand (%)

Energy	1971	1990	2002	2004	2010	2020	2030
Coal	25.42	25.00	25.09	24.75	22.66	22.17	21.84
Oil	43.59	36.43	35.53	35.17	35.53	35.22	34.97
Natural gas	16.11	19.24	21.17	20.55	22.17	23.96	25.05
Nuclear	0.52	6.01	6.69	6.38	6.37	5.39	4.63
Hydro	1.88	2.12	2.17	2.16	2.26	2.23	2.21
Biomass and waste	12.41	10.57	10.82	10.50	10.37	9.91	9.73
Another renewables [a]	0.07	0.64	0.53	0.51	0.83	1.12	1.55
Total primary energy	100	100	100	100	100	100	100
Total fossil- fuels [b]	85.12	80.66	79.80	80.46	80.16	81.35	81.86
Total non—renewables [c]	85.64	86.67	86.49	86.84	86.54	86.73	86.50
Total renewables [d]	14.36	13.33	13.51	13.16	13.46	13.27	13.50

Source: World Energy Outlook. IEA (2004, 2006a)

a Geothermal, solar, wind, tidal and wave energy.

b Coal + oil + natural gas.

c Fossil fuels + nuclear.

d Hydro + biomass and waste + other renewables.

1.1.2 Problems related to the usage of non-renewable energy resources

As observed in the above section, the world economy has a high dependence on non-renewable energy resources. However, a key feature of non-renewable energy resources is that their stocks (reserves) are finite. Therefore, the usage of non-renewable energy resources calls attention to the "survival" (i.e., economic growth and development) of the economic system due to the limited availability of these resources.

- The reserves of oil and natural gas will last, respectively, 41 and 64 years at current rates. Moreover, the coal reserves will last around 155 years. Hence, since the world economy shows a high dependence on fossil fuels, one concludes that the usage of non-renewable energy resources (in particular, fossil fuels) raises the question of the maintenance of economic growth and development in medium and long-term. [1a]
- Even if enough energy is somehow indefinitely pretended up for everyone who wants it, without risking conflict and disorder in bringing it back home, there would still be an enormous problem - how to use the energy without causing unacceptably high levels of damage to the natural world.
- The most obvious threat is the prospect that burning fossil fuels is intensifying natural climate change and heating the Earth to dangerous levels. Carbon emissions - thought to be a major cause of global climate change - are set to increase by 60%. As developing countries' share of world energy demand surges from 38% to a predicted 48%, poor countries are expected to contribute two-thirds of the projected increase in carbon emissions.
- Not only the greenhouse effect is a problem but also there are still real costs that go with the quest for and use of energy: air and water pollution, impaired health, acid rain, deforestation, and the destruction of traditional ways of life. It is one of the most vicious circles the planetary crisis entails.
- In general, the world’s energy use is unsustainable. One alternative way of coming out of this energy crisis is to use renewable energy which is obtained from inexhaustible natural sources.

Renewable energy sources (RES) capture their energy from existing flows of energy, from on-going natural processes, such as sunshine, wind, flowing water, biological processes, and geothermal heat flows. The notion of going green is not strictly a new technological concept, and any naturally occurring and theoretically inexhaustible energy such as wind, biomass, solar, tidal, wave, hydroelectric power that is not derived from fossil or nuclear fuel is referred to as renewable energy. The relevance of these emerging fields became more pronounced when the need to produce clean, safe and efficient energy devices without trading off environmental friendliness arise. The present situation of energy use in Ethiopia differs fundamentally from the situation in industrialized countries. In Ethiopia still approximately 70-80% of the primary energy shares are taken from biomass. But the biomass, basically wood which is processed to charcoal, is neither cultivated in a sustainable way nor is it used efficiently. Deforestation and with it soil erosion, loose of farm yield potential and desertification are the consequences. In 2006, the energy consumption per capita was assessed at about 32.94 kWh, which is extremely low compared to most other countries in the world [1b]. Just like in most other countries in the world, the total energy consumption in Ethiopia is increasing. The annual rate of growth for the use of electric energy amounts up to 10 %. It is planned to expand the national grid and with it to increase the share of the people who have access to electricity. But the goal to offer electricity to all Ethiopians is still very far away. Being the most abundant and well-distributed form of renewable energy, solar energy constitutes a big asset for arid and semi-arid regions. A range of solar technologies is used throughout the world to harvest the sun ‘s energy. In the last years, an exciting innovation has been introduced by researchers called **solar updraft**. It is a solar thermal driven electrical power generation plant that converts the solar thermal energy into electrical power in a complex heat transfer process. The implementation of this project is of great significance for the development of new energy resources and the commercialization of power generating systems of this type and will help developing countries to promote the rapid development of the solar hot air-flows power generation [2]. The basic physical principles of centralized electricity generation with solar updraft power plants (SUPP) were described by Haaf et al., in 1982. After the pilot plant in Manzanares had gone into operation in June 1982, the first experimental results confirmed the main assumptions of the original physical model. Later, on the basis of experimental data from July 1983 to January 1984, a semi-empirical, parametrical model was proposed for predicting the monthly mean electrical power output of the pilot plant as a function of solar irradiation. Solar energy is viewed as a clean and renewable source of energy for the future. Energy from the sun offers probably the best potential for energy options in Ethiopia. An assessment study indicated in 2002, that the average daily solar radiation reaching the ground for Ethiopia as a whole is 5.2 kWh/m2. The strength of solar radiation in Ethiopia is expected to be the highest category in the world. Therefore, the radiation can qualify to be the sole resource of energy for the country. So, solar energy can bring an important contribution to sustainable and central energy for Ethiopia [1b]. And solar energy can be developed directly in many methods. In one particular method, solar radiation hits the absorber surface of a solar thermal collector and the surface warms. The heat energy is carried away by a fluid (air) flow to the place where the energy is required at the turbine. The solar updraft power plant works in this method [2]. A typical Solar updraft power Plant (SUPP) consists of a circular greenhouse type collector and a tall tower (chimney) at its center. Air flowing radially inwards under the air collector is heated from the collector floor and roof, and through a turbine enters the chimney. Thereby staging a pressure build-up along with the tower, and the heat transfer fluid, HTF is warmed up in order to drive the turbine, hence produces energy in the form of electricity. Air is heated by solar radiation under a low circular glass roof open at the periphery; this and the natural ground below it forms a hot air collector. Continuous 24 hours-operation is guaranteed by placing tight water-filled tubes under the roof. The water heats up during the daytime and emits its heat at night. These tubes are filled only once, no further water is needed. In the middle of the roof, there is a vertical chimney with large air inlets at its base. The joint between the roof and the chimney base is airtight. As hot air is lighter than cold air it rises up the chimney. Suction from the chimney then draws in more hot air from the collector, and cold air comes in from the outer perimeter. Thus, solar radiation causes a constant up draught in the chimney. The energy this contains is converted into mechanical energy by pressure-staged wind turbines at the base of the chimney, and into electrical energy by conventional generators.

Many researchers around the world have introduced various projects of the solar tower. Around 1500, Leonardo Da Vinci made sketches of a solar tower called a smoke jack (figure 1-a) [3]. The idea of using a solar updraft to produce electricity was first proposed in 1903 by the Spanish engineer Isodoro Cabanyes (figure 1-b). Another earlier description was elaborated upon in 1931 by the German science writer Hans Gunther [4]. He proposed a design in the 25 August 1903 issue of La Energia Electrical, entitled Projecto de motor solar. In this bizarre contraption, a collector resembling a large skirt heats air and carries it upwards towards a pentagonal fan inside a rectangular brick structure vaguely resembling a fireplace (without a fire). The heated air makes the fan spin and generates electricity, before it escapes up a tall chimney, cools, and joins the atmosphere [5]. In 1926, Prof Engineer Bernard Dubos proposed to the French Academy of Sciences the construction of a Solar Aero-Electric Power Plant in North Africa with its solar updraft on the slope of the high height mountain after observing several sand whirls in the southern Sahara [6]. The author claims that an ascending air speed of 50 m/s can be reached in the chimney, whose enormous amount of energy can be extracted by wind turbines [7].

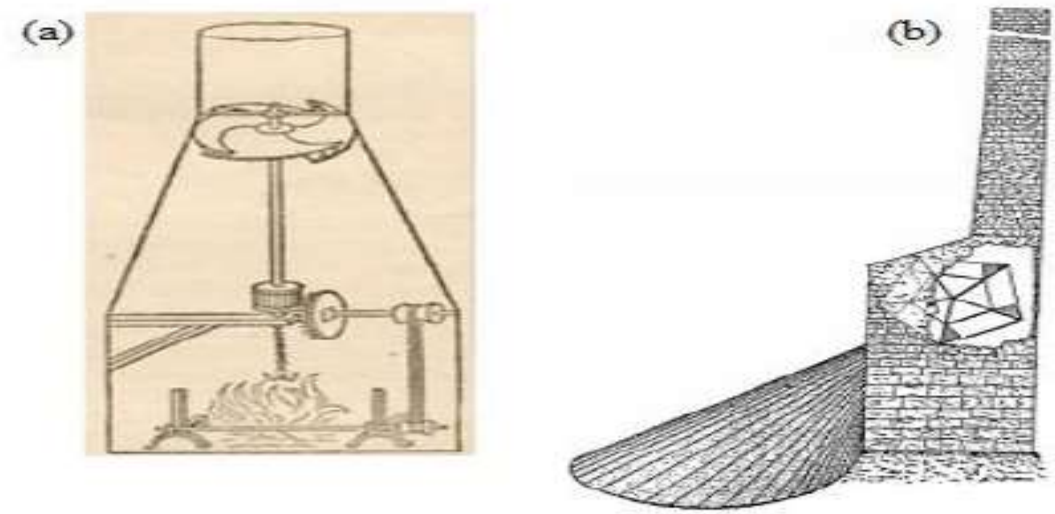

Figure 1.1 (a) The spit of Leonardo da Vinci (1452-1519) (Library of Entertainment and knowledge (b) Solar engine project proposed by Isodoro Cabanyes.

The idea of using solar radiation to generate air convection that can subsequently be converted to an energy source has been around since the start of the 20th century, when a Spanish Colonel called "Isidoro Cabanyes", proposed it in a scientific magazine. The French academy of sciences recommended the Dubos 's idea be followed up, especially in French North Africa, which has no fuel and needs power. As a matter of fact, Dubos had the North African Atlas Mountains in mind when he developed his plans **[6**]. In 1956, he filed his first patent in Algeria. It was artificially generating ancestry atmospheric vortex in a sort of round-shaped Laval nozzle and recover some energy through turbines. Nazare received a French patent for his invention in 1964 (figure 3) [7]. In 1975 the American Robert Lucier filed a patent request based upon a more complete design. This patent was granted in 1981 **[8**]. Starting in 1982, a team led by the German civil engineer Jorg Schlaich took the initiative and constructed a prototype in Manzanares Spain, with a 195 m high and a maximum power output of 50 kW **[**8]. In 2002 Time Magazine identified this project as one of the best inventions of the year. The operating principle is considered revolutionary but is based on very common knowledge: Warm air rises [9].

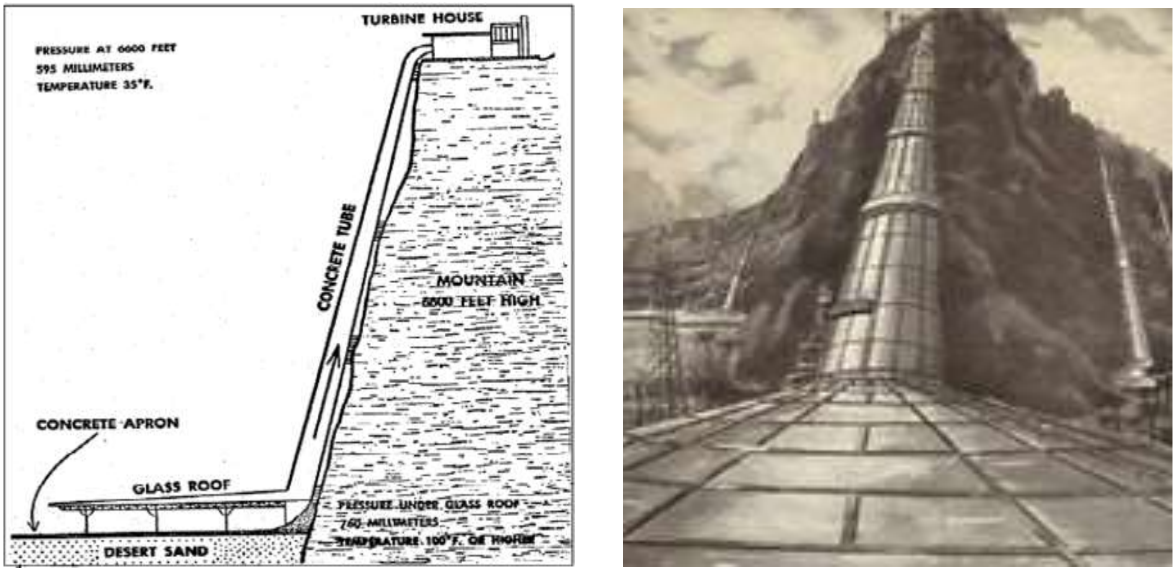

Fig 1.2. Principle of Professor Dubos 's power plant description [12]

Figure 1.3. the solar tower of the professor NAZARE. (Source: L 'Ere nouvelle n° 52 July 1985)

Solar Updraft towers provide a very simple method for renewable electricity generation, with constant and reliable output. Other renewable energy sources such as wind turbines and solar arrays suffer from high diurnal and seasonal fluctuations or unpredictable patterns of output. Sensible technology for the wide use of renewable energy must be simple and reliable, accessible to the technologically less developed countries that are sunny and often have limited raw material resources. It should not need cooling water and should be based on environmentally friendly production from renewable or recyclable materials. Invariably, solar updraft tower meets these requirements. A typical pictorial illustration of the robust setup and technology behind the solar updraft tower is shown in figure 4. below. It uses solar insolation to increase the temperature of the air, and the buoyancy force causes the flow of the air stream inside the solar updraft system. Air is warmed up due to the greenhouse effect under a transparent collector **[**10**]**.

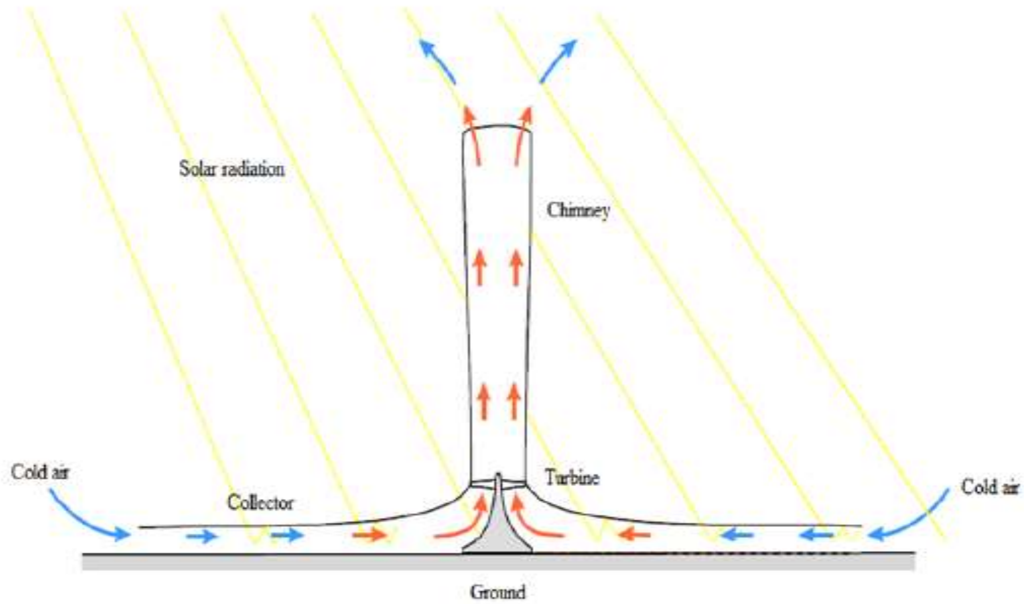

Figure 1.4: Principle of the solar updraft: glass roof collector, chimney tube, wind turbines [10]

1.2 Working Principle

As presented in figure 1.4 above, a Solar Updraft Tower converts solar radiation into electricity by combining three well-known principles: the greenhouse effect, the tower, and wind turbines in a novel way. Hot air is produced by the sun under a large glass roof [9]. Direct and diffuse solar radiation strikes the glass roof, where specific fractions of the energy are reflected, absorbed and transmitted. The quantities of these fractions depend on the solar incidence angle and optical characteristics of the glass, such as the refractive index, thickness and extinction coefficient. The transmitted solar radiation strikes the ground surface; a part of the energy is absorbed while another part is reflected back to the roof, where it is again reflected the ground. The multiple reflections of radiation continue, resulting in a higher fraction of energy absorbed by the ground, known as the transmittance-absorptance product of the ground. Through the mechanism of natural convection, the warm ground surface heats the adjacent air, causing it to rise. The buoyant air rises up into the chimney of the plant, thereby drawing in more air at the collector perimeter and thus initiating forced convection which heats the collector air more rapidly. Through mixed convection, the warm collector air heats the underside of the collector roof. Some of the energy absorbed by the ground surface is conducted to the cooler earth below, while radiation exchange also takes place between the warm ground surface and the cooler collector roof. In turn, via natural and forced convection, the collector roof transfers energy from its surface to the ambient air adjacent to it [8]. As the air flows from the collector perimeter to the chimney, it's temperature increases while the velocity of the air stays approximately constant because of the increasing collector height. The heated air travels up the chimney, where it cools through the chimney walls. The chimney converts heat into kinetic energy. The pressure difference between the chimney base and ambient pressure at the outlet can be estimated from the density difference. This, in turn, depends upon the temperatures of the air at the inlet and at the top of the chimney. The pressure difference available to drive the turbine can be reduced by the friction loss in the chimney, the losses at the entrance and the exit kinetic energy loss [9]. As the collector air flows across the turbine(s), the kinetic energy of the air turns the turbine blades which in turn drives the generator(s) [10]. Warm air, lighter than cold air, moves inwards and eventually rises through the central chimney passing through the turbine where it yields a large fraction of its energy. The latter will be converted into mechanical energy then into electrical energy. The warm-up drafting air will be replaced by the fresh ambient air entering from the periphery of the collector which becomes warm and escapes also through the chimney [11].

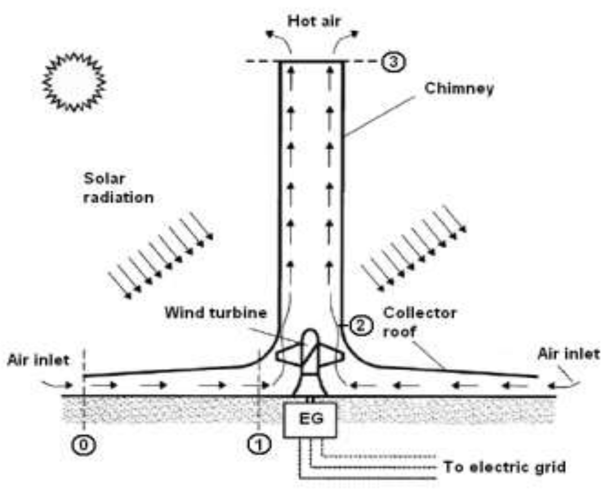

Figure 1.5 Solar tower power plant component description [11].

The chimney situated in the collector center is the actual thermal engine of the solar updraft power plant. The upthrust of the air heated in the collector is proportional to the rise in air temperature flowing in the collector and its volumetric flow rate. Suitable turbines located at the base of chimney convert kinetic energy of the up flowing air inside chimney to mechanical power in the form of rotational energy [12]. The typical solar updraft turbine is of the axial flow type. The principle of operation of these turbines is similar to the turbo generators used in hydroelectric power stations, where the static pressure is converted into mechanical work. The power output achieved is proportional to the product of the volume flow rate and the pressure drop across the turbine. The air flow through the turbine can be regulated by varying the turbine blades pitch angle. This mechanical energy can be converted into electric energy by coupling the turbine to the generator. The solar updraft does not necessarily need direct sunlight. They can exploit a component of the diffused radiation when the sky is cloudy. The lack of system dependence on the natural occurrence of wind, which is intermittent, makes it a very attractive development. The collector is composed of soil as a system of heat storage, a transparent surface located a few meters above the ground and a field of air circulation. This one opened at the two ends, recovers incidental solar energy while heating and containing the air which circulates there. The air is heated by the absorption of the solar flow, which crosses the transparent upper surface of the collector. It circulates within the collector subjected to phenomena of convection [13].

The collector

Hot air for the solar updraft is produced by the greenhouse effect in a simple air collector consisting only of a glass or plastic film covering stretched horizontally two to six meters above the ground. The height of the covering increases adjacent to the chimney base so that the air is diverted to vertical movement with minimum friction loss. This covering admits the short-wave solar radiation component and retains long-wave radiation from the heated ground. Thus, the ground under the roof heats up and transfers its heat to the air flowing radially above it from the outside to the chimney.

The energy storage

Water filled black tubes are laid down side by side on the soil under the glass roof collector. They are filled with water once and remain closed thereafter so that no evaporation can take place. The volume of water in the tubes is selected to correspond to a water layer with a depth of 5 to 20 cm depending on the desired power output characteristics.

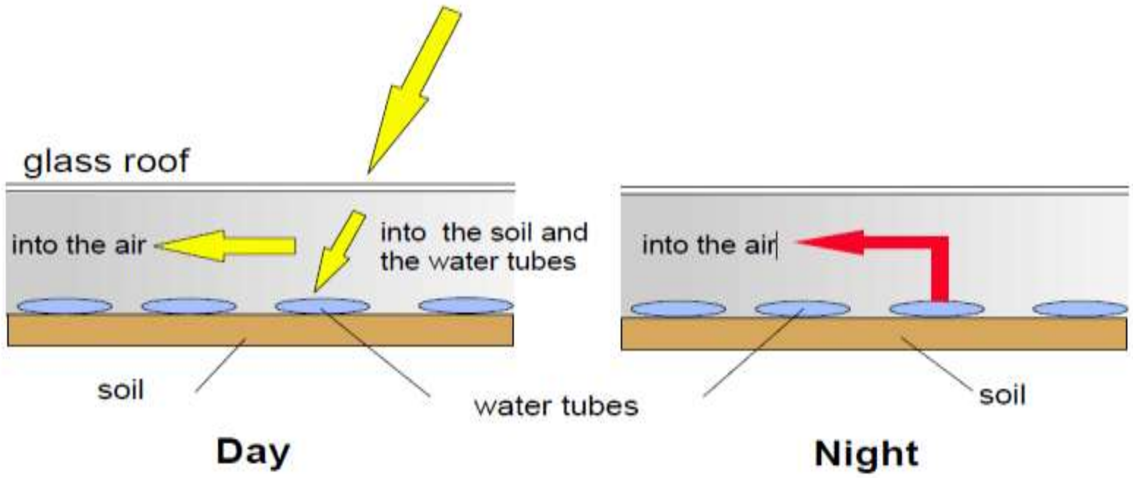

Figure 1.6: Principle of heat storage underneath the roof using water-filled black tubes [13].

Since the heat transfer between black tubes and water is much larger than that between the ground surface and the deeper soil layers, even at low water flow speed in the tubes, and since the heat capacity of water (4.2 kJ/kg) is much higher than that of soil (0.75 - 0.85 kJ/kg) the water inside the tubes stores a part of the solar heat and releases it during the night, when the air in the collector cools down.

The chimney

The chimney itself is the plant's actual thermal engine. It is a pressure tube with low friction loss (like a hydroelectric pressure tube or penstock) because of its optimal surface- volume ratio. The upthrust of the air heated in the collector is approximately proportional to the air temperature rise ΔTc in the collector and the volume, (i.e. the height Hc multiplied by the diameter Dc) of the chimney. In a large solar updraft, the collector raises the temperature of the air by about 35^{o}C. This produces an updraft velocity in the chimney of about 15m/s. It is thus possible to enter into an operating solar updraft plant for maintenance without difficulty. There are many different ways of building this kind of chimney. They are best built freestanding, in reinforced concrete. But guyed tubes, their skin made of corrugated metal sheet, as well as cable-net designs with cladding or membranes are also possible. All the structural approaches are well known and have been used in cooling towers. No special development is needed.

The turbines

Using turbines, mechanical output in the form of rotational energy can be derived from the air current in the chimney. Turbines in a solar updraft do not work with a staged velocity like a free-running wind energy converter, but as a cased pressure-staged wind turbo-generator, in which, similarly to a hydroelectric power station, static pressure is converted to rotational energy using a cased turbine in this application installed in a pipe. The power output of a cased pressure-staged turbine of this kind is about eight times greater than that of a speed-stepped open-air turbine of the same diameter. Air speed before and after the turbine is about the same. The output achieved is proportional to the product of volume flow and the fall in pressure at the turbine. With a view to maximum energy yields the aim of the turbine regulation system is to maximize this product under all operating conditions. Blade pitch is adjusted during operation to regulate power output according to the altering airspeed and airflow. If the flat sides of the blades are perpendicular to the airflow, the turbine does not turn. If the blades are parallel to the air flow and allow the air to flow through undisturbed there is no drop-in pressure at the turbine and no electricity is generated. Between these two extremes there is an optimum blade setting: the output is maximized if the pressure drop at the turbine is about two-thirds of the total pressure differential available.

1.3 Problem Statement

Ethiopia as a developing country faced with a lot of challenges. One of the most pressing challenges lies in the power sector. Many rural areas in the country are not yet connected to the national grid due to the high costs and the complex technology of rural electrification. Two major problems, poverty and worldwide dependence on fossil fuels, are widespread in society. Fossil fuels are a non-renewable source of pollution, and poverty negatively affects the livelihood of millions in arid and semi-arid areas in Ethiopia. Overall, this location is a perfect spot for a solar updraft power plant due to the abundance of solar radiation. Therefore, SUPP which depends on green, safe and environmentally friend solar energy is a suitable option for this area and studied using CFD software fluent.

1.4 Objectives

General objective: To study the performance of a conventional solar updraft tower power plant for power generation in eastern part of Ethiopia.

The Specific Objectives are:

- ✓ Study of solar collector under Adama weather condition
- ✓ Studying suitable thermal energy storage for the system
- ✓ Specifying and studying of the chimney for the system
- ✓ Examining the scaling effects on the power output and fluid flow through the system
- ✓ The study of air flow through a solar updraft tower power plant using the CFD software FLUENT.

1.5: Conceptual Framework

An axisymmetric solar updraft is used to determine the boundary conditions to best account for the heat transfer occurring between the chimney's surfaces and the air moving through the system. Axis symmetric criteria reduces 3D problems into 2D problem. The main benefits of 2D approximation is reducing the computing time, as number of elements are less the most accurate mesh can be generated and convergence error will be reduced therefore very accurate results will be obtained. But in case of 3D analysis too many elements too much of care required while meshing takes more computing time chances of errors will be more therefore whenever the problem meets the 2D approximation criteria it is best to go with 2D FE analysis. Incorporating a layer of thermal storage in the ground is required to accurately model the chimney system and greatly impacts the airflow. The thermal storage dissipates heats throughout the night, transferring heat from the ground into the air. Forced-advection wells can also be incorporated into solar updraft systems to increase the air temperature. The wells are located in the thermal storage and transfer the heat from the ground into the airstream.

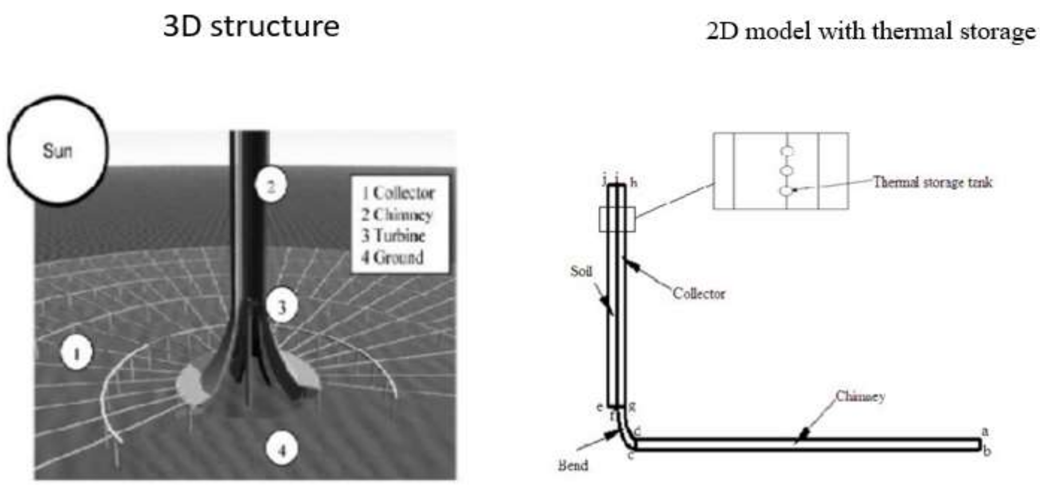

Figure 1.7: 3D structure and 2D model with thermal storage [10]

The tasks are highlighted as:

i. Create a model based on plant design parameters to assess the performance of SUPP.

ii. In this stage, the model depends the optimal SUPP dimensions (chimney height and collector diameter) by considering the total cost of the system.

iii. In the next stage, using the predicted optimal plant size, the system reliability is determined.

Additionally, the thesis:

i. Offers the study of energy storage layer to ensure the continuous operation of the SUPP even in the period when there is no solar radiation.

ii. Incorporates chance constraint into the model to account for randomness in the solar radiation and ambient temperature data.

iii. Validates the developed model using a case study involved in different countries so far.

iv. It offers valuable managerial insight on the effect of some important parameters on both the optimal plant size and economic feasibility of the proposed SUPP.

1.6 Scope, Limitations and Significance of The Study

1.6.1 Scope of the study and contribution to the body of knowledge

This study presents a CFD model that can be used for the design of SUPP so as to stand-in the adoption of the technology. The main contribution of this thesis to the body of knowledge is the development of CFD model for the optimal design of SUPP and importance of the study. The developed model is general and can be utilized in any location of Ethiopia for SUPP design and assessment. Therefore, it is very necessary to adopt this technology in every part of Ethiopia like other conventional sources which we are using regularly.

1.6.2 Significances of the Study

Solar updraft power stations are particularly suitable for generating electricity in deserts and sun-rich wasteland. It provides electricity 24 hours a day from solar energy alone. Without using fuel and cooling water, it is suitable in extreme drying regions. This power plant is particularly reliable and a little trouble-prone compared with other power plants. The materials concrete, glass and steel necessary for the building of solar tower power stations are everywhere in sufficient quantities. Unlike others (biomass) no ecological harm and no consumption of resources have undergone.

Solar updraft operates simply and have a number of other advantages:

- ✓ The collector can use all solar radiation, both direct and diffused. This is crucial for tropical countries where the sky is frequently overcast. The other major large scale solar-thermal power plants, parabolic through and central receiver systems, which apply concentrators and therefore can use only direct radiation, are a disadvantage there.

- ✓ Due to the heat storage system, the solar updraft will operate 24h on pure solar energy. The water tubes laying under the glass roof absorb part of the radiated energy during the day and release it into the collector at night. Thus, solar updraft s produce electricity at night as well.
- ✓ Solar updraft is particularly reliable and not liable to break down, in comparison with other solar generating plants. Turbines, transmission, and generator subject to a steady flow of air are the plant's only moving parts. This simple and robust structure guarantees operation that needs little maintenance and of course no combustible fuel.
- ✓ Unlike conventional power stations (and also other solar-thermal power station types), solar updraft does not need cooling water. This is a key advantage in the many sunny countries that already have major problems with drinking water.
- ✓ The building materials needed for solar updraft s, mainly concrete and glass, are available everywhere in sufficient quantities. In fact, with the energy taken from the solar updraft itself and the stone and sand available in the desert, they can be reproduced on site.
- ✓ Solar updraft can be built even in less industrially developed countries. The industry already available in most countries is entirely adequate for their requirements. No investment in a high-tech manufacturing plant is needed.
- ✓ Even in poor countries, it is possible to build a large plant without high foreign currency expenditure by using their own resources and work-force; this creates large numbers of jobs and dramatically reduces the capital investment requirement and the cost of generating electricity.

1.6.3 limitation

As a delimitation, the cost of generating electricity from a solar updraft is high. Although fuel is not required, solar updraft s have a very high capital cost due to the huge structure that requires a lot of capital to construct. This study focuses on providing a model for SUPP design assuming that the proposed plant would be modeled by CFD, however, it fails to provide detailed insight into the complex mechanism of building and operation including risk.

The SUPP also faces the challenge of little or no power generation in the night due to a lack of energy supply from the sun or alternative sources. The energy generated by the SUPP fluctuates over the day and varies with time of the year due to the position of the sun at various times and seasons. Conventional SUPP requires a large expanse of flat land with no competing values. Furthermore, the mass flow rate of air in the SUPP is limited to the collector size and the stack effect of the chimney.

1.7 Research Questions

- ✓ What are the technologies available in harnessing solar energy to produce power?
- ✓ How do solar updraft tower power plant (SUPP) works and in what areas are they practically feasible?
- ✓ What factors affect or influence the power output of a solar updraft power plant?
- ✓ What affects the performance of a solar updraft power plant?
- ✓ How does the air flow through the solar updraft tower?
- ✓ Can the solar updraft tower operate at the night-time?

CHAPTER TWO

LITERATURE REVIEW

2.1 Introduction

This chapter concerns some general information on SUPP technology, solar energy harnessing technology by SUPP and solar thermal energy storage system. In addition, previous research works on SUPP, solar energy collector and solar thermal energy storage are used as input for the current work. SUPP is a promising for large-scale utilization of solar energy and extensive research has been carried out to investigate its huge-potential over the world. Based on an analysis of the geographical conditions and solar-energy resources in many countries, the feasibility of constructing a solar hot air-flows power generating system was demonstrated [14]. Detailed theoretical preliminary research and a wide range of wind tunnel experiments led to the establishment of an experimental plant with a peak output power of 50 kW on a site made available by the Spanish utility union Electrica Fenosa in Manzanares about 150 km south of Madrid in 1981-82 **(**Schlaich & Schiel) [17] with funds provided by the German Ministry of Research and Technology. The aim of this research project was to verify, through field measurements, the performance projected from calculations based on theory and to examine the influence of individual components on the plant's output and efficiency under realistic engineering and meteorological conditions. These results show that the components are highly dependable and that the plant as a whole is capable of highly reliable operation. The single global radiation is exploited and the thermodynamic cycle is a characteristic feature of the system. Continuous operation throughout the day is possible and even abrupt fluctuation in energy supply is effectively mitigated. The plant operated continuously even on cloudy days even if at reduced output [15,16].

2.2 Related Works Done by Previous Researchers

Schlaich [17] has demonstrated the technical feasibility of electricity generation with solar updraft power plants and stated electrical power output is a function of global irradiation, depends on meteorological and environmental conditions**.** The pilot project worked for about eight years until the chimney support wires rusted out and the chimney was blown over in a storm, but it did prove that the concept was scientifically sound. To get meaningful amounts of power out of such a system (that is to get megawatts instead of kilowatts) requires the construction of a substantially taller chimney. The taller the chimney, the stronger the updraft and the stronger the updraft, the more power you can generate [18].

Table 2.1 Data and design values of the pilot plant of Manzanares parameters

Parameters	unit	Value
Chimney height	m	195
Tower radius	m	5.08
Collector radius	m	120
Collector height	m	1.85
Collector weight	kg	125000
No. of turbine blades		4
Turbine blade profile		FXW-151
Collector temperature increase (ΔT)	℃	20
Nominal output power	kw	50
Glass roof- collector area	m^2	6000
Roof covered with polymer sheets	m^2	40000
Irradiation	W/ m^2	1000
Rotor blade radius	m	5
Fresh air temperature	K	302
Collector efficiency Turbine Friction loss factor		0.32 0.85 0.9

Haaf [19] did an in-depth analysis of the chimney system to optimize the power output prior to construction and mentioned the environmental factors, including soil characteristics and the Sun's irradiation, were considered in the energy balances performed on the ground and solar collector. Through extensive research, Haaf [19] determined that the materials, ground storage, and size of the plant impacted the efficiency of the solar updraft. Using these findings, the chimney in Spain was constructed to have a height of 195 meters and a diameter of ten meters. The collector, two meters in height, radiated out from the chimney and had a radius of 122 meters. The prototype solar updraft power plant at Manzanares in Spain Haaf [19] showed that the solar updraft is a practical technology capable of generating electrical power from the sun. Solar updraft power plant systems are being considered as feasible options to produce energy in countries where unexploited desert areas are abundant, like South America, Africa, Asia and Oceania [20-21]. Enviro- mission is set to build the tallest structure of solar updraft power plant in North America with its innovative solar updraft tower design, which provides baseload power [22]. The solar updraft tower uses a solar energy collector canopy and a central tower to generate and updraft airflow that drives the rotation of pressure-staged turbines at the base of the tower and generates electricity. Enviro Mission plans to build its first commercial solar updraft tower on public lands in L Paz County, Arizona. If we imagine a sunny day in Arizona where the outside temperature would be 40 degrees Celsius, the temperature under the collector would be 80 to 90 degrees Celsius and the temperature at the top of the tower would be 32 degrees Celsius. This creates the ideal temperature differential that Enviro Mission desires.

Figure 2.1 Enviro Mission Arizona USA

To evaluate the performance of solar updraft power plants in some locations in Egypt theoretically and to make an approximation of the quality of the generated electrical energy, a simple mathematical model [23], based on the energy balance was developed to estimate the power output of solar updraft s as well as to observe the effect of various ambient conditions and structural dimensions on the power generation. It was found that the wind speed inside chimney reaches more than 7 times the value of the free wind speed outside chimney. The solar updraft power plant with 500 m chimney height, 50 m chimney diameter and 3000 m collector diameter capable of producing yearly between 1.6-1.7 x 10^8 kW hr. in the selected locations in Egypt. Therefore, the use of solar updraft power plants in many locations in Egypt will be attractive. It can cover a considerable section of the increasing demand for energy. It can save the use of conventional sources of energy like oil and natural gas and consequently reduces the emissions of harmful gases. Analysis of a solar updraft power plant in the Arabian Gulf region of UAE was carried by Hamdan [24]. The developed analytical model was used to evaluate the effect of geometric parameters on the solar plant power generation. The analysis showed that **chimney** height and turbine pressure head are the most important physical variables for the solar updraft design. The study showed that second –law efficiency has no monotonic relation with turbine pressure head. The model shows that second-law efficiency and power harvested increase with the increase of chimney height and/or diameter. The developed model is used to analyze the feasibility of solar updraft power plants for the UAE climate which possesses typical characteristics of the gulf climate. The solar characteristics of the UAE are shown along with characteristic metrological data. Hamdan 2011[24] in his work presents a numerical thermal model for steady-state airflow inside a solar updraft power plant using adapted Bernoulli equation with buoyancy effect and ideal gas equation. The outcome shows that using a constant density assumption through the solar updraft can simplify the analytical model however it over predicts the power generation. This outcome shows that the chimney height, the collector radius, the solar irradiance, and the turbine head are important parameters for the design of solar updraft. The maximum power generation depends on the turbine head and the relation is not monotonic. Kasaeian [25] has investigated the air velocities and different temperature were considered for 5 m collector radius and 12 m height of chimney, after designing and making a solar updraft pilot power plant with 5 m collector radius and 12 m height of chimney, the temperatures, and air velocities were investigated. The temperature and velocity readings were carried out for some specified places of collector and chimney with changeable some parameters on different days. The inversion of air at the lower of the chimney was investigated after sunrise, on both summer and winter seasons. The inversion of air shows with increasing solar radiation from a minimum point and after a while, it is broken by the collector warm-up. Kristein [26] has found out the good agreement between experimental model and numerical model, for evaluating the coefficient of loss and mean exit swirl angle of the flow passing through the collector-to-chimney transition section of a full-scale solar updraft power plant as dependent on IGV stagger angle and collector roof height. The numerical analysis flow angles, velocity components, and internal and wall static pressures. The resulting agreement between numerical and experimental model predicted total pressure loss coefficient was reasonable when considering how small it is. The numerical model predicts optimized geometry parameters. Mathematical equations were created to predict the loss coefficient and turbine mean inlet flow angles of solar updraft power plants as dependent on collector deck height and inlet guide vane setting angle. The comparison of experimental equations very useful in solar updraft power plant optimization.

Koonsrisuk [27] in his study compared the prediction of the performance of solar updraft plants by using simple theoretical models that have been proposed in the literature. The parameters used in the study were various plant geometrical parameters and insolation. Computational fluid dynamics (CFD) simulation was also conducted and its consequences compared with the hypothetical prediction. The power out and the efficiency of the solar updraft plants as functions of the considered parameters were used to compare relative merits of the hypothetical models. Koonsrisuk [28] in his paper, the performance of solar updraft power plant based on second law study is investigated for different configurations. A comparison is made between the conventional solar updraft power plant (CSUPP) and SCSPP. The appropriate entropy generation number and second law efficiency for solar updraft power plants are proposed in this study. Results show that there is the optimum collector size that provides the minimum entropy production and the maximum second-law efficiency. The second-law efficiency of both systems increases with the increasing of the system height. The study reveals the influence of various effects that change pressure and temperature of the systems. It was found that SSUPP is thermodynamically better than CSUPP for some configurations. The results obtained here are expected to provide information that will assist in improving the overall efficiency of the solar updraft power plant. Larbi [29] in his paper presented the performance analysis of a solar updraft power plant expected to provide the remote villages located in Algerian southwestern region with electric power. Solar energy and the psychometric state of the air in the south of Algeria are important to encourage the full development of solar updraft power plant for the thermal and electrical production of energy for various uses. We are interested in Adrar where solar radiation is better than other areas of Algeria. The obtained results show that the solar updraft power plant can produce from 140 to 200 kW of electricity on a site like Adrar during the year, according to an estimate made on the monthly average of sunning. This production is sufficient for the needs of isolated areas. Liu [30] proposed a comprehensive theoretical model for the performance evaluation of a solar updraft power plant (SUPP) and has been verified by the experimental data of the Spanish prototype. This model considers effect of flow, heat losses, and the temperature gap inside and outside the chimney. There is a maximum power output for a certain SUPP under a given solar radiation condition due to flow and heat losses and installation of the turbines. In addition, the design flow rate of the turbine in SUPP system is found beneficial for power output when it is lower than that at the maximum power-point. Furthermore, a limitation on the maximum collector radius exists for the maximum attainable power of the SUPP whereas no such limitation exists for chimney height in terms of contemporary construction technology. Maia [31] found that Sustainable improvement is closely associated with the use of renewable energy resources. In order to achieve a viable development, from an environmental point of view, the energy efficiencies of the processes can be increased using renewable energy resources. There is a relationship between energy and sustainable development since energy is consumed due to irreversibilities. The solar updraft has been highlighted in studies of using solar energy to produce electric power.

Krisst and Kulunk [32] demonstrated different types of small-scale solar updraft devices with power outputs not exceeding 10 W. Its collector had a diameter of 6 m and the chimney was 10 m tall. In 1997, a solar updraft thermal power generating demonstration model was built and modified twice on the campus of the University of Florida, and both theoretical and experimental investigation on their performances was carried out. A micro-scale model with a chimney of 3.5 cm in radius and 2m in height on a patch of area of 9 m^2 was built by Kulunk in lzmit, Turkey, which produces an electric power of 0.14W [32]. Pasumarthi and Sherif and Padki and Sherif et al [33] developed a mathematical model to study the effects of various environment and geometry conditions on the heat and flow characteristics and power output of a solar updraft. Lodhi presented a comprehensive analysis of the chimney effect, power production, efficiency, and estimated the cost of the solar updraft power plant set up in developing nations [34]. Gannon and von Backstrom presented a thermodynamic cycle analysis of the solar updraft power plant for the calculation of limiting performance, efficiency, and the relationship between the main variables including chimney friction, system, turbine and exit kinetic energy losses [35]. Pastohr et al., presented a numerical simulation result in which the energy storage layer was regarded as solid [36]. Liu et al., carried out a numerical simulation for the MW-graded solar updraft power plant, presenting the influences of pressure drop across the turbine on the draft and the power output of the system [37]. Schlaich presented a simplified theory, some practical experience results and a detailed economic analysis of solar updraft s for the design of commercial solar updraft power plant systems like the one being planned for Australia [38]. Pretorius et al., reviewed most of the outstanding issues. Different calculation approaches with a variety of considerations have been applied to calculate chimney power plant performance [39]. The available work potential that atmospheric air acquires while passing through the collector has been determined and analyzed by Ninic [40]. In this study, the dependence of the work potential on the air flowing into the air collector from the heat gained inside the collector, air humidity and atmospheric pressure as a function of elevation are determined. Various collector types using dry and humid air have been analyzed. The influence of various chimney heights on the air work potential was established. Bilgen and Rheault [41] designed a solar updraft system for power production at high latitudes and evaluated its performance. Pretorius and Kroger [42] evaluated the influence of a developed convective heat transfer equation, more accurate turbine inlet loss coefficient, quality collector roof glass and various types of soil on the performance of a large-scale solar updraft power plant. Koonsrisuk and Chitsomboon [43] proposed dimensionless variables to guide the experimental study of flow in a small-scale solar updraft. Computational fluid dynamics (CFD) methodology was employed to obtain results that are used to prove the similarity of the proposed dimensionless variables. Bernardes [44] carried out numerical simulations to study the performance of two schemes of power output control applicable to solar updraft power plants. Either the volume flow or the turbine pressure drop is used as independent control variable. Values found in the literature for the optimum ratio of turbine pressure drop to pressure potential vary between 2/3 and 0.97. It is shown that the optimum ratio is not constant during the whole day and it is dependent of the heat transfer coefficients applied to the collector. This study is a contribution towards understanding solar updraft power plant performance and control may be useful in the design of solar updraft turbines. Cao [45] studied the solar updraft power plant (SUPP) is a promising technology for the large-scale utilization of solar energy. Due to the significant difference of weather conditions, the performance of SUPPs varies from one place to another, and thus, specific design work is required for different regions. In addition, little effort has been done to evaluate the SUPPs precisely. Also, the configuration size design and techno-economic analysis of commercial SUPPs are carried out for location than to the ambient temperature. The SUPP with higher generation capacity holds better cost-benefit characteristics. Chen [46] in his paper, the chimney is assembled with porous absorber for the indirect mode solar dryer. The thermal conductivity and specific heat capacities have remarkable effects on the average temperature of solar porous absorber in the system. The inclined angle of porous absorber influences the airflow and temperature field in the solar dryer greatly. The mean temperature of the higher aluminous solar absorber is lower and the top temperature of porous absorber delays due to lower thermal conductivity. The higher airflow velocity and the lower temperature at chimney exit can be achieved with the height of solar dryer changing from 1.41 m to 1.81m. Dai [47] analyzed a solar updraft power plant which is expected to provide electric power for remote villages in northwestern China. Three counties in Ning Xia Hui autonomous region, that is, Yinchuan, Pingluo, and Helan, where solar radiation is better than other regions of China, were selected as experimental locations to construct solar power plant. The solar power plant chimney in which the height and diameter of the chimney are 200 m and 10 m, respectively, and the diameter of the solar collector cover is 500 m is able to generate 110-190kW electric power on a monthly average all the year. Some parameters such as chimney height, diameter of the solar collector, ambient temperature, solar irradiance and the efficiency of wind turbine which influence the performance of power generation are also analyzed. Saeed [48] has investigated optimization method for various parameters for configuration of solar updraft power plant. This method used for system optimization and if the output power of the system is maximum while capital cost of the component is minimized. In this paper, design parameters include collector diameter, chimney height and chimney diameter. In addition, effect of variation in design variables on both objective functions is performed. This objective optimization method is very needful and effective for selecting optimal geometrical parameters of solar updraft power plants. The result shows that power output of the plant rise linearly when solar irradiation increases and increase in ambient temperature causes slight decrease in power output of the plant. Al-Kayiem [49]. create a mathematical model to find the following parameters: pressure drop across the turbine, max chimney height, power output, air flow velocity- temperature and the overall efficiency. Hermann [50] has investigated solar updraft power plants numerically using FE software (ANSYS Fluent) and developed CFD code. Analytical laws are verified by considering a large range of scales with the chimney heights between 1 m and 1000 m. Complete time-dependent high-resolution simulations of the flow in the collector and chimney of the model provide detailed insight into the fluid dynamics and heat transfer mechanisms. Both lateral and longitudinal convection rolls are recognized in the collector, indicating the presence of a Rayleigh- Bernard-Poiseuille instability. Local separation is investigated near the chimney inflow. The flow inside the chimney is fully turbulent. Furthermore, the research indicated that large winds and changing ground temperature impacted the movement of air through the chimney. Despite the small amount of data acquired over a few months, Haaf et al was confident that the Manzanares power plant was a success and encouraged the research and development of solar towers. The power plant remained operational for most of the 1980’s and had a maximum power output of 50 kW**.** The data collected from the plant is still used today to validate computational fluid dynamic (CFD) models of solar updraft power plants. Although the solar updraft was constructed in the 1980s, most research on the subject has been done since the early 2000s. One of the first CFD models of a solar updraft power plant was conducted in 2004 by Pastohr [36]. Pastohr et al., carried out an analysis to advance the description of the operation mode and efficiency. The pressure drops at the turbine and the mass flow rate have a significant influence on the efficiency. This can be determined only by coupling of all parts of an upwind power plant. In this study the parts ground, collector, chimney and turbine are modeled together numerically. The basis for all sections is the numerical CFD program FLUENT. This program solves the basic equations of the thermal fluid dynamics, Model improvement and parameter studies essentially arise with this tool. Additional to the calculations using FLUENT a simple model is developed for comparison purposes and parameter studies. The numerical results with FLUENT compare well with the results given by the simple model, therefore, we can use the simple model for parameter studies. The basis for the geometry is the prototype Manzanares. FLUENT was used to create an axisymmetric solar updraft modeled using the Spanish power plant and included two meters of ground thermal storage. Pastohr [36] did not include a radiation model; instead, the authors believed that the radiation from the sun could be modeled as a heat source in a thin layer at the top of the ground. After simulating different levels of solar irradiation, it was concluded that the more energy in the system the higher the velocity of the air moving through the chimney. Pastohr also formulated (and solved) mathematical models based on energy balances on the ground and the collector.

Comparing the FLUENT results to the mathematical results led the authors to the conclusion that a time-dependent simulation needed to be conducted in order for FLUENT to properly calculate the heat transfer from the ground to the air. Xu [51] also created an axisymmetric FLUENT model based on the plant in Manzanares. Using the precedent set by Pastohr et al., a thin heat source was used to model the radiation of the sun. The main difference between the approaches of these two authors was the way the thermal storage was modeled. Pastohr et al., treated the thermal storage as a solid material, while Xu [51] considered the material porous. Xu also included a turbine in his simulation, the turbine was modeled as a pressure drop at the junction between the collector and the chimney. The magnitude of the pressure drop was determined by the theoretical turbine efficiency and power output of the turbine. Xu concluded that energy loss in the system and power output of the turbine are both directly related to the amount of solar radiation and the turbine’s efficiency.

The use of porous material in CFD simulations of a thermal storage layer was first studied by Ming [52]. A solid material only considers conductive heat transfer; however, there is convective, radiative, and conductive heat transfer in a porous media. Comparing different mediums for thermal storage, Ming [52] found that materials, such as gravel, with a higher thermal conductivity, are better suited for a thermal storage layer because a higher ratio of the heat was stored during the day. A study was carried out to determine how the solar radiation impacts the static pressure, velocity magnitude, and the temperatures of the outlet and energy storage layer. Ming [53] have created a mathematical model for mathematical simulations on the solar updraft power plant system coupled with turbine. The system has been categorized into three regions: collector, chimney and turbine, and the heat transfer mathematical models of and flow have been set up for these three regions. Using the prototype as an experimental example, numerical simulation results for the prototype with a three-blade turbine show that the maximum power output of the system is a little higher than 50,000 W. The effect of the turbine speed on the geometrical parameters has been analyzed. Thereafter, design and simulation of a MW-grade solar updraft power plant system with a 5- blade turbine have been presented, and the numerical simulation results show that the power output and turbine efficiency are 10MW and 50%, respectively, which present a reference to the design of large-scale solar updraft power plant systems. It was found that the temperatures and velocity increased with a radiation increase while the pressure decreased. The study helps to gain an understanding of how the Sun's energy powered a solar updraft and impacted the material properties of the air. In the previous studies discussed, researchers did not include a radiation model to calculate the fluid properties in a solar tower power plant**.** Guo [54] performed simulations to determine if a radiation model was necessary to correctly model a solar updraft. It was concluded that the temperature in a chimney system was greater without incorporating a radiation model because the energy losses in the system were not calculated correctly. Guo et al., concluded that the temperature differences between using and not using a radiation model were significant enough that it is necessary to incorporate radiation. After deciding it was necessary to use a radiation model while simulating a solar updraft, the authors went on to study how the magnitude of solar radiation, the turbine pressure drop, and the ambient temperature impacted the system. Guo [54] found that the temperature in the chimney increases when either the solar radiation increased or the pressure drop is increased**;** However, the updraft velocity decreases with an increase in pressure drop. Finally, the authors determined that the ambient temperature had a negligible impact on the system.

Guo [55] observed that in a solar updraft power plant, only a fraction of the available total pressure difference can be used to run the turbine to produce electric power. The optimal ratio of the turbine pressure drops to available total pressure difference in a solar updraft system is investigated using theoretical analysis and 3D numerical simulations. The values found in the literature for the optimal ratio vary between 2/3 and 0.97. In this study, however, the best possible ratio was found to vary with the intensity of solar radiation and to be around 0.9 for the Spanish prototype. In addition, the optimal ratios obtained from the analytical approach are close to those from the numerical simulation and their differences are mainly caused by the neglect of aerodynamic losses coupled with skin friction, flow separation, and secondary flow in the theoretical analysis. This study may be useful for the preliminary estimation of power plant performance and the power-regulating approach selection for solar updraft turbines. A radiation model and the inclusion of a thermal storage system is necessary to develop and accurately model the greenhouse effect in a solar updraft. The greenhouse effect is when the ground absorbs some of the sun's energy and re-radiates it back into the system. The release of heat from the ground is important to keep air circulating in a solar updraft at night.

Gholamalizadeh [56] used the Discrete Ordinates radiation model in FLUENT to simulate the greenhouse effect in a three-dimensional chimney. The authors alter the amount of irradiation focused on the collector and studied how it impacted the temperature and the velocity in the chimney system. It was found that increasing solar irradiation increased the velocity and temperature in the system. By comparing temperature profiles to other authors (e.g., [53, 54]), Gholamalizadeh et al., [56] found that incorporating the greenhouse method greatly altered the profile in the chimney. The following design parameters were selected: collector radius, chimney height, and chimney diameter. Two different solar updraft power plant configurations were considered: The Kerman pilot power plant and Manzanares prototype power plant. A set of possible optimal solutions was obtained. Based on the optimal solution, the best configuration for each power plant was selected. The performance and expenses of the optimal solution and the built power plant were compared. The outcome shows that the increment of power output was higher than the increment of the expenditure in the optimal configuration. A parametric study was conducted to evaluate the effect of changing design parameters on different objective functions. This paper provides very useful design and optimization methodology for solar updraft power plant systems.

Xiao [57] in his work is intended at optimizing the geometry of the major components of the SUPP using a computational fluid dynamics (CFD) software ANSYS -CFX to study and get better the flow characteristics inside the SUPP. The collector inlet opening was varied from 0.05 m to 0.2 m. The collector outlet diameter was also varied from 0.6 m to 1 m. The overall chimney height and the collector diameter of the SUPP were kept constant at 8 m and 10 m correspondingly. These proposed collectors were tested with chimneys of different divergence angles (0°-3°) and different chimney inlet openings of 0.6 m to 1 m. The diameter of the chimney was also varied from 0.25 m to 0.3 m. Based on the CFX computational results; the best arrangement was achieved using the chimney with a divergence angle of 2° and chimney diameter of 0.25 m together with the collector opening of 0.05 m and collector outlet diameter of 1 m. The temperature inside the collector is higher for the lower opening resulting in a higher flow rate and power. Sangi [58] in his study evaluated the performance of solar updraft power plants in some parts of Iran theoretically and to estimate the amount of the produced electric energy. The solar updraft power plant is a simple solar thermal power plant that is capable of converting solar energy into thermal energy in the solar collector. In the second stage, the generated thermal energy is converted into kinetic energy in the chimney and ultimately into electric energy using a combination of wind turbines and a generator. A mathematical model based on the energy balance was developed to estimate the power output of solar updraft s as well as to examine the effect of various ambient conditions and structural dimensions on the power generation. The solar updraft power plant with 350m chimney height and 1000m collector diameter is capable of producing monthly average 1-2MW electric power over a year. Von Backstrom [59] develop computation methods for the pressure drop in extremely high tower, as in solar tower power plants. The methods permit for density and flow area changes with elevation, for wall friction and inner refreshing drag. It presents equations for the vertical density and pressure distributions in expressions of Mach number. One of these is a simplification of the adiabatic pressure lapse ratio equation to include flow at modest Mach numbers. The other is analogous to the hydrostatic relationship between pressure, density, and height, but extends it to small Mach numbers. Its incorporation leads to an accurate value of the average density in the tower. Zhou **[**60**]** in his study, the maximum chimney height for convection avoiding negative buoyancy at the latter chimney and the optimal chimney height for maximum power output is presented and analyzed using a theoretical model validated with the measurements of the only one prototype in Manzanares. Current in a solar updraft power plant that drives turbine generators to generate electricity is driven by buoyancy resulting from higher temperature than the surroundings at different heights. The result based on Manzanares prototype shows that as standard lapse rate of atmospheric temperature is used, the maximum power output of 102,200 W is obtained for the optimal chimney height of 615m, which is lower than the maximum chimney height with a power output of 92300W. Sensitivity analyses are also performed to examine the influence of various lapse rates of atmospheric temperatures and collector radii on maximum height of chimney. The result shows that the maximum height gradually increases with the lapse rate increasing and go to infinity at a value of around $0.0098Km^{-1}$ and that the maximum height for convection and optimal height for maximum power output increase with a large collector radius.

Zhou [61] evaluated the performance of compressible flow through a solar updraft. Developed an accurate numerical model including three-dimensional (3D) steady Navier–Stokes equations in Cartesian coordinate system. This model is validated by comparison with the previous numerical simulated results for one-dimensional compressible flow in a proposed 1500-m-high solar updraft with an inner diameter of 160 m. Results for this 3D numerical model of compressible flow through a solar updraft is more accurate compared to those from the Boussinesq model and full buoyancy model. Normally, an incompressible flow is considered in the Boussinesq model, and enthalpy loss is not included in the energy equation in both the Boussinesq model and full-buoyancy model. Moreover, buoyancy reference density is kept as constant in the energy equation in the full-buoyancy model. The results show that the use of the Boussinesq model and full-buoyancy model with some commercial numerical computational fluid dynamics programs usually result in large errors, and the developed model in this article could give more accurate results than the previous commercial Boussinesq model and full-buoyancy model. The convection was induced by setting constant temperature boundaries on the chimney walls. The temperature difference in the chimney was calculated based on the Rayleigh number. The hot temperature was applied to the ground boundary and low temperature was specified on the collector wall. The chimney boundary was considered adiabatic. It was found that increasing the Rayleigh number increased the airflow through the chimney.

Also, the flow started transitioning from laminar to turbulent in simulations with large Rayleigh numbers. Chergui [62] found turbulence did not fully develop until the Rayleigh number was greater than 10^8.

Tahar [63] expanded on Chergui [62] experiment by changing the inlet boundary condition and the shape of the chimney. Tahar also considered the boundary condition of the chimney wall to be the low temperature in the system. The same conclusions were made by both authors, except Tahar et al., found that turbulence began with Rayleigh numbers as low as 10^5.

Creating an accurate model of a solar updraft power plant using CFD is an important step toward the development of more plants. It has been determined that including a radiation model is important to calculate realistic heat losses in the plant system [55]. Also, it is important to model the system transiently and with a thermal storage layer to most accurately calculate the heat transfer in the ground and with the air. It was found that a porous medium is best for the thermal storage because convective, conductive, and radiative heat transfer is considered [54]. Despite the different models, many of the same conclusions about air flow in a solar tower have been reached. There is a clear connection between the amount of solar irradiation on a plant and the temperature and velocity of the air moving through the tower system [53, 54, 55 and 56]. It was also found that the turbine pressure impacted the airflow in the system. When there were greater pressure drops and the less efficient the turbine, the velocity magnitude in the tower system was lower [53, 55]. While researchers have come a long way in understanding the mechanics of a solar tower power plant thirty-two years, the solar tower continues to be a challenge to model. Despite number trials and research studies that have been done, an accurate CFD model still remains elusive to researchers. Numerical studies using CFD are becoming indispensable computing tools for engineers. The CFD simulation provides insight into the details of how the solar updraft tower works and allows modification and new concepts to be evaluated using a computer simulation. The output of the solar updraft tower can be predicted before the actual plant is being constructed. The simulation also allows engineers to locate and identify problems in the design and further optimize the system before the construction. It is very suitable for large scale products such as the solar updraft tower to be simulated and results to be obtained near to the actual based on the assumptions made. It is impossible to build a large prototype within this kind of scale. Therefore, CFD simulation is the solution. Several researchers have contributed to the construction, numerical simulation of the solar tower collector. Pasumarthi & Sherif have tested two different types of collector which are the extensions of the collector base and also the intermediate absorber is being introduced. The results of the experiment show that the temperature reported is higher than the theoretically predicted temperatures. The results indicate the fact that the experimental temperature reported is the maximum value of the temperature attained inside the solar updraft tower where the theoretical model predicts the bulk air temperature. Schlaich also presented an analytical model of the solar updraft tower system. A boundary layer analysis was performed to determine the pressure differential due to frictional effects and the heat transfer coefficient during turbulent flow between two approximately parallel disc and surface where it applied to the flow at the inlet of the collector of the solar updraft tower collector. A comprehensive analysis of the helio-aero-gravity concept, power production, efficiency, and estimating the cost of the solar tower power plant set up in developing nations was conducted. Padki, Sherif and Pasumarthi et al [52] developed a mathematical model of differential equations to study the effects of various environment and geometry conditions on the heat and flow characteristics and power output. Earlier numerical models had been presented by Backstrom, where tower friction, system turbine, and exit kinetic energy losses were introduced. Other researches also contributed to the improvement of the solar updraft tower numerical analysis by Hedderwick **[**64**]** and Beyers [65**].**

Pretorius and Kroger [66] also evaluated the influence of a developed convective heat transfer equation, a more accurate turbine inlet loss coefficient, various types of soil and quality collector glass roof and the performance of a large-scale solar tower power plant. Bernardes [67] developed a comprehensive analysis of the solar updraft tower both analytical and numerical model to describe the performance of the system based on estimated power output of the solar updraft tower as well as to evaluate the effects of various types of ambient condition and structural dimension of the tower to the power output of the plant. A mathematical model was proposed that could predict the effects of parameter of the solar updraft tower such as tower height, the collector radius and the effects of the solar radiation from the sun, on the relative static pressure, the driving force, the power output and the efficiency of the solar updraft tower. Another simulation study was carried out to investigate the performance of the power generating system based on a developed mathematical model. The simulated power outputs in steady-state were obtained for different global solar radiation intensity, collector area, and tower height. The effects of the solar radiation intensity on the flow of the solar updraft tower were analyzed by Huang [68] where a Boussinesq model was adopted for natural convection, a discrete ordinate radiation model (DO) was employed for radiation and ground under collector cover was seen as a constant inner heat source. Koonsrisuk **[**69**]** compared theoretical models from previous works to study the accuracy of those theoretical models for the prediction of the solar updraft tower performance varying the plant geometry. Computational fluid dynamics (CFD) studies were conducted to compare the results with these theoretical models and found that the results were very well compared with the CFD results and thus were recommended for the prediction of solar updraft tower performance. A numerical model was presented for the process of laminar natural convection in a solar tower. They have focused on airflow and heat transfer inside the system and analyzed the effect of the geometry and Rayleigh number. A mathematical model based on the Navier–Stokes, continuity, and energy equations were developed to describe the solar tower power plant mechanism in detail. Numerical simulation was performed using the CFD software FLUENT that can simulate a two-dimensional axisymmetric model of a solar tower power plant with the standard *k*-epsilon turbulence model [70]. A comprehensive theoretical model had been developed by taking account of the detailed thermal equilibrium equations in the collector, the system driving force and the flow losses based on existing experimental data or formulas for the tower height and collector radius. The effect of the geometric dimensions on the fluid dynamics and heat transfer was investigated. The thermal efficiency of the collector was found to improve with increasing scale, due to an increase in the heat transfer coefficient. The performance evaluation of the solar tower power plant was done by FLUENT software by changing three parameters including collector slope, tower diameter and entrance gap of collector. The results were validated with the solar tower power plant which was constructed in Manzanares. Another numerical research was conducted to study the influence of solar radiation and ambient temperature on the electrical energy produced by a solar tower. The results indicated that the production of electrical energy is closely related to solar radiation and ambient temperature. Up until recently, a mathematical model based on the Navier Stokes, continuity and energy equations were developed to describe the solar updraft power plant mechanism.

The numerical simulation was performed using the CFD software FLUENT that can simulate a two-dimensional axisymmetric model of a solar tower power plant with the standard *k*-epsilon turbulence model and Discrete ordinates irradiation model. Optimizing the geometry of the major components of the solar updraft tower power plant using a computational fluid dynamics (CFD) software ANSYS-CFX was to study and improve the flow characteristics inside the solar updraft tower power plant.

The researches were now mainly to optimize the previous design such as performance evaluation of a solar updraft tower which was carried out based on the parameters such as roof angle, inlet height and for different irradiation values using ANSYS Fluent. A 3D CFD (Computational fluid dynamics) model of a Solar Updraft Tower Power Plant was developed and validated through comparison with the experimental data of the Manzanares plant. Then, it was employed to study the system performance for different locations in Ethiopia. A mathematical model was developed to estimate the performance of SUPP based on tracing solar collector consideration in Manzanares. The objective was to verify the suggested model and to optimize the slope angle of tilted tracking solar collector and the results were promising for implementation in Ethiopia. Lately, Computational Fluid Dynamics modeling was used to calculate the specific parameters, energetic and exergetic efficiencies of the solar updraft tower where the results from experimental and simulation were statistically assessed and very close to the measured data. A model for time-dependent analysis of solar towers was presented. The energy balances for three components of solar towers, absorbing plate, cover glass, and air-gap were considered for plant models. In this article, it will promote new solar renewable energy for reducing the conventional type of power generation and this has motivated us to look for alternative technologies and try to improve existing current system of the solar updraft tower.

(Robera and Abebayehu, 2011); presented the Modeling and Simulation of Solar updraft Power Plant with and without the Effect of Thermal Energy Storage Systems. The main focus of their study was on the economic feasibility of installing energy storage units in the system. The analysis showed that if the total project cost is $2,336,158.18 without the storage unit, the Levelized Cost of electricity will be $0.56 per KWh-1 then adding an investment cost of $56857.57 on energy storage unit will result reduced cost of electricity to $0.24 per KWh^{-1}.

In 2014, (Bisrat and Nigussie Mulugeta) presented the energy-storing effect of the ground and compare the power output of the plants. An unsteady solution for the solar updraft without thermal energy storage system gave an average power of about 14.27 kW for the data provided at Dire Dawa. Irradiation is zero starting from the 19th hour, but the velocity and the power have values greater than zero. This is an indication of the fact that the ground stores energy during day time (maximum solar radiation) and releases it during night (minimum solar radiation). In different journals the effects of collector diameter chimney height and solar irradiation on power output of the plant is presented.

2.3 Gap Analysis on The Previous Work

Many modifications and optimizations can be carried out to convert the simple systems to moderated and obtain the optimum dimensional harmony between the chimney and collector dimensions, compare different sizes and optimize the systems totally. Also, there is a big gap for manufacturing and testing specified turbines for SUPPs.

Many experimental works have been done without any investigation on the turbine which is the main moving part of these systems. Many reports are available on the data of air velocity, temperature, and the ideal output power, neglecting the presence of any turbine.

Among many reports on experimental works, there are only a few reports related to the large-scale solar updrafts, which call for more studies.

The gaps are related to CFD modeling of solar updraft system is lack of variety in the validation references.

Most studies have only focused on optimizing the geometrical parameters and the total size of the SUPP to achieve a higher air mass flow rate. Manipulating and optimizing the plant geometrical dimensions and sizes were common objectives published in most papers which had consequences of high investment cost and increased thermal losses. However, an attempt to naturally induce a higher amount of air-stream into the system has not stated well. Air-vents at the collector's absorber is as an option to induce additional air-stream into the system, thus, increasing the mass flow rate of the working fluid in the greenhouse with respect to the increase in the temperature of the greenhouse.

The possibility of incorporating the thermal storage of SUPP by using the packed-bed absorber increases the heat regenerators during the night time.

CHAPTER THREE

NUMERICAL MODELING OF SOLAR UPDRAFT TOWER POWER PLANT

The study involves identifying existing works carried out on the SUPP technology and develop a mathematical model that can be used in Ethiopia to design SUPP. This entails developing mathematical models for the solar collector, chimney, wind turbine, and wind flow within the chimney. For the solar collector, an analysis of a single and double cover air heater made of glass or plastic and the ground as the backplate will be evaluated in terms of radiative and convective heat transfer as well as the overall loss coefficient, the overall temperature gain within the collector and the heat transfer to the air mass and finally the air movement.

The optimum chimney height, diameter and optimum position of the turbine within the chimney will be determined. Pressure variations in the chimney are critical in establishing air movement and eventually energy output.

A collector can be analyzed by identifying incident radiation on its surface, determining heat transfer and loss coefficients. The air temperature gain in relation to ambient air temperature, air density, and air mass flow rate inside the collector can be determined. The effect of collector height, diameter in-relation to chimney height determines the power output for the power plant. The mathematical model of the SUPP is divided into the subsystem components for conciseness. Power output from SUPP depends on geometric parameters of the plant (the collector and the chimney), and the environmental conditions (ambient temperature, and solar insolation).

3.1. Analytical Modeling

The goal of this work is to determine an appropriate way to model the solar updraft to predict the energy output with a turbine without modeling the actual turbine. The modeling of the turbine can be achieved by specifying a pressure drop that would equate to the actual performance, as reported by Xu et al., [51]. Therefore, the approach here will be to first model the chimney without a turbine load and validate the results with published literature. Then, the turbine load will be modeled and further studies will be presented. Finally, a study on the effects of the turbine will be presented including a way to create a predictive equation for the output. The analyses will be used to determine if it is possible to create an efficient solar updraft power plant while also reducing the tower height.

3.1.1 Maximum Velocity Without Turbine Load

The solar updraft is analyzed to determine the maximum velocity that the air can theoretically travel through the tower due to solar radiation. The tower converts the heat produced by the collector into kinetic energy, therefore, the density difference caused by the increase in temperature within the collector works as the driving force. The air within the tower is lighter than the air at the outlet, which causes buoyancy. Without the turbine, the theoretical power that can be achieved by the flow in the tower, *Ptower*, is defined using the kinetic energy [76]:

$$P = \frac{1}{2} m V^2 \text{ ------------------------------------ } (1)$$

where p is the power, m mass and v is the velocity of the air. The equation based on the pressure difference between the bottom of the tower and ambient air at the tower exit can be expressed as:

$$P_{tower} = \Delta P_t \text{ x } V_{nt} \text{ x } A_t \text{ -------------------------------- } (2)$$

Where, V_{nt} is the velocity at the entrance of the tower and A_t is the cross-sectional area at the exit of the tower. The pressure difference in Equation (2) is expressed as:

$$\Delta P_t = \text{gH} \left(\boldsymbol{\rho_a} - \boldsymbol{\rho_t} \right) \text{ ---------------------------------- } (3)$$

where H is the height of the tower. If Equations (1) and (2) are set equal to each other along with substituting Equation (3) and the **Boussinesq approximation** (3) the form of V_{nt} is:

$$V_{nt} = \sqrt{2gH \frac{\Delta T}{Ta}} \text{ ---------------------------------- } (4)$$

where $\Delta T = T_t - T$a and T_t is the average temperature within the tower. Equation (4) is used to represent the velocity entering the tower without the turbine load and is proportional to the square root of the tower height and temperature difference. The Boussinesq approximation states that the density variation is important in the buoyancy term. The temperature and pressure-dependent density ρ, have been replaced by a constant density ρ_o, except in the body force term representing the buoyancy force. Other approximations used in analysis of fluid flows are those listed as follows.

- ✓ Steady-state vs time-dependent flow
- ✓ Two-dimensional vs three-dimensional flow
- ✓ Incompressible vs compressible flow
- ✓ Inviscid vs viscous flow
- ✓ Hydrostatic vs non-hydrostatic flow
- ✓ Depth-averaged (shallow-water) equations

- ✓ Reynolds-averaged equations (turbulent flow)

3.1.2. Maximum Power Output

The solar updraft is now analyzed to determine the maximum power output due to solar radiation received by the collector. According to Schlaich [10], the power output from the turbine is:

$$P = Q_s\, \eta_{tb}\eta_c\eta_t \text{ ------------------------------------ } (5)$$

where the η variables represent the efficiencies of the turbine, collector, and tower, respectively.

Q_s is amount of energy into the system through the collector from the sun which is written as:

$Q_s = \mathrm{A_c q_s}$ where $\mathrm{A_c}$ is the cross-sectional area of the collector top surface and qs" is the global horizontal solar radiation. Therefore, to solve Equation (5), the efficiencies of the collector and tower are required. The efficiency of the collector represents the energy received by the collector to the total solar radiation to the system.

The collector efficiency is defined as:

$$\eta_c = \frac{Q_c}{Q_s} \text{ ------------------------------------ } (6)$$

where $\dot{Q}c$ is the heat transfer below the collector and expressed as:

$$\dot{\mathrm{Q}}\mathrm{c} = \dot{\mathrm{m}}\mathrm{cp}\ \Delta\mathrm{T} \text{ ------------------------------------ } (7)$$

If Equations (5) and (6) are substituted into (7), the collector efficiency can be calculated as:

$$\eta_c = \rho\, V_{nt}\, A_t C_p \frac{\Delta T}{\mathrm{A_c\ qs}} \text{ ------------------------------ } (8)$$

$$\eta_c = 1.23 \text{ x } 62.1 \text{ x } 78.5 \text{ x } (1006)\ x\ \frac{20}{46735.7\ x\ 5200} = 0.51 = 51\%$$

Where: $\rho_{\mathrm{air}=1.23}$, $\mathrm{A_{chim=78.5}}$, and $\mathrm{C_{p\ air=1006}}$

Equation (8) shows that the temperature difference and cross-sectional area of the tower are inversely related. The efficiency of the tower represents the kinetic energy of air in the tower versus the heat transfer at the base, and therefore, expressed as:

$$\eta_t = \frac{P_t}{Q_t} \text{ ------------------------------------ } (9)$$

Where P_t and Q_t are the power and energy flow rate into the system.

The heat transfer at the base is represented by:

$$\dot{Q}t = \dot{m}\ cp\ \Delta T \text{ ------------------------------ } (10)$$

then the efficiency of the tower is simplified by the equation below.

$$\eta_t = \frac{\mathrm{gH}}{\mathrm{Cp\ Ta}} \text{ ------------------------------ } (11)$$

where the tower efficiency is determined by the height of the tower and ambient air temperature. Theoretically, increasing the tower height increases the tower efficiency, and increasing the ambient temperature decreases tower efficiency.

The relationship for the turbine power output:

$$P_t = \tfrac{1}{2}\pi \ \eta_t \ \rho \ V^3 \ r_t^2 \quad ------------------------------ (12)$$

where tower efficiency is in terms of velocity. According to Haaf et al., [19] for the Spanish prototype, when the peak power output from the turbine is achieved, the vertical air velocity across the turbine is about 0.8 of the maximum velocity without the turbine load. Therefore, Equation (12) can be manipulated by substituting Equation (4) multiplied by 0.8. The resulting equation is:

$$P_t = \tfrac{1}{2}\pi \ \eta_t \ \rho \ (0.8 \text{ x } \sqrt{2gH\frac{\Delta T}{Ta}})^3 \text{ x } r_t^2 \quad ---------------------- (13)$$

where ΔT is the temperature difference without the turbine. In addition, Pastohr et al., [36] used the Betz power limit 16⁄27, to calculate the peak pressure drop. If Equation (13) is multiplied by the Betz limit, the power output of the turbine can be expressed:

$$P_t = \frac{8}{27}\pi \ \eta_t \ \rho \ (0.8 \text{ x } \sqrt{2gH\frac{\Delta T}{Ta}})^3 \text{ x } r_t^2 \quad ---------------------- (14)$$

Equations (12) and (13) are analytical relationships to calculate the maximum power output of a designated solar updraft knowing the tower height and radius and temperature difference without using the actual characteristics of the turbine.

3.2 Solar Collector Design for The Solar Updraft Power Plant System.

The solar updraft collector utilizes solar radiation as fuel to heat a working fluid. The collector comprises a large plate (collector cover) placed at a height above the ground to create an airflow channel. The collector cover function is to transmit the radiant energy received to heat both the ground and flowing ambient air in-between. The heated ground reflects the energy received to increase the radiant of the flowing air. The major component of a solar updraft power station is the solar collector. Solar energy collectors are a special kind of heat exchangers that transform solar radiation energy into internal energy of the transport medium. The collector is the part of the chimney that produces hot air by the greenhouse effect. It has a roof made up of plastic film or glass plastic film. The roof material is stretched horizontally two-meter above the ground (Figure 3.1). The height of the roof increases adjacent to the chimney base so that the air is diverted to the chimney base with **minimum friction loss**. This covering admits the short-wave solar radiation component and retains long-wave radiation from the heated ground. Thus, the ground under the roof heats up and transfers its heat to the air flowing radially above it from the outside to the chimney. The structure of the collector changes to the covering material we used.

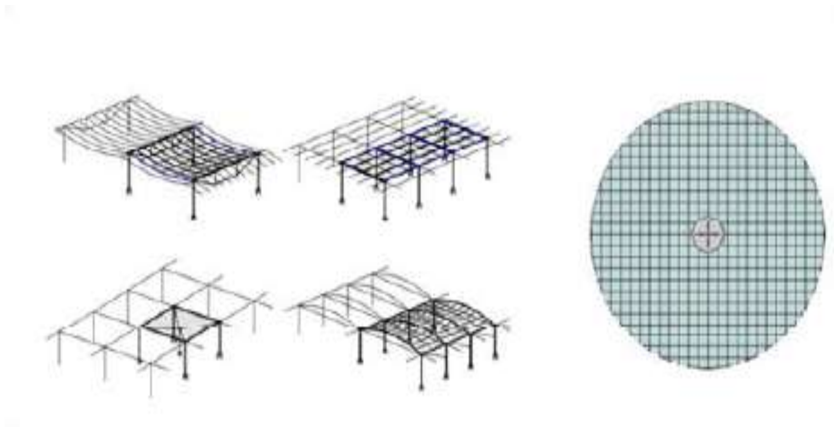

Figure: 3.1 collector design option [54]

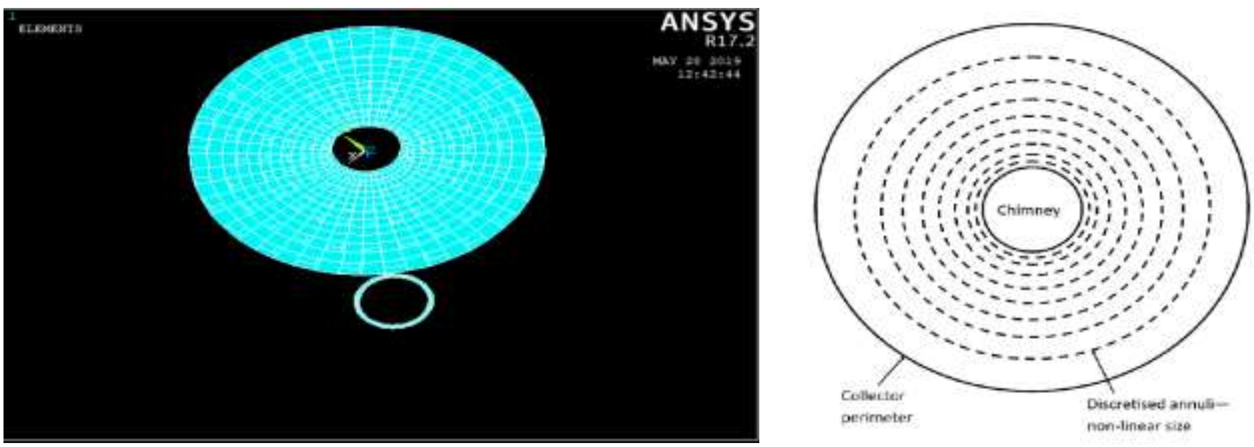

Figure:3.2 a) Solar collector modeled on Ansys b) discretized collector annuli

Collector has a diameter of 244 m and area of a collector is πr^2.

Hence $A_c = 3.14(122)^2 = 46735.7\text{m}^2$.

Updraft tower (chimney) has diameter of 10m and $A_t = \pi r^2 = 3.14 \; x \; 25 = 78.5m^2$

3.2.1 Collector Discretization

The model discretizes the one-dimensional flow path (from the inlet at the collector periphery to the outlet at its center) into a large number of small collector sections. Each discretized section has an inlet and outlet value for each variable, the inlet values being equal to the outlet value of the previous discretized section. Investigations into SUPP performance have shown the largest change in flow variables at low radial values (close to the collector outlet), as the reducing flow area of most canopy profiles causes an increase in flow velocity and a drop in static pressure. Several formulations are available in the literature for the estimation of collector efficiency [72,73]. These formulations define the collector efficiency as a function of the available solar radiation and the temperature difference between the surroundings and the inlet of the chimney. In reality, the associated heat losses via convection and radiation affect the air temperature and, thus, the efficiency of the collector. A recent study by Guo *et al.,* [54] revealed that the efficiency of the solar updraft collectors is overestimated when radiation model is not taken into consideration. This overestimation can introduce errors in the economic feasibility of SUPP and ultimately lead to the wrong conclusion. The figure 3.3 shows the flow of energy and the thermal network of the flat plate collector.

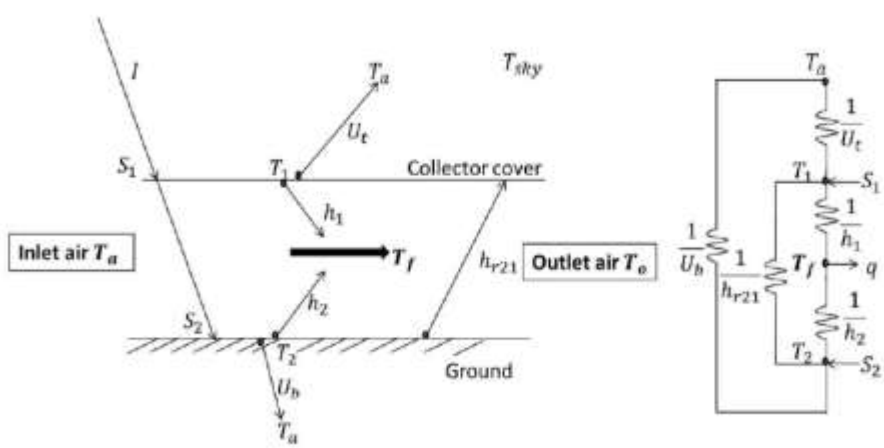

Figure 3.3 Air flow, energy interactions and thermal resistances in the collector [55].

The energy balances in the collector are outlined at the collector cover, for the air flow, and ground absorber, respectively, as:

$$S_1 + h_{r21}\,(T_2 - T_1) + h_1\left(T_f - T_1\right) = U_t(T_1 - T_a) \text{ --------------------- } (15)$$

$$h_1(T_1 - T_f) + h_2\left(T_2 - T_f\right) = q \text{ ------------------------------ } (16)$$

$$S_2 + h_2\left(T_f - T_2\right) + hr_{21}(T_1 - T_2) = U_b(T_2 - T_a) \text{ --------------------- } (17)$$

Where, S_1 is the incident solar radiation in the collector cover, T_2 is the ground temperature, T_1 is the collector cover temperature, T_f is the air flow temperature, S_2 is the solar radiation absorbed by the ground, U_t is the overall heat loss coefficient in the top of the collector cover, U_b is the ground loss coefficient, $hr_{21,}$ h_1 and h_2 are the heat transfer coefficients between the ground and the collector cover, the collector cover and air flowing inside the collector, and the collector cover and air flowing inside the collector, respectively. The complication arising from the heat balance equation presented above is that there is no straight-forward analytical solution for solving the temperatures T_1 , T_2 and T_f since the heat transfer coefficients $hr_{21,}$ h_1, h_2 , Ut and Ub are dependent on them. For this reason, numerical iteration solution is imperative, in which guess temperature values are initially utilized. The equations for calculating the variables which appear in equation are outlined as follows. Incident solar radiation on the collector cover and the ground absorber is given as:

$$S_1 = \alpha_1 \text{ I and } S_2 = \alpha_{2\ I}\tau_1 \text{------------------------} (18)$$

Where α_1 is the absorptivity of the collector cover, I is the available solar radiation, α_2 and τ_1 are the corresponding absorptivity of the ground and transmissivity of the collector cover, respectively. The formulation and procedure for calculating the absorbed and transmitted incident solar radiation are obtained from Duffie and Beckman [75]. Additionally, the overall heat loss coefficient in the top of the collector cover U_t is obtained as:

$$U_t = h_w + h_{rs} \text{--------------------------------} (19)$$

where the wind convective heat transfer, h_w and h_{rs} the radiation heat transfer coefficient between the collector cover and the sky are respectively, as follows:

$$h_{w=} \ 5.67 + 3.86\,(V) \text{------------------------------} (20)$$

$$h_{rs} = \frac{\sigma\varepsilon_1(T_{sky}+T_1)(T^2{}_{sky}+T^2{}_1)(T_1-T_{sky})}{(T_1-T_a)} \text{------------------} (21)$$

Where (V) is site location wind speed and ε is the emissivity of the collector cover, T_{sky} is the sky temperature expressed as:

$$T_{sky} = 0.0552(T_a)^{1.5} \ [74] \text{-----------------------------} (22)$$

The radiation heat transfer coefficient between the cover and the ground absorber can be estimated by:

$$hr_{21} = \frac{\sigma\ (T_2 + T_1)(T^2{}_2 + T^2{}_1)}{\frac{1}{\varepsilon_2} + \frac{1}{\varepsilon_{1-1}}} ------------------------(23)$$

The free convection heat transfer coefficient between the collector cover and the air flow h_1, and that between the absorber plate and the air flow h_2, are found using:

$$h_k = Nu\ \frac{k_{air}}{Dh}\ \text{for k= 1,2}\ ----------------------------(24)$$

In the equation, Nu is Nusselt number, k_{air} is thermal conductivity of the air. For the circular shaped collector with diameter D_c and height H_c, the hydraulic diameter D_h is calculated as:

$$D_h = \frac{2\ (\pi D_c\ x\ H_c)}{(\pi D_c + H_c)} --------------------------------(25)$$

For solar updraft power plants where $H_c << D(c\ )/2$, Bernardes *et al.*, [67] and Larbi *et al.*, [29] used the approximation $D_c = 2H_c$.

3.2.2 Incident radiation on the collector

The solar updraft technology is dependent on the solar radiation incident on the collector. Therefore, it follows that the number of daylight hours for a place has a bearing on the performance of the plant. Duffie and Beckman 2013 [75] showed that the monthly average extra-terrestrial radiation on a surface is given by:

$$Ho = 24\ x\ 3600 Gsc\ /\Pi\ (1+0.033\cos 360n\ /365x\ (\cos\Phi\cos\delta\cos ws + \ \Pi ws\ /180\sin\Phi\sin\delta)) ---(26)$$

Where Φ is the latitude, n is the day number and δ is the declination angle which is given by:

$$\delta = 23.45\ \sin\ (360\ x\ \frac{284+n}{365}) ----------------------------(27)$$

Where n the average day of the year, Taking July 17th as the average day of the month day, n = 198, $\delta = 23.45\ \sin\ (360\ x\ \frac{284+198}{365} = 21.2^o$

The mathematical model uses the average day of the month to compute the declination angle. The average day for the month is defined by Duffie and Beckman 2013 [75] as shown below:

Table 3.1: Average day for each month (Duffie and Beckman)

Month	Date	Average Day n
January	17	17
February	16	47
March	16	75
April	15	105
May	15	135
June	11	162
July	17	198
August	16	228
September	15	258
October	15	288
November	14	318
December	10	344

The hour angle (Ws) which defines the displacement of the sun east or west of the local meridian with each hour traversing 15^o, was used to determine when the sun rises and sets.

And $ws\ is\ the\ sunset\ hour\ angle = \cos^{-1}(-\tan\Phi\tan\delta)$ ------------------ (28)

From equation (28), the sunset hour angle:

$w_S = \cos^{-1}(-\tan 8.33 \tan 21.2) = 93.2^o$

The monthly average extraterrestrial radiation, from equation (26)

$H_o = 24 \text{ x } 3600G/\pi\ (1 + 0.033 cos 360n/365) \times (cos\emptyset cos\delta sin\ ws + \pi ws/180 \text{ x } \sin\phi\ sin\delta))$

$H_o = 24\times3600\times1367/\pi\ (1 + 0.033 cos 360\times198/365) \times cos 8.33 \times cos 21.2 \times sin\ 93.2 + \pi\times 93.2/180 \sin 8.33 \times sin 21.2$

$= 37595198.69\ (0.968167732)\ (0.92840034 + 0.049549809)$

$H_o = 37595198.69\ (0.968167732)\ (0.977950149)$

$H_o = 30.60 MJ/m^2$

The monthly average daily solar clearness index is determined as follows,

$$K_T = \frac{H}{H_o} \qquad (29)$$

3.2.3 Collector energy balance

The collector is composed of soil as a system of heat storage, a transparent surface located a few meters above the ground and a field of air circulation. This one opened at the two ends, recovers incidental solar energy while heating and containing the air which circulates there. The air is heated by the absorption of the solar flow, which crosses the transparent upper surface of the collector. It circulates within the collector subjected to phenomena of convection. For simplicity, theoretical investigations have considered that the energy equation balance of the collector is given by:

$$Q = mC_p\,\Delta T = \tau\alpha\, A_c G - h_{conv}\,\Delta\, T_a\, A_c \qquad (30)$$

Where *m* denotes the mass flow rate of air passing in the solar collector and which is expressed by:

$m = \rho\, A_2\, V_2$ and velocity at the exit of the collector can be given by:

$$V = \frac{\tau\alpha\, A_c G - h_{conv}\,\Delta\, T_a\, A_c}{\rho A_2 C_p\,\Delta\, T} \qquad (31)$$

Where *G*=solar radiation; *A*coll=collector area; Q =heat output of warm air; *Cp*=specific heat capacity of air; $\tau\alpha$ =transmittance-absorptance product, a=ambient, ρ=air density

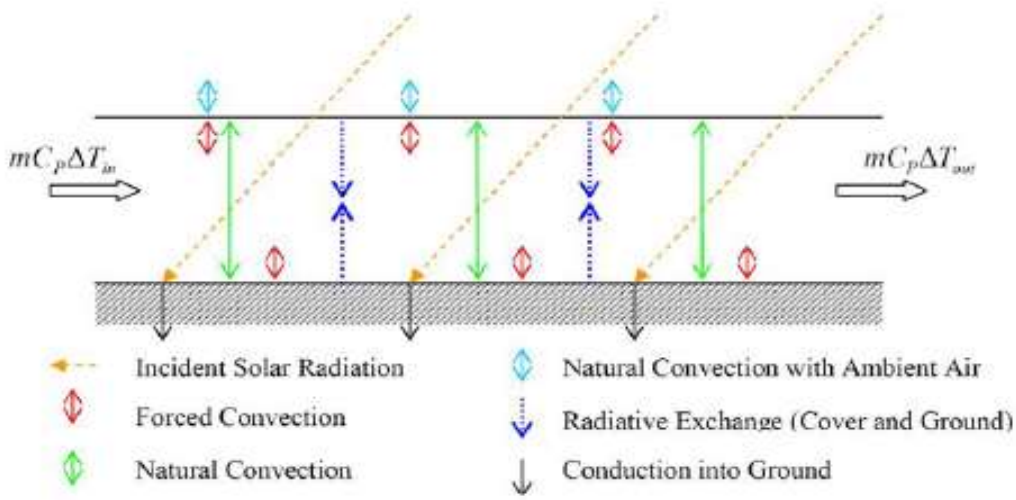

Figure 3.4: collector thermal energy balance scheme [19]

Theoretical analysis of the collectors

a) The temperature of the air inside the collector during the night (Tf)

The temperature of the air inside the collector can be written as follows:

$$T_f = T_{pm} - T_a \qquad (32)$$

b) Collector efficiency factor(F′)

Collector efficiency factor is the ratio of the actual thermal collector power to the power of an ideal collector whose absorber temperature is equal to the fluid temperature.

c) The amount of heat stored by the pebble

The amount of heat stored from pebble is found from (Antia and Etuk, 2017)

$$Q_s = M_s \; x \; C_{ps} \; x \; T_{pb} \text{---------------------------} (33)$$

The from the design specification the heat stored by the pebble is equal to 75% heat from the sun radiation incident on the absorber plate. Again, using the equation of (Antia and Etuk, 2017) the heat stored can be rewritten as follows.

$$Q_s = qA_{abs-surf} \; x \; 0.75 \; x \; t_{exposed} \; to \; sun \; light \text{--------------------} (34)$$

The re arranging eq (33) and eq (34), the temperature of the pebble can be found as:

$$\mathrm{T_{pb}} = \frac{\mathrm{qA_{abs-surf}\ x\ 0.75\ x\ t_{exposed}\ to\ sun\ light}}{\mathrm{M_s C_{ps}}} \text{--------------------} (35)$$

Solar intensity reaching the pebble is written as:

$$q_b = G(\tau\alpha) \text{-----------------------------------} (36)$$

d) The amount of heat gained by the pebble (Antia and Etuk, 2017)

$$\mathrm{Q_{gain}} = \mathrm{M_s\ x\ Cp_s}\left(\mathrm{T_{pb}} - \mathrm{T_a}\right) \text{----------------------------} (37)$$

a). Heat gain per second for pebble bed storage

The amount of heat gain per second for the storage material is found from the following equation (Antia and Etuk, 2017)

$$\mathrm{Q_{charged}} = \frac{\text{Heat gained by the pebble (KJ)}}{\text{Average sun-shine hours(sec)}} = \mathrm{M_s Cp_s}\left(\mathrm{T_{pb}} - \mathrm{T_1}\right) \text{---------} (38)$$

b). Heat discharged per second pebble bed storage

The amount of heat discharged to the air from heat stored in the pebble is found from (Antia and Etuk, 2017)

$$\mathrm{Q_{discharged}} = \frac{\text{Heat stored in a pebble (Qs in KJ)}}{\text{Required discharged time (sec)}} = \frac{\mathrm{M_s C_{ps} T_{pb}}}{\mathrm{t_{req}}} \text{-----------------} (39)$$

Note: For this design, the rate of heat discharge only occurs during the night time when the ambient temperature drops down drastically following the sun radiation.

c). Heat gain by the air from the thermal storage during the night.

Then the heat gain by the pebble is calculated using**,** (Antia and Etuk, 2017)

$$\mathrm{Q_{air}} = \mathrm{mC_p}\ (\mathrm{T_f} - \mathrm{T_a}) \text{------------------------------} (40)$$

In the glazing the heat transfer modes are listed as follows:

i. Radiation heat transfer from glazing to ambient
ii. Convection heat transfer from glazing to airstream
iii. Radiation heat transfer from ground to glazing
iv. Radiation heat transfer from absorber plate to glazing

3.2.4 Collector Inlet Pressure Drop

Due to its acceleration and a loss at the collector inlet, the pressure decreases as the air is drawn towards the collector. And this collector inlet pressure drops and total pressure outside the collector inlet is Pa.

$$\Delta P_i = \rho_i {V_i}^2\ K_i + \rho_i {V^2}_i \text{------------------------------} (41)$$

Where i refer inlet to collector and *K* is static pressure correction factor. In this case Value of the loss coefficient is approximately zero for a well-rounded inlet while a value of unit is more approximate for the case of the sharp-edged inlet. Since the inlet pressure drop is smaller than the total pressure drops any possible error in this approximation will be negligible

3.2.5 Collector Drag Pressure Drop

There are collector supports for the collector roof above the surface of the ground. These are positioned as shown in the Figure 3.5 on radii with a radial pitch pr and spaced tangentially on these radii pt apart. And those collector supports produces drag force that causes radial pressure gradient on the air in the collector and we can find this pressure gradient by considering the force exerted by each support on the air

$$F_{SD} = ½\ C_{SD}\ d_S\ \rho V2 \text{------------------------------} (42)$$

Where V is the local free stream velocity with H is the height of the collector at radius r and m is the mass flow rate.

$$V = m/(2\rho\pi rH) \text{------------------------------} (43)$$

$$F_{SD} = \frac{CSD}{8\pi^2}\left(\frac{ds}{H}\right)\frac{m^2}{\rho r^2} \text{------------------------------} (44)$$

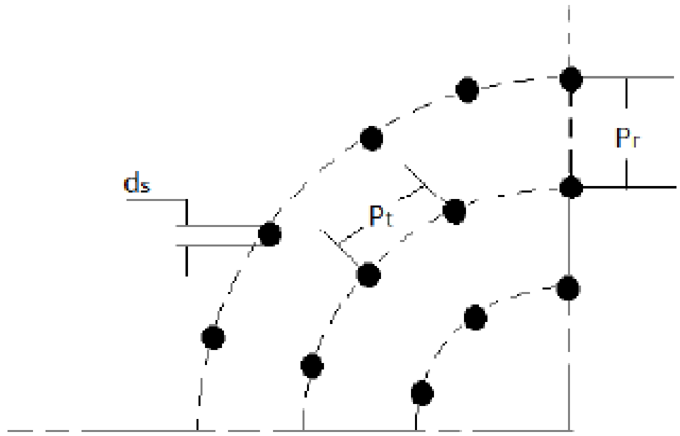

Figure 3.5 Schematic Plan View of the Position of the Collector Supports [37].

The number of supports along the circumference at radius r is given by equation (45) with a tangential pitch.

$$n_{st} = \frac{2\,\pi\, r}{P_t} \quad (45)$$

The force required to move air is thus given by the equation below:

$$F_{SrD} = F_{BD} n_{st} = \frac{C_{SD} m^2 d_s}{4\pi r P_t H\, \rho} \quad (46)$$

This is the force required by the air to move radially inwards through one row of supports. The resultants corresponding pressure difference required is thus given by:

$$\Delta P_s = \frac{F_{srd}}{2\pi\, rH} = \frac{C_{SD}\, m^2 d_s}{8\pi^{\,2} \rho\, P_t H^2 r^2} \quad (47)$$

3.2.6 Overall Loss Coefficient and Heat Transfer Correlations

It is convenient from the point of view of analysis to express the heat lost from the collector in terms of an overall loss coefficient defied by the equation.

$$\dot{Q}_L = U_L A_L (T_{pm} - T_a) \quad (48)$$

Where: UL = overall loss coefficient

AC = area of the collector

Tpm = average temperature of the absorber plate and Ta = temperature of surrounding air (assumed to be the same on all sides of the collector).

The heat lost from the collector is the sum of the heat lost from the top, the bottom and the sides. Thus,

$$\dot{Q}_L = \dot{Q}_t + \dot{Q}_b + \dot{Q}_s \quad (49)$$

Where $\dot{Q}_t$ = rate at which heat is lost from the top

$\dot{Q}_b$ = rate at which heat is lost from the bottom and $\dot{Q}_s$ = rate at which heat is lost from the sides

Each of these loses is also expressed in terms of coefficients called the top loss coefficient, the bottom loss coefficient and the side loss coefficient and defined by the equations:

$$\dot{Q}_t = U_t A_c (T_{pm} - T_a) \text{------------------------------} (50)$$

$$\dot{Q}_b = U_b A_c (T_{pm} - T_a) \text{------------------------------} (51)$$

$$\dot{Q}_s = U_s A_c (T_{pm} - T_a) \text{------------------------------} (52)$$

Each of the losses can be described briefly in the following form.

1) Top Loss Coefficient

The top loss coefficient Ut is evaluated by considering convection and re-radiation losses from the absorber plate in the upward direction. For the purpose of calculation, it is assumed that the transparent cover and the absorber plate constitute a system of infinite parallel surfaces and that the flow of heat is one- dimensional and steady (Hottel and Woertz). It is further assumed that the temperature drop across the thickness of the cover is negligible and that the interaction between the incoming solar radiation absorbed by the cover and the outgoing lose may be neglected. The outgoing re-radiation is of long wavelengths. For these wavelengths, the transparent cover will be assumed to be almost opaque.

Convective Heat Transfer Coefficient

a) From the plate to the cover

For the prediction of the top loss coefficient, the evaluation of natural convection heat transfer between two parallel plates tilted at some angle to the horizontal is of obvious importance. The natural convection heat transfer coefficient h1c is related to three dimensionless parameters, the Nusselt number Nu, the Rayleigh number Ra, and the Prandtl number Pr, that are given by:

$$N_u = \frac{h_{1c} L}{K}, \quad R_a = \frac{g \beta_v \nabla T L^3}{v \alpha}, \quad P_r = \frac{v}{\alpha} \text{--------------------------} (53)$$

Where: L is the plate spacing,

g is the gravitational constant, ΔT is Temperature difference between the plate and the glass, and

β v, is the volumetric coefficient of expansion of air.

b**)** From the Glazing cover to the ambient

The convective heat transfer coefficient (h2c) at the glass cover is calculated from the following empirical correlation.

$$h_{2c} = 5.7 + 3.8V \text{------------------------------} (54)$$

Where: h_{2c} is in W/m2 k, and V is the wind speed in m/s.

Radiative Heat Transfer Coefficient

a) From the plate to the cover

The radiative heat transfer coefficient from the plate to the glass cover is expressed as:

$$h_{1r} = \varepsilon_{eff}\sigma\left\{\frac{(T_p+273)^4-(T_g+273)^4)}{T_p-T_g}\right\} \text{-----------------------------} (55)$$

The effective emissive of plate-glazing is given by the equation (56)

$$\varepsilon_{eff} = \left[\frac{1}{\varepsilon_p}+\frac{1}{\varepsilon_g}-1\right]^{-1} \text{-------------------------------} (56)$$

b) From the Glazing Cover to the ambient

Sky Temperature

The effective temperature of the sky is usually calculated from the following simple empirical relation in which temperatures are expressed in Kelvin.

$$T_{sky=}\ T_a - 6 \text{----------------------------------} (57)$$

The radiative heat transfer coefficient from the glass cover to the ambient is expressed as:

$$h_{2r} = \varepsilon_g\sigma\left\{\frac{(T_g+273)^4-(T_{sky}+273)^4)}{T_g-T_a}\right\} \text{-----------------------------} (58)$$

The total heat transfer coefficient from collector plate to cover h1 is expressed as:

$$h_1 = h_{1c} + h_{1r}$$

The total heat transfer coefficient from the cover to ambient h2 is expressed as:

$$h_2 = h_{2c} + h_{2r}$$

The effective heat transfer coefficient from plate to ambient (i.e. the top loss coefficient) is given by:

$$U_t = \left[\frac{1}{h_1}+\frac{1}{h_2}\right]^{-1} \text{-----------------------------------} (59)$$

2) Bottom Loss Coefficient

The bottom loss coefficient Ub is evaluated by considering conduction and convection losses from the absorber plate in the downward direction through the bottom of the collector. It will be assumed that the flow of heat is one dimensional and steady. In most cases, the thickness of insulation provided is such that the thermal resistance associated with conduction dominates. Thus, neglecting the convective resistance at the bottom surface of the collector casing, we have:

$$U_b = \frac{K_i}{\delta_b} \text{-------------------------------------} (60)$$

Where: K_i = thermal conductivity of the insulation and δ_b = back insulation thickness

3) Side Loss Coefficient

As in the case of the bottom loss coefficient, it will be assumed that the conduction resistance dominates and that the flow of heat is one-dimensional and steady. The one-dimensional approximation can be justified on the grounds that the side loss coefficient is always much smaller than the top loss coefficient.

$$U_s = \frac{A_1}{A_c}\frac{K_i}{\delta_e} ------------------------------------(61)$$

Where: $A_1 = Pd_e$

P = perimeter of the absorber plate, de = height of the edge, δ e = edge insulation thickness.

4) Overall Heat Loss Coefficient

The overall heat loss coefficient UL is the sum of the top, bottom and edge loss coefficient. That is:

$$U_L = U_t + U_b + U_s ---------------------------------(62)$$

5) Thermal Analysis of Flat Plate Collector and Useful Heat Gained by the Fluid

The procedure for calculating the overall loss coefficient is described in the above section. If the average plate temperature or mean plate temperature Tpm is known, then the heat lost from the collector can be calculated. Tpm can be related to the value of the inlet fluid temperature T_{fi} by considering the flow of heat in the absorber plate and across the fluid tubes to the fluid. In order to simplify the problem, a number of one-dimensional analyses will be conducted. The one-dimensional flow of heat in the absorber plate in the direction of fluid will be first considered, and then it will be followed by a consideration of the heat flow from the plate to the fluid across the tube wall. Finally, the one-dimensional heat transport inside the tube will be considered.

6) ***Collector Efficiency Factor***

The collector efficiency factor, ' F, represents the ratio of the actual useful heat collection rate to the useful heat collection rate when the collector absorber plate (Tp) is at the local fluid temperature (Tf).

7) Useful Heat Gained by the Fluid

The performance of a flat-plate solar collector can be described by the useful gain from the collector per unit time of a collector area Ac and it is the difference between the absorbed solar radiation and the thermal loss or the useful energy output of a collector.

$$\dot{Q_u} = A_c\dot{q_u} = A_c\left[\dot{q_{ab}} - U_L\,(T_p - T_a)\right] -------------------------(63)$$

Where: $q_{ab} = (\dot{\tau_o}\alpha_o)I_{T(t)}$ $--------------------------------(64)$

τo and α o are the transmissivity of the glass cover and the absorptivity of the absorber respectively.

8) Collector Heat Removal Factor

It is an important design parameter since it is a measure of the thermal resistance encountered by the absorbed solar radiation in reaching the collector fluid. It represents the ratio of the actual useful heat gain rate to the gain which would occur if the collector absorber plate was at the temperature T_{fi} everywhere. Its value will range between 0 and 1. The total useful energy collection rate $\dot{Q}_u$ may be expressed as:

$$Q_u = \dot{m}C_p(T_{fo} - T_{fi}) ---------------------------- (65)$$

Substitution of T_{fo} gives:

$$Q_u = A_c F_R[\dot{q_{ab}} - U_L(T_{fi} - T_a)] ------------------------ (66)$$

And collector heat removal factor can be expressed as follows:

$$F_R = \left[\frac{\dot{m}C_p}{A_c U_L}\right]\left[1 - e^{\frac{A_c U_L \dot{F}}{\dot{m}C_p}}\right] ---------------------------- (67)$$

Where: FR is the heat removal factor of the collector. Physically the collector heat removal factor is equivalent to the effectiveness of a conventional heat exchanger.

9) Effects of Various Parameters on Collector Performance

A large number of parameters influence the performance of flat-plate collector.

These parameters could be classified as:

- ✓ Design parameters,
- ✓ Operational parameters,
- ✓ Meteorological parameters, and
- ✓ Environmental parameters

9.1) Effects of Design Parameters

a) Selective Absorber coatings

An ideal selective coating is one that is a perfect absorber of solar radiation while being a perfect reflector of thermal radiation. Such a coating will make a surface, a poor emitter of thermal radiation. Hence a selective coating increases the temperature of an absorbing surface. Absorber plate surface which exhibit the characteristics of a high value of absorptivity for incoming solar radiation and a low value of emissivity for out-going re-radiation are called selective surfaces. Such surfaces are desirable because they maximize the absorption of solar energy and minimize the emission of the radiative losses. A large number of non-selective coatings are available and are in widespread use as flat-plate collector coatings. These are primarily organic coatings such as flat black coatings. Most of these coatings have absorptances exceeding 0.95 and emittances of 0.90-0.95.

b) Number of Covers

The number of covers (glazing) used in a collector is usually one or two. As the number of covers increases the value of τα decrease. Thus, the flux $\dot{q_{ab}} = (\tau\alpha)I(t)$ absorbed in the absorber plate decreases. The addition of more covers also causes the value of Ut, and hence the heat loss, to decrease. However, the amount of decrease is not the same in both cases. For this reason, the efficiency goes through a maximum. This kind of result is obtained with all collectors, a maximum efficiency being usually obtained with one or two covers. Since the flat-plate collectors currently available in our country are single glass this design is based on this parameter.

c) Spacing

The proper spacing has to be kept between the absorber plate and the cover. From the point of view of the heat loss from the top, it is evident that the spacing must be such that the values of the convective heat transfer coefficients are minimized.

d)Effect of Shading

The main problem associated with the use of larger spacing is that Shading of the absorber plate by the side walls of the collector casing increases. Whenever the angle of incidence is not normal, some of the structure will intercept the solar radiation. Some of this radiation will be reflected to the absorbing plate if the side walls are of a high reflectance material. Some shading always occurs in every collector and needs to be corrected for. The shading is particularly important in the early morning and late evening hours. It is estimated that for most designs using spacing of 2 to 5 cm between the cover and the plate, shading reduces the radiation absorbed by about 3 percent (RAI, G.D, 2001).

3.2.7 Transient Analysis of Flat Plate Solar Collector Using Finite Difference Method

In order to obtain the appropriate heat power for a particular installation of a flat plate solar collector, knowledge about the collector operating parameters is necessary. These parameters (e.g. the temperature of the working fluid at the collector outlet) depend on the level of sun exposure, and thus they are variable. The solar collector works under transient conditions. In this section, the mathematical model used to simulate the dynamic behavior of liquid flat plate collectors is developed. The collector is divided in to five nodes (cover, air gap, absorber, fluid, and insulation) perpendicular to the flow direction. For each node, the equation describing the energy balance is derived. The derived differential equations are solved using the explicit finite-difference method. All the thermo-physical properties of the operating fluid, absorber, air gap, glass and insulation can be considered as constant. The transient temperatures are evaluated iteratively, using relations derived for the equation of energy balance for each node.

i. Single Glass Cover

$$\mathrm{C_g \rho_g V_g \frac{dT_g}{dt}} = \left[\mathrm{h_2(T_a - T_g) + hr1(F(T_p - T_g) + hc1(T_{ag} - T_g) + \alpha IT}\right]\mathrm{w\Delta y} - - - - - - - - (68)$$

Where, h2 =hc2 +hr1

ii. Air Gap between Glass Cover and Absorber

$$\mathrm{C_{ag}\rho_{ag}V_{ag}}\frac{dT_{ag}}{\mathrm{dt}} = \left[hc1F\left(T_p - T_{ag}\right) + hc1(T_g - T_{ag})w\Delta y\right] - - - - - - - - - - - - - - - (69)$$

iii. Absorber

$$C_p\rho_pV_p\frac{dT_p}{dt} = \left[hr1\left(T_g - F\left(T_p\right)\right) + hc1(T_{ag} - F\left(T_p\right) + \alpha\tau IT + k_{ins}\delta_{ins}(T_{ins} - F(T_p)\right]w\Delta y + \pi Dihfi\Delta y\left(T_f - FT_p\right) - (70)$$

iv. Working Fluid

$$C_f\rho_fA\frac{dT_f}{dt} = \pi Dihfi(F\left(TP - T_f\right) - \dot{m}_fC_f\frac{dT_f}{dy} - (71)$$

Where, A= $\frac{\pi Di^2}{4}$

v. Insulation

$$\mathrm{C_{ins}\rho_{ins}V_{ins}\frac{dT_{ins}}{dt}} = \mathrm{[k_{ins}\sigma_{ins}(FTP - T_{ins}) + hc2(T_a - T_{ins})]w\Delta y} - - - - - - - - - - - - - (72)$$

The explicit finite-difference method is proposed to solve the system of equations. The time derivatives are replaced by a forward difference scheme, whereas the dimensional derivative is replaced by a backward difference scheme.

$$\frac{dT_g}{dt} = T_{g,jt+\Delta t} - T_{g,jt\Delta t} - (73)$$

$$\frac{dT_{ag}}{dt} = T_{ag,jt+\Delta t} - T_{ag,jt\Delta t} - (74)$$

$$\frac{dT_p}{dt} = T_{p,jt+\Delta t} - T_{p,jt\Delta t} - (75)$$

$$\frac{dT_{ins}}{dt} = T_{ins,jt+\Delta t} - T_{ins,jt\Delta t} ---------------------------(76)$$

$$\frac{dT_f}{dt} = T_{f,jt+\Delta t} - T_{f,jt\Delta t} --------------------------- \quad (77)$$

$$\frac{dT_f}{dy} = T_{f,jt+\Delta t} - T_{f,j-1t} + \Delta t \Delta y ------------------------(78)$$

$$\frac{dT_a}{dt} = T_{a,jt+\Delta t} - T_{a,jt\Delta t} ---------------------------(79)$$

After some transformations, the following formulae were obtained:

For the glass cover,

$$Tg,jt+\Delta t = EE * \Delta t * Tg,jt + BB * \Delta t * Ta,jt + CC * F * \Delta t * Tp,jt + DD * \Delta t * Tag,jt + GG * \Delta t * ITt ------------------------------------(80)$$

For the air gap,

$$Tag, jt+\Delta t = (1 - 2 * HH * \Delta t)\, Tag, jt + HH * \Delta t * Tg, jt + HH * F * \Delta t * Tp, jt ------ \ (81)$$

For the plate (absorber),

$$Tp, jt+\Delta t = (1 - OO * F * \Delta t)\, Tp, jt + NN * \Delta t * ITt + JJ * \Delta t * Tg, jt + KK * \Delta t * Tag, jt + LL * \Delta t * Tins, jt + MM * \Delta t * Tf, jt ---------------------------(82)$$

For the working fluid,

$$Tf, jt+\Delta t = (1 - PP * \Delta t - \Delta y)\, Tf, jt + PP * F * \Delta t * Tp, jt + \Delta y * Tf, j{-}1t -------- \ (83)$$

For the insulation,

$$Tins, jt+\Delta t = (1 - SS * \Delta t)\, Tins, jt + QQ * F * \Delta t * Tp, jt + RR * \Delta t * Ta, jt -------- \ (84)$$

Where, T is for temperature, the abbreviations g, ag, p, f, and ins are for the glass, air gap, plate (absorber), working fluid and insulation respectively. Di is for the internal diameter of the tube, F

is for the fin efficiency of the absorber plate, t is the time, Δt is the time increment, C is for the specific heat capacity, ρ is for the density, k is for thermal conductivity, α is the thermal absorptivity of plate, τ is the thermal transmissivity of the glass, δ is for the thickness, $\dot{m}$ is for the mass flow rate, N is the number of nodes in the flow direction, and V is for the volume.

Divide the length of the tube in to 10 number of points with the interval of 0.2 m length shows 11 nodes from inlet to the outlet in the above equations:

$$BB = \frac{h_2}{\rho_g C_g \delta_g} \text{-------------------------------} \quad (85)$$

$$CC = \frac{h_{r1}}{\rho_g C_g \delta_g} \text{-------------------------------} \quad (86)$$

$$DD = \frac{h_{c1}}{\rho_g C_g \delta_g} \text{-------------------------------} \quad (87)$$

$$\mathrm{EE} = 1 - (\mathrm{BB} + \mathrm{CC} + \mathrm{DD}) \text{--------------------------} \quad (88)$$

$$GG = \frac{\alpha}{\rho_g C_g \delta_g} \text{-------------------------------} \quad (89)$$

$$HH = \frac{h_{c1}}{\rho_{ag} Ca_g \delta_{ag}} \text{-----------------------------} (90)$$

$$JJ = \frac{h_{r1}}{\rho_p C_p \delta_p} \text{-------------------------------} (91)$$

$$KK = \frac{h_{c1}}{\rho_p C_p \delta_p} \text{-------------------------------} \quad (92)$$

$$LL = \frac{k_{ins}}{\rho_p C_p \delta_p \delta_{ins}} \text{-----------------------------} (93)$$

$$MM = \frac{\pi Dihfi}{\rho_p C_p \delta_p w} \text{-----------------------------} \quad (94)$$

$$NN = \frac{\alpha\tau}{\rho_p C_p \delta_p} \text{-------------------------------} \quad (95)$$

$$\mathrm{OO} = \mathrm{JJ} + \mathrm{KK} + \mathrm{LL} + \mathrm{MM} \text{-------------------------} \quad (96)$$

$$PP = \frac{\pi Dihfi}{\rho_f C_f A} \text{-------------------------------} \quad (97)$$

$$QQ = \frac{k_{ins}}{\rho_{ins} C_{ins} \delta ins^2} \text{-----------------------------} \quad (98)$$

$$RR = \frac{h_{c2}}{\rho_{ins} C_{ins} \delta_p \delta_{ins}} \text{-----------------------------} \quad (99)$$

$$SS = QQ + RR \text{-------------------------------} \quad (100)$$

Initial conditions (At time equal to zero (at 12:00 PM)):

The heat transfer fluid is at a temperature of 66℃.

$Tfat\ j$ (0) = 339.15 K

The glazing and insulation materials maintain an ambient temperature.

$Tfat\ j$ (0) = 298.15 K

The plate temperature equals to ambient temperature plus ten degree Celsius.

$Tfat\ j$ (0) = 308.15 K

The air gap temperature between plate and glazing equals average of plate and glazing temperature.

$Tfat\ j$ (0) = 303.15 K

3.3. Design of thermal energy storage for solar updraft power plant

Using an energy storage system in a solar thermal power plant has many advantages: higher annual solar contribution, reduction of part-load operation, power management and buffer storage [78]. The energy storage system has the function of a buffer during the day as the solar irradiation onto the earth's surface varies with time (e.g. night and day, seasonal changes, diurnal variation, and weather) [79]. With the aid of the storage the security of the energy supply is increased. A solar thermal power plant without an energy storage system can therefore only operate between sunrise and sunset unless it is hybridized. Hence either an energy storage system and/or fossil cofiring should be integrated into the plant.

3.3.1 Selection of Thermal energy Storage Mechanism and Media

From a technical point of view, the crucial requirements while selecting a storage medium are [83]:

- ✓ The high energy density (per-unit mass or per-unit volume) in the storage material
- ✓ Mechanical and chemical stability of storage material/media
- ✓ Compatibility between the storage medium and other materials
- ✓ Complete reversibility for a large number of charging/discharging cycles or prolonged use
- ✓ Minimized thermal losses
- ✓ Ease of control

3.3.2 Thermal Energy Storage Types

In the following section, thermal energy storage types for the application in solar thermal power plants are described. The current thermal energy storage types can be divided into four main groups:

(1) *Thermal Energy Storage Systems for Sensible Heat*

a) Indirect Storage system

b) Direct Storage Systems

(2) Latent-Heat Storage

(3) *Steam Accumulator*

(4) *Thermo-Chemical Storage System*

3.3.3 Thermal Energy Storage Systems for Sensible Heat

The term sensible heat describes the heat which is absorbed or released by a material as a result of a change in temperature, whereupon the material does not undergo a change of aggregate state. Thermal energy storage systems for sensible heat are distinguished **in *indirect storage*** and **direct storage**. Four indirect storage concepts are introduced here:

i. 2-***Tank Molten Salt Indirect Storage***

ii. ***Packed-Bed Thermal Energy Storage system***

iii. ***Sand Storage***

iv. ***Concrete Storage***

With indirect storage systems, it must generally be considered that there is a pressure drop of the HTF in the charging and discharging process of the storage. The pressure drops results in an increase in the work needed to be done by the turbine. This leads to reduced storage efficiency [79].

In addition, there are energy losses and temperature drop in the heat exchanger when transferring the heat from the HTF to the storage medium and vice versa.

i. 2-Tank Molten Salt Indirect Storage

The 2-tank molten salt indirect storage system is a commercially available technology, which is based on nitrate salts [78]. This storage type finds application predominantly in parabolic trough power plants and is the most widely-used technology.

A storage system with two tanks has also disadvantages:

It is relatively expensive [80]. The investment cost of a storage system with two tanks is effectively doubled compared to a single tank solution and other energy storage options because two tanks and duplicate piping is required [81].

Using nitrate salts as a storage medium has the disadvantages that it has high **freezing points** (120 – 220°C) [78] and that the price for nitrate salts can fluctuate because it is a commodity product that is subject to price pressures [81].

ii. Packed-Bed Thermal Energy Storage (Regenerator)

Thermal energy storage material stores the heat energy gained from solar radiation during the day and release it when there is no sun radiation (night).

Specifications:

Material: pebbles (stone granite)

Initial Design requirements (assumption):

- ✓ Pebble is assumed to store 75% solar energy transferred from the absorber plate.
- ✓ Pebble Charging time is assumed to be 6 hours per day and
- ✓ Discharging time of 5 hours per day.

Table 3.2. Thermal property of pebble. [Y. Cengel]

Number	property	Symbol	values
1	Density ($kg/m3$)	ρ	3300
2	Thermal conductivity ($W/m.\ K$)	K	2.4- 2.6
3	Specific heat capacity ($kJ/kg.\ K$)	CP	0.88
4	Thermal diffusivity ($m2$/s)	Kr	0.79 -1.8

Packed-Bed thermal energy storage (also known as pebble bed or rock pile storage) consists of a container filled with a bed of loosely packed particulate material with a high heat capacity e.g. pebbles, gravel or rocks. This storage type was designed to utilize air as the heat transfer fluid (HTF). However, it would also be possible to use liquid media. The following descriptions are based on the HTF air. At both the top and bottom of the storage there is a duct through which the air is forced. When charging, the hot air enters the storage through the top duct, passes through the pebble bed transferring the heat to the storage material, and leaves the storage through the bottom duct. In the discharge process, the direction of the air circulation is reversed. Cold air enters the storage through the bottom duct and is heated up as it travels upwards to the top where it exits through the top duct. [75], [82]. Illustration Shown in Figure 3.6 is a temperature–storage height plot of the thermal stratification (temperature distribution) in the packed bed. The plot contains five lines, covering a range of storage loads between 0% (completely discharged) and 100% (completely charged). For ease of explanation these conditions will be referred to as the blue line and the red line respectively.

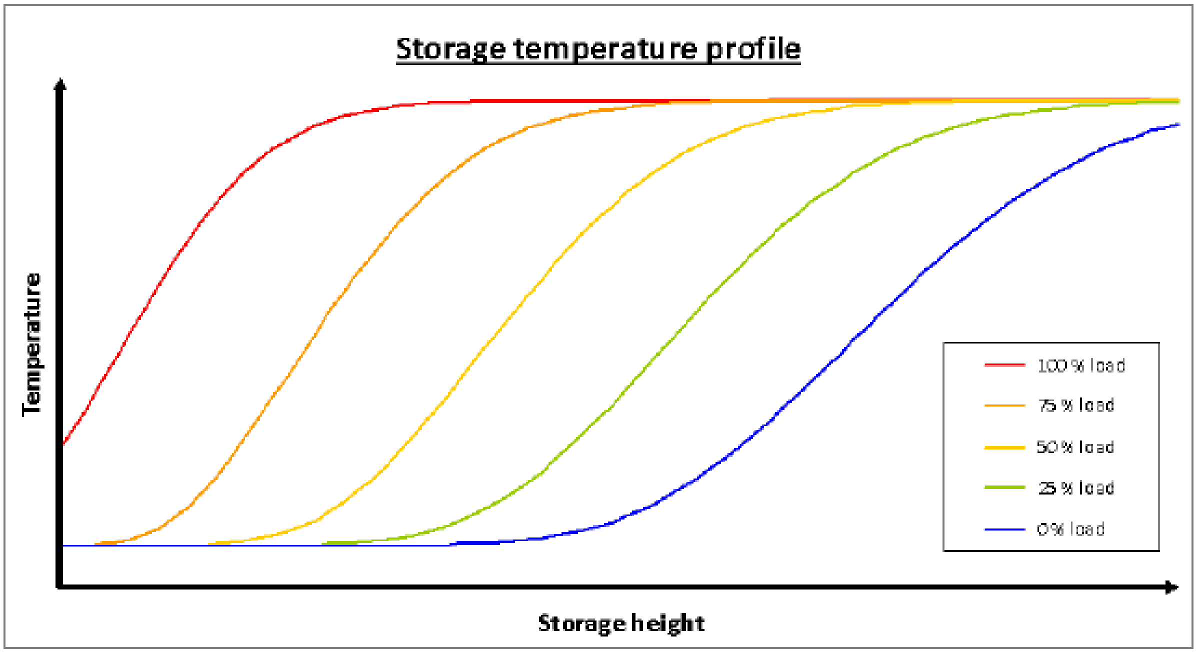

Fig.3.6. The temperature profile of a packed-bed thermal energy storage for a range of load percentages [82]

Blue line: Up to approximately 1/3 of the storage height, ambient temperatures overcome. The temperatures then begin to rise along the height of the storage. At the top of the pebble-bed, the temperatures are close to, but still below the maximum material temperature. Therefore, this condition is referred to as having 0% load, as the maximum air temperature has not yet been reached [82]. **Red line**: In the process of charging the storage, hot air passes through the pebble-bed in the downward direction. The time needed to fully charge the storage depends on the design of the storage. When beginning the charging process, only the pebbles near the top are heated to maximum temperature and less heat is available for the lower levels. This is due to the rapid heat transfer. When the material at the top level has reached maximum temperature (i.e. the temperature of the hot air), the hot air then passes through the top layer without transferring any heat until a layer at a lower temperature is reached. Over time the lower layers will also have been heated to maximum temperature. This is a continuous process of the material layers being heated from the top to the bottom. The storage is said to be fully loaded when the hot air passing through it transfers so little heat to the material that on exiting, the air temperature is near to the maximum allowed by system boundary conditions. Moreover, the warmer the exiting air exiting the storage at the bottom is, the greater would be the loss of energy. The condition that a storage system is defined to be fully loaded therefore depends on the power plant air system's configuration and component limitations. According to the red line in the graph the storage is fully charged when approximately 2/3 of the storage material from the top has reached maximum temperature [82]. The storage chamber is fitted with several thousand ceramic structures that are piled next to and on top of each other. When charging, hot air passes through the channels and transfers its heat on the thin walls. When discharging, the walls transfer the heat to cold air, heating it up on its way to the duct at the top of the chamber [82]. Generally speaking, ceramic bodies can be designed in many different forms (Figure 3.7). All these ceramic bodies are porous and can be easily set. The ceramic bodies are used in industrial facilities, e.g. in the iron-works industry in high-temperature industrial regenerators (hot blast stoves), which are commercial wind heaters (the supplied air to be preheated is referred to as wind). In this application, several of these storage types are constructed in parallel and operated sequentially, resulting in quasi-continuous heat exchanger operation.

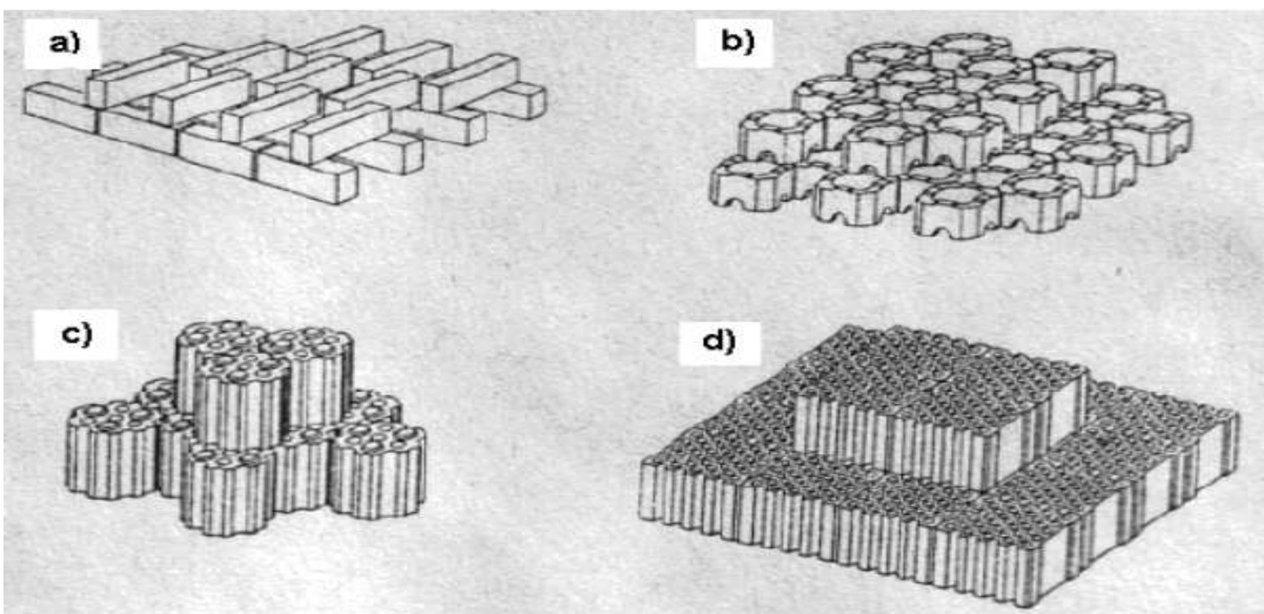

Figure 3.7. Shapes of ceramic bodies for high-temperature regenerators *[79]*

The following presented formulae are quoted (and translated) from source [83]:

The thermal capacity Q, which is transferred from the airflow to the bodies (e.g. pebbles) in the the charging process is calculated by the following equation:

$$Q = \alpha_v V(T_a + T_b) \text{ ------------------------------------ } (101)$$

where αv is the volume-dependent heat transfer coefficient between the airflow and the pebbles [W/(m^{3}K)], V is the usable storage volume of the pebbles [m^3], T_{air} is the airflow temperature and T_b is the temperature of the bodies [°C].

The volume - dependent heat transfer coefficient α_v between the airflow and the bodies in the packed-bed thermal energy storage system is calculated as follows:

$$\alpha_v = 650\left(\frac{\rho w}{d}\right)^{0.7} \text{ ------------------------------------ } (102)$$

where ρ is the density of the air [kg/m3], w is the airflow velocity [m/s] and d is the equivalent diameter of the bodies and is calculated by:

$$d = \left[\frac{6V(1-\varepsilon)}{\pi n}\right]^{1/3} \text{ ------------------------------------ } (103)$$

where ε is the porosity (relative void volume) of the packed bed and n is the number of bodies in the packed bed.

The Biot number Bi is calculated from the convection heat transfer coefficient h [W/m^{2}K], the radius R of the body [m] and the thermal conductivity k [W / (m K)]:

$$B_i = \frac{hR}{K} \text{ ------------------------------------ } (104)$$

The Biot number is the ratio of the inner resistance of a body (R/ k) to the resistance at the surface (1/ h) of a body. At the values of $Bi \leq 0.1$, the inner thermal resistance of the body is small in comparison to the surface resistance and therefore the internal temperature gradients are negligible. The pressure loss in packed-bed thermal energy storage for a range of $100 < Re < 13{,}000$ can be calculated from the following equation (from Cole).

$$\Delta p = \rho w^2 \left(\frac{L}{d}\right)\left[\frac{(1-\varepsilon)^2}{Re\,\varepsilon^3}\right]\left[\frac{1.24Re}{(1-\varepsilon)} + 368\right] \text{ ------------------------- } (105)$$

where L is the length (height) of the packed bed in flow direction, d is the equivalent diameter of the bodies, w is the air velocity [m/s], ε is the porosity of the backed bed (from 0.35 to 0.5)

Re is the Reynolds number Re= wd/v, v is the kinematic viscosity of the air [m^2/s]. For bodies with an uneven form, a form factor *f* is used in order to take the deviation of the spherical shape into account. The form factor *f* is the ratio of the area of the body to the area of a sphere of the same size. There are no sure descriptions of *f* values but specific approximate values can be used. Example for assumed values: *f* = 1.5 for round gravel; *f* = 2.5 for small granite bodies that are broken into pieces and *f* = 1.5 if these granite bodies have a diameter > 50 mm. With the values of ε and *f* the pressure loss can be calculated:

$$\Delta P = \rho w^2 \left(\frac{L}{d}\right)(1-\varepsilon)\ \frac{f}{\varepsilon^{3/2}}\left[4.74 + 166(1-\varepsilon)\ \frac{f}{\varepsilon^{3/2 Re}}\right] \text{-----------------} \quad (106)$$

If the values of ε and *f* are not known then the following simplified equation is used:

$$\Delta P = \rho w^2 \left(\frac{L}{d}\right)\left(21 + \frac{1750}{Re}\right) \text{---------------------------} \quad (107)$$

The entire area of the bodies in the packed bed *Ap* is calculated by:

$$A_p = \frac{6(1-\varepsilon)Vf}{d} \text{------------------------------} \quad (108)$$

The equation for calculating the area-related heat transfer coefficient α is:

$$\alpha = \frac{\alpha_v\, d}{6(1-\varepsilon)f} \text{------------------------------} \quad (109)$$

The heat transfer in packed-bed thermal energy storage with a total packed bed height H, which is divided into layers of equal length Δx = H/n, shall now be considered. The discretization scheme of the packed-bed thermal energy storage in a mathematical model is shown in Figure 3.8. Due to the low thermal conductivity of the packed bed, the radial temperature gradients can be neglected so that every layer i at a time t can be marked with a uniform temperature $T(s\ i\ )$ of the bodies. The instantaneous energy balance for the i-th layer of the packed-bed thermal energy storage in the charging process can be described with the following differential equation:

$$(1-\varepsilon)\ \rho_b\ c_b \frac{dT_{b,i}}{dt} = \alpha_v \mathrm{Vi}\,(T_{air\ ,i} - T_{b\ ,i}) - Q_{loss\ ,i}\ \ [\mathrm{w}] \text{-------------------} (110)$$

Where, ρ_b is the density of the body [kg/m3], c_b is the specific heat capacity of the body [J/ (kg k)] Vi is the volume of the i-th layer [m3], $T_{b\ ,i}$ is the temperature of the body [°C], t is the time [s], $T_{air\ ,i}$ - is the temperature of the airflow from the (i-1)-th layer [°C] and $Q_{loss\ ,i}$ - is the heat loss to the surrounding air. The heat loss of the i-th layer to the surrounding is calculated from the equation:

$$Q_{loss\ ,i} = k_{st}(T_{b\ ,i} - T_{amb})\ \Delta \mathrm{X\ P}\ [\mathrm{w}] \text{------------------------} (111)$$

Where, k_{st} is the heat loss coefficient of the thermal energy storage [W/(m2K)], T_{amb} is temperature surrounding the thermal energy storage [°C], Δx is the height of the i-th layer [m] and P is the circumference of the thermal energy storage cross-section [m]. Because the specific heat capacity of the air can be neglected when compared to that of the bodies, the following energy balance is valid for the i-th layer of the thermal energy storage in the charging process:

$$Q = (m_{air}\, c_{p\,air})\,(T_{air,\ i-1} - T_{air,i}) = \alpha_v\, v_i\,(T_{air,\ i-1} - T_{b,i}) \text{ -------------- } (112)$$

This follows that the air temperature in the i-th layer of the thermal energy storage is calculated with the equation:

$$T_{air,i} = T_{air,\ i-1} - \alpha_v\, v_i\,(T_{air,\ i-1} - T_{b,i}) \Big/ (m_{air}\, c_{p\,air}) \text{ -------------- } (113)$$

where $T_{air,i}$ is the air temperature in the i-th layer [°C], $T_{air,\ i-1}$ is the air temperature in the (i-1)-th layer [°C], m_{air} is the air mass flow [kg/s] and $c_{p\,air}$ is the specific heat capacity of air [J/(kgK)].

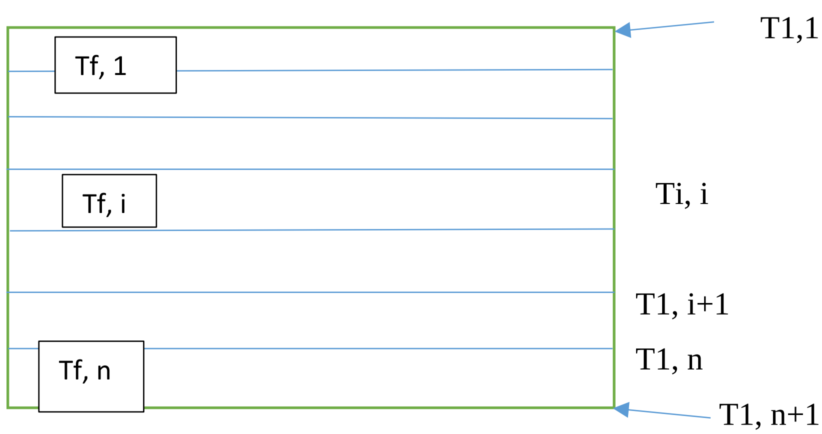

Figure 3.8 Model of the packed-bed thermal energy storage system

3.3.4 Selection of Insulating Material

Most insulation is used to prevent the conduction of heat. A good insulator is obviously a poor conductor. Less dense materials are better insulators. The denser the material, the closer its atoms are together. That means the transfer of energy of one atom to the next is more effective. Thus, gases insulate better than liquids, which in turn insulate better than solids [85]. An interesting fact is that poor conductors of electricity are also poor heat conductors. Wood is a much better insulator than copper. The reason is that metals that conduct electricity allow free electrons to roam through the material. This enhances the transfer of energy from one area to another in the metal. Without this ability, the material-like wood-does do not conduct heat well. Insulation is defined as a material or combination of materials, which retard the flow or loss of heat and is used in heating, air conditioning and refrigeration systems to insulate piping, ducts, vessels, thermal storage devices, and equipment's in order to conserve thermal energy, prevent surface condensation and control heat input to the contained fluids. Generally, the thermal insulation can be used to control heat flow in wide temperature ranges when the appropriate insulating material is selected. Insulation reduces the transfer of heat from the thermal storage to the surrounding. The basic requirement for thermal insulation is to provide significant resistance to the flow of heat across the insulation material. To accomplish this, the insulation material must reduce the rate of heat transfer by conduction, convection, or any combination of these mechanisms that would occur during charging and/or backing. Type and thickness of insulation material are the basic parameters in thermal insulation selections. It is advisable to select the correct thickness and material type. The general criteria needed to make a choice among various thermal insulation materials are as follows [85]:

- ✓ Surface temperature expected
- ✓ The R-value of the material
- ✓ Cost of the complete insulating system
- ✓ The reason insulation is needed
- ✓ The location where insulation will be needed
- ✓ Accessibility for the insulated area

3.3.5 Temperature of Working Surfaces

The temperature of the working surface is a decisive factor in the selection of insulating material thickness. The recommended insulation thickness based on upper limit hotness of surfaces at specified temperatures is given in the table below [86].

Table 3.3: Surface temperature and recommended insulation material thickness

Surface temperature **(℃)**	Insulation thickness (cm)
66	5.1 0
121	7.60
177	10.20
288	15.20
360	17.20
400	22.90
510	25.44

3.3.6 R-value of Insulating Material

The R-value [K/W] is the reciprocal of the amount of heat energy per area of material per temperature difference between the outside and inside of the insulation. It is an indication of resistance to heat flow and is its ability to insulate. The higher the R-value, the better the insulation property will be [85]. For cylindrical insulation (such as circular pipe insulation) of inner radius $r1$, outer radius $r2$, and length L having average thermal conductivity K with thermal resistance can be given by the table listing insulating materials with their R-value as shown in appendix A.2.

3.3.7 Cost of Insulating Material

The other variable in the selection of insulating material is the cost per service time of the insulator. The optimum thickness can be determined by obtaining an expression for the total cost which is the sum of the expressions for the lost heat cost and insulation cost as a function of thickness. As thickness of insulation increases, the cost of material will go up. On the other hand, the energy cost savings also goes up, but at a slower rate of increase than the cost of materials and installation [87]. Due to their availability, affordable cost and appropriate thermal insulating property, selecting combined insulating material in order to achieve better insulation with minimized cost. These materials are Cellulose fiber and Fiberglass having a total thickness of about 15cm.

3.3.8 Advantages of Insulation Systems

The following are the basic advantages of insulating systems [87]:

Energy Savings: Substantial quantities of heat energy are wasted because of un-insulated heated surfaces. Properly designed and installed insulation systems will immediately reduce the need for energy and benefits to the industry include enormous cost savings, improved productivity, and enhanced environmental quality.

Process Control: By reducing heat loss or gain, insulation can help maintain process temperature to a pre-determined value or within a predetermined range.

Personnel Protection: Thermal insulation is one of the most effective means of protecting workers from burns resulting from skin contact with surfaces of hot surfaces and equipment operating at higher temperatures. Insulation reduces the surface temperature of piping or equipment to a safer level, resulting in increased worker safety and the avoidance of worker downtime due to injury.

Fire Protection: Used in combination with other materials, insulation helps provide fire protection in fire stop systems designed to provide an effective barrier against the spread of flame, smoke, and gases at penetrations of fire-resistance-rated assemblies by ducts, pipes, and cables.

3.4 Design of a chimney for solar updraft power plant

The chimney is the main characteristic of the solar updraft station. The chimney is located at the center of the collector and is the thermal engine for the plant. The chimney creates a temperature differential between the cool air at the top and the heated air at the bottom. The change in the air temperature induces a pressure differential, which drives the air from the bottom of the chimney out of the top. A well-designed solar updraft must minimize **frictional losses** and maximize the pressure **difference** in the chimney. The pressure difference in the chimney is proportional to the chimney height, given by the relation.

$$\Delta P_{Sc} = (\rho_o - \rho_2)\, \mathrm{g} H_{sc} \quad (114)$$

therefore, maximizing the height of the chimney is very essential in improving the efficiency.

Schlaich (1995) stated that, the efficiency of the chimney is given by:

$$\eta_{Sc} = \frac{P_{tot}}{Q} = \frac{g\, H_{sc}}{C_p\, T_a} \quad (115)$$

The relation in equation (115) explains the significance of the chimney's height on the efficiency. The chimney efficiency is again seen to be inversely proportional to the outside air temperature, therefore the lower the air temperature the better the efficiency. This explains why the solar updraft plant is yet able to produce a substantial amount of electrical power during the night and overcast weather conditions. This is made possible as the plant is able to make good use of the low rise in air temperature produced by the heat emitted by the ground.

The material for the chimney construction could be reinforced concrete tubes, steel sheet tubes supported by guy wires, or cable-net construction with a cladding of sheet metal or membranes (Figure3.9). Schlaich (1995) suggests that reinforced concrete would be a cost-effective way to create a stable tower with a lifespan of up to 100 years.

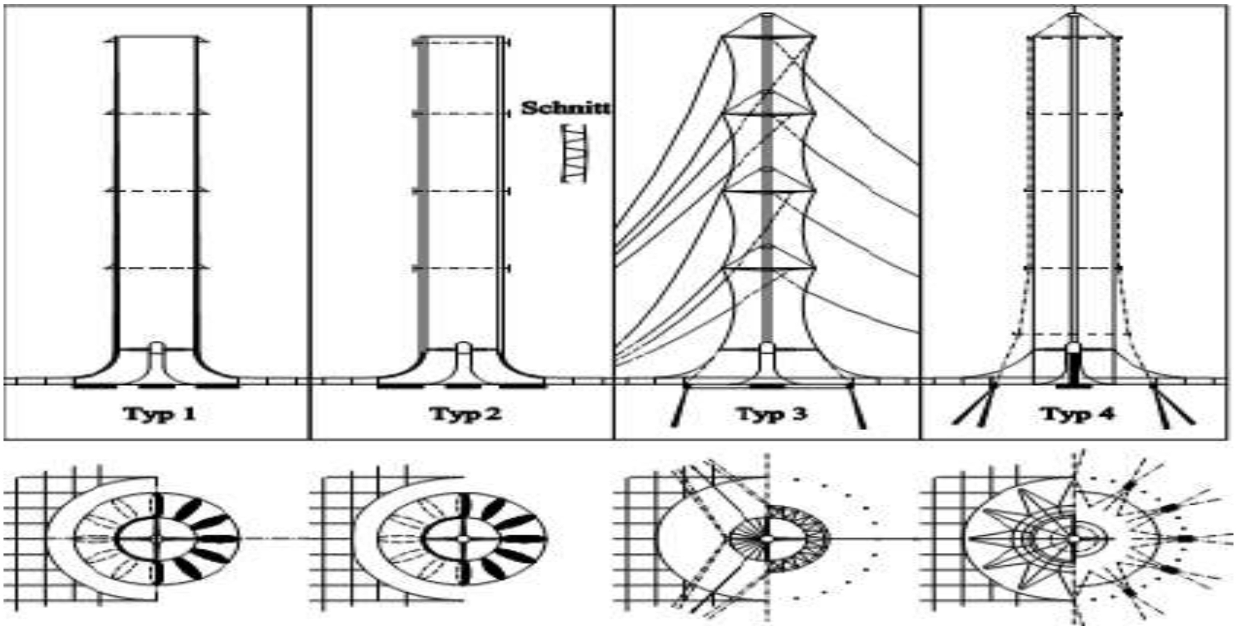

Figure 3.9. Chimney construction shapes (Bernardes, 2010) [44].

In other to achieve high wind velocities and efficiency, chimney heights are often made very tall. A chimney of height 200 m and diameter 10 m is considered and the airflow velocity through the chimney will be estimated.

3.4.1 The total pressure developed in the chimney

The total pressure developed due to buoyancy from equation (116) is determined as

$$\Delta P_{tot} = \rho_{air}\ g\left(H_{Sc} + \frac{H_c}{2}\right) \text{-----------------------------} (116)$$

ΔP_{tot} = 1.23 x 9.81 x (200 +2/2) = 2425.326 pa

3.4.2 The wind speed through the chimney

In the absence of a wind turbine, a maximum airflow speed is achieved and the whole pressure difference is used to accelerate the air and converted into kinetic energy (Schlaich, et al 2005). The maximum chimney airflow rate and the maximum air velocity is therefore expressed as (Zhou, et al 2008): The maximum chimney airflow rate and the maximum air velocity in the chimney in the absence of a wind turbine from equation (117) is expressed as:

$$V_{max} = \sqrt{\frac{2\Delta P_{\ tot}}{\rho_{air}}} \text{-----------------------------} (117)$$

$$V_{max} = \sqrt{\frac{2x\ 2425.326}{1.23}} = 62.8\,\frac{m}{s}$$

Zhou, et al (2008) stated again that, the maximum power is drawn when the chimney airflow rate velocity V_{SC} is one-third of the maximum speed V_{max} in the case of turbine being on load.
The actual wind speed through the 200 m tall chimney when a turbine is installed from equation (118) is found to be:

$$V_{Sc} = 1/3\sqrt{\frac{2\,\Delta P_{tot}}{\rho_{air}}} ------------------------------(118)$$

$$= \frac{1}{3}\ x\ \sqrt{\frac{2\ x\ 2425.326}{1.23}} = \frac{1}{3}(62.8) = 20.93\ \frac{m}{s}$$

3.4.3 The dynamic pressure

From equation (119) the dynamic pressure needed to accelerate the air through the chimney is determined as

$$P_d = ½\ \text{x}\ \rho_{air}\ VSc^2 ---------------------------------(119)$$

P_d = ½ x 1.23 (20.93) $^{2\,=}$ 269.4 pa

P_d = 269.4 pa

3.4.4 Static pressure drops at the turbine

The static pressure drops at the turbine from equation (120) is determined as

$$\Delta P_t = \Delta P_{tot} - \frac{1}{2} x\ \rho\ Vsc^2 ----------------------------(120)$$

ΔP_t = 2425.326 – 269.4 = 2155.9 pa

3.5 Chimney efficiency

The efficiency of the chimney can be found as follows.

$$\eta_{Sc} = \frac{p_{tot}}{Q} = g\ H_{Sc}/C_pT_a$$

$$\eta_{Sc} = \frac{9.81\ x\ 200}{1006\ x\ 298} = 0.65\%$$

3.6 Electrical power output

The maximum electrical power output of the plant from equation (121) below is therefore estimated as expressed by:

$$P_e = P_{t,max} = V_{Sc}A_{Sc}\Delta P_t\eta_{ge} ----------------------------(121)$$

where Δp is the pressure drop that represents the turbine work and v_{sc} is the outlet velocity.
The outlet velocity and tower radius are used because the volumetric flow rate is constant throughout the system. Equation (70) has a turbine efficiency of unity because the turbine effects are assumed in the definition of the pressure drop across the turbine. Therefore, the pressure drop represents the work

extracted from the system. When the solar radiation is 1000 $\frac{w}{m^2}$, the Spanish prototype reaches a vertical velocity of 15 m/s, a temperature difference of 20 K and a pressure drop with a range of (0-320) [19]. Therefore, using the equation (121) with the outlet velocity of 11 m/s and turbine pressure drop of 60pa, the power output can be obtained as follows assuming generator as perfect efficient.

$P(e\ ) = 60x\ 3.14\ x\ (5x5)x11 = 51.81\ kw$

3.7 The plant overall efficiency

The overall efficiency of the SUPP can be considered as the product of the partial efficiency contributed by each of the plant components, i.e. the turbine, the collector and the chimney.

$$\eta_{\ Scpp}\ =\ \eta_C \eta_{SC} \eta_t \quad ------------------------------(122)$$

$$\eta_{\ Scpp}\ =\ 0.51 \text{ x } 0.0065 \text{ x } 0.85$$

$$\eta_{\ Scpp}\ =\ 0.3\ \%$$

Where: η is a term efficiency which is described as follows:

ηc= the effectiveness of the collector to convert solar radiation into heat.

ηsc=effectiveness of the chimney to convert heat delivered by the collector into flow energy

ηt=effectiveness of the wind turbine to convert the kinetic energy of the flow into mechanical energy

3.8 Scaling effect on the power output

The SUPP with the following physical dimensions; 244 m diameter collector size, 200 m tall chimney with internal diameter 10 m employing a wind turbine of efficiency 85% output a theoretical electrical current of around 51.81 Kw based on the climatic conditions of Adama city which exhibit an average daily solar radiation of 5200 kWh/m2 day. From the results obtained, the electrical power output of the plant is seen to be influenced by the following factors discussed below:

1. The collector diameter

Increasing the size of the solar collector i.e. the collector area improves the amount of solar energy absorbed. The power is seen to be directly influenced by the collector area, therefore, increasing the collector size causes a rise in the energy input, which contributes, greatly to the power output produced by the plant. The effect of various collector sizes on the power output and the results depict how the power output is influenced by size of the collector.

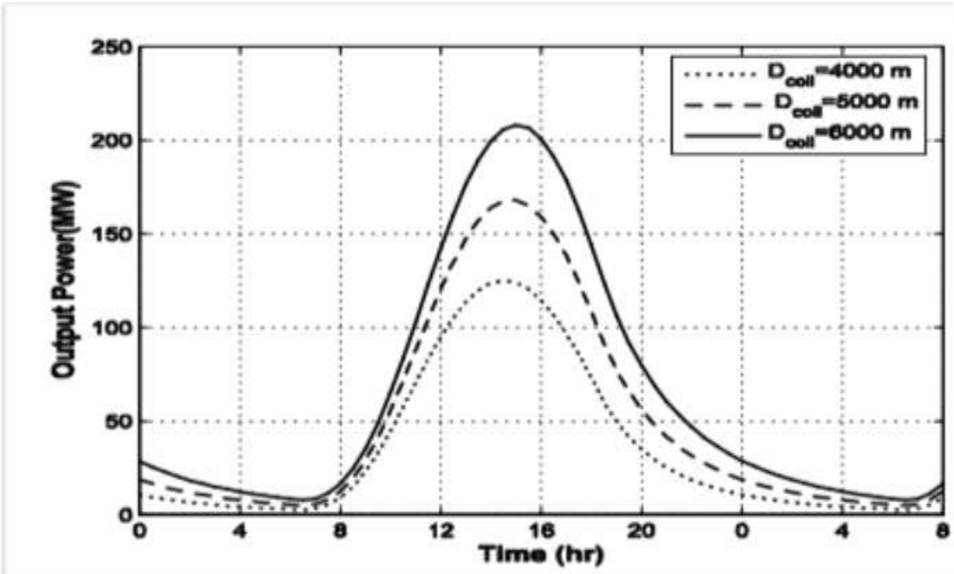

Figure 3.10. The effect of various collector sizes on the power output. Hammadi, (2008)

2. The height of the chimney

Raising the height of the chimney to an appreciable limit increases the pressure difference which improves the airflow and the draft. The various chimney heights have a dominant effect on power productivity and confirmed that a rise in the chimney height influences the power output. The major challenge to this effect has been the difficulty in putting up tall structures and the huge capital investment that is required. Generally, the SUPP represents very poor overall efficiency and this is attributed to the low efficiency of the chimney. The chimney efficiency is directly proportional to its height and as a result, increasing the height improves its efficiency which interns affect the overall plant efficiency. For instance, if a huge solar updraft with a height of 1000 m is being proposed, the efficiency of the chimney will be increased to about 35 %. Owing to this reason Mullet, (1987) in his report on SUPP concluded that the SUPP is essentially a power generator of large scale.

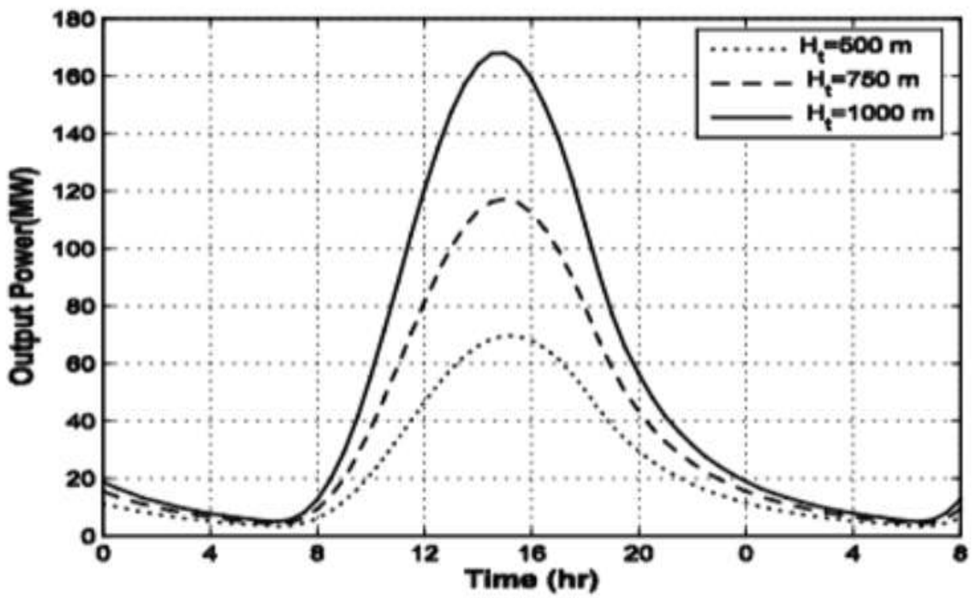

Figure 3.11: The effect of chimney height on the power output. Hammadi, (2008)

3.10 CFD Modeling and Simulation

A numerical model of the solar updraft power plant is created in a three-dimensional domain with the numerical methods investigated in the validation cases: pressure-based solver with the SIMPLE method, **standard *k-ε* turbulence model**, second-order upwind spatial discretization and first-order time discretization. This is the baseline two-transport-equation model solving for k and ε and is the default k–ε model. Coefficients are empirically derived. Options to account for viscous heating, buoyancy, and compressibility are also shared with other k–ε models.

The schematic for the current model is shown in Figure 3.12. The dimensions of the model and the environmental conditions used are explained as follows. The tower has a height of 100 m and a diameter of 10 m, the collector has a height of 2 m and diameter of 244 m, and the turbine is placed within the tower at a height of 10 m. The average ambient temperature at the location of the model is about 25˚C, so the ambient temperature for the model is 298 K. The boundary conditions are similar to the ones from Xu et al., [77]. The collector is modeled as a convection boundary condition with a convection coefficient of 10 W/ (m^2 K). The chimney and bend are both adiabatic no-slip walls. To model the solar rays traveling through the collector to heat the ground and air, varying heat fluxes are applied to the ground boundary condition. The peak solar radiation q_S'', during the January and March months in Adama, Ethiopia is about 5200 KWh/m^2 day. Using some value of ground heat flux, q_G '', analysis can be done. Therefore, representative ground heat fluxes are chosen to be 600, 700, and 800 W/m^2. Finally, different pressure drops from (0 – 320) Pa is used to model how the turbine affects the flow.

3.10.1 Model Simplification

The model needs to be simplified to ease the computation of the simulation. As the sun's radiation intensity changes within the day and the peak, solar radiation will be near noontime of the day and during that time it should be a very stable point for a fair-weather condition. For the model validation purposes, the experimental data of Manzanares based on the longitude and latitude of Adama, Ethiopia. The numerical study requires a steady-state condition; therefore, the mathematical model can be simplified with the following assumption.

a) The modeled fluid is Newtonian and incompressible

b) The flow is a Three-dimensional flow and it is assumed as turbulent

c) The viscous dissipation and compressibility properties of the fluid are assumed negligible

d) The solar radiation intensity is uniform throughout the surface of the collector (I_o = 800W/m$_2$)

e) The Solar radiation transmittance is 100%

f) Heat is being absorbed into the ground with the absorption of 0.8

g) The ambient temperature at the inlet and outlet are assumed as 298 K.

h) There is no heat loss at the inner wall of the collector, soil cover and tower wall

i) The air density changes using Boussinesq hypothesis and properties of air is assumed to be constant in all formulations

j) The fluctuation of wind effects is neglected

k) The overall process is at steady state

l) Loss of head due to the strutting and support columns for the solar collector and the loss of head for the pressure type turbine are neglected.

Based on the assumption above, the solar updraft tower will be assumed as a three-dimensional steady compressible forced convective heat transfer system. Therefore, the standard *k-e*psilon turbulence model is used with the radiation model of discrete ordinates.

3.10.2 Governing Equation

As explained in the previous chapter, the solar updraft tower consists of the solar collector and the updraft tower which function is to increase the energy in the air by utilizing the greenhouse concept where the air flow is driven by the buoyancy effect due to the vertical column of hot air at the updraft tower. The modeled fluid which flows within the system is described through the conservation equation of mass, momentum, and energy. The unknowns in the equations can be computed by the application of suitable turbulence model. The standard *k*-epsilon models are used to solve the equations and standards values for constants are adopted. With the above assumptions and the system is assumed as steady-state condition, the basic equations can be written as follows:

Continuity Equation

$$\frac{1}{r}\frac{d}{dr}(ru) + \frac{dw}{dz} = 0 \quad \text{------------------------------------} (123)$$

Momentum Equation

$$\rho\left(\frac{udu}{dr} - \frac{V^2}{r} + w\frac{du}{dz}\right) = -\frac{dp}{dr} + \mu\left[\frac{1}{r}\frac{d}{dr}\left(r\frac{du}{dr}\right) - \frac{u}{r^2} + \frac{d^2u}{dz^2}\right] \text{-----------------} (124)$$

$$\rho\left(\frac{udv}{dr} - \frac{uv}{r} + w\frac{dv}{dz}\right) = \mu\left[\frac{1}{r}\frac{d}{dr}\left(r\frac{dv}{dr}\right) - \frac{v}{r^2} + \frac{d^2v}{dz^2}\right] \text{----------------------} (125)$$

$$\rho\left(\frac{udw}{dr} + w\frac{dw}{dz}\right) = -\frac{dp}{dz} + \rho g \beta(T - T_c) + \mu\left[\frac{1}{r}\frac{d}{dr}\left(r\frac{dw}{dr}\right) + \frac{d^2w}{dz^2}\right] \text{---------------} (126)$$

Energy Equation

$$\frac{1}{r}\frac{d}{dr}(\rho ruT) + \frac{d}{dz}(\rho vT) = \frac{1}{r}\frac{d}{dr}\left(r\frac{\lambda}{C_p}\frac{dT}{dr}\right) + \frac{d}{dz}\left(\frac{\lambda}{C_p}\frac{dT}{dz}\right) \text{--------------------} (127)$$

3.10.3 Turbulence Modelling

A turbulence model is a method of computational procedure to close the system of mean flow equations. For most of the engineering applications in the industry, it is unnecessary to resolve the details of the turbulent fluctuations. Therefore, the turbulence models enable the calculation of the mean flow without first calculating the full time-dependent flow field. The reason is to identify and know the effects of turbulence on the mean flow. The Reynolds number quantifies the relative importance of these two types of forces for given flow conditions and is a guide to when turbulent flow will occur in a particular situation.

$$\text{Reynolds number} = \frac{inertial\ forces}{viscous\ forces} = \frac{ma}{\tau A} = \frac{\rho V\frac{du}{dt}}{\mu\frac{du}{dy}.A} \propto \frac{\rho L^3\frac{du}{dt}}{\mu\frac{du}{dy}L^2} = \frac{\rho L\frac{dy}{dt}}{\mu} \propto \frac{\rho u_o L}{\mu} = \frac{u_o L}{\nu}$$

Where: t is the time, y is cross-sectional position, u *is* (local) flow speed, τ is the sheat stress (Pa), A is the cross-sectional area of the flow, V is the volume of the fluid element, uo is the maximum speed of the object relative to the fluid (m/s), L is a characteristic linear dimension (m), μ is the dynamic viscosity of the fluid (Pa·s), ν the kinematic viscosity ($\nu = \mu/\rho$) (m^2/s) and ρ is a density of the fluid (kg/m^3).

$$\text{Re} = \frac{\rho\, vD}{\mu} ---------------------------------- (128)$$

Where ρ = density of air (kg/m3)

v = velocity of the fluid (m/s)

μ = Dynamic viscosity of air (kg/m. s)

D = Diameter of pipe (m)

$$\text{Re} = \frac{(1.23 \text{ x } 62.1 \text{ x } 10)}{(1.84 \text{ x } 10{-}5)}$$

Re = 415.125 x 10^5 which is greater than 2300 and therefore, the flow is turbulent. Therefore, a turbulent model can be used for this application. The standard *k*-epsilon equations are used for analysis. It is the simplest and complete of turbulence using two-equation models in which the solution of two separate transport equations allows the turbulent velocity and length scales to be independently determined.

- ✓ The most widely-used engineering turbulent model for industrial applications
- ✓ Robustness, economy, and reasonable accuracy for a wide range of turbulent flows
- ✓ explain its popularity in industrial flow and heat transfer simulations.
- ✓ This leads to stable calculations that converge relatively easily.
- ✓ Reasonable predictions for many flows
- ✓ It contains sub-models for compressibility, buoyancy, combustion, etc.

The turbulent kinetic energy which is the transport equation obtained from the exact equation and its rate of dissipation is derived using physical reasoning:

***k* equation**

$$\rho\left(\frac{1}{r}\,\frac{d(ruk)}{dr} + \frac{d(kv)}{dz}\right) = \frac{d}{dz}\left(\left(\mu + \frac{\mu_t}{\sigma_k}\right)\frac{dk}{dz}\right) + \frac{1}{r}\,\frac{d}{dr}\ \left(r\left(\mu + \frac{\mu_t}{\sigma_k}\right)\frac{dk}{dr} + G_k - \ \rho\varepsilon ------(129)$$

$\mu t = \ \rho c\mu \frac{\mathrm{k}^2}{\epsilon}$ where μt is turbulent viscosity, $c\mu$ depends on the mean rate of strain and rotation, angular velocity and system rotation.

Epsilon equation

$$\rho\left(\frac{1}{r}\frac{\partial(ru\varepsilon)}{\partial r} + \frac{\partial(\varepsilon v)}{\partial z}\right) = \frac{\partial}{\partial z}\left(\left(\mu + \frac{\mu_t}{\sigma_\varepsilon}\right)\frac{\partial\varepsilon}{\partial z}\right) + \frac{1}{r}\,\frac{\partial}{\partial r}\left(r\left(\mu + \frac{\mu_t}{\sigma_\varepsilon}\right)\frac{\partial\varepsilon}{\partial r}\right) + \frac{\varepsilon}{k}\,(C_1\,G_k - C_2\rho\varepsilon) --(130)$$

Referring to the standard *k*-epsilon equations above, G_k represents the generation of turbulence kinetic energy due to the mean velocity gradients. The variable r, which stands for the radial coordinate, corresponds to the radial direction in the collector and the variable z, which represents the axial coordinate, corresponds to the tower axial direction. The standard k-epsilon equation was used when calculating, the wall adopted standard wall function method and also the simple method was used to treat pressure-velocity coupling. The equations also consist of some adjustable constants $\sigma k, \sigma \varepsilon,$ C1 ε and $C_2 \varepsilon$. The values of these constants have been arrived at by numerous iterations of data fittings for a wide range of turbulent flows. These are as follows $\sigma_k = 1.00$, $\sigma \varepsilon = 1.30$, C1 $\varepsilon = 1.44$, $C_2 \varepsilon = 1.92$ & $C_\mu = 0.09$

3.10.5 Geometry Generation

The geometry was constructed using the ANSYS design modeler. The solar updraft tower is split into three different zones. There are three different zones which are:

a) The Solar Collector

b) Transition Section in between solar collector and tower

c) Tower

The mesh of each part is generated separately and the parts where the face size is too wide, secondary mesh refinement is being introduced to provide smooth and better-quality mesh. The transition zone is the most sensitive area of the computational domain as it is a very small area on which there is a strong pressure gradient. Therefore, refinement is also added to this area to improve mesh quality. The overall mesh quality is checked to reduce the skewness ratio to approximately 0.8. The system geometry consists of a tower with 200 meters height and 10-meter diameter surrounded by a collector with a 244-meters radius and 2-meter height. The physical domain was modeled and meshed using the ANSYS mesh editor. Grid generation is considered as the first necessary step for CFD modeling and has an impact on numerical results.

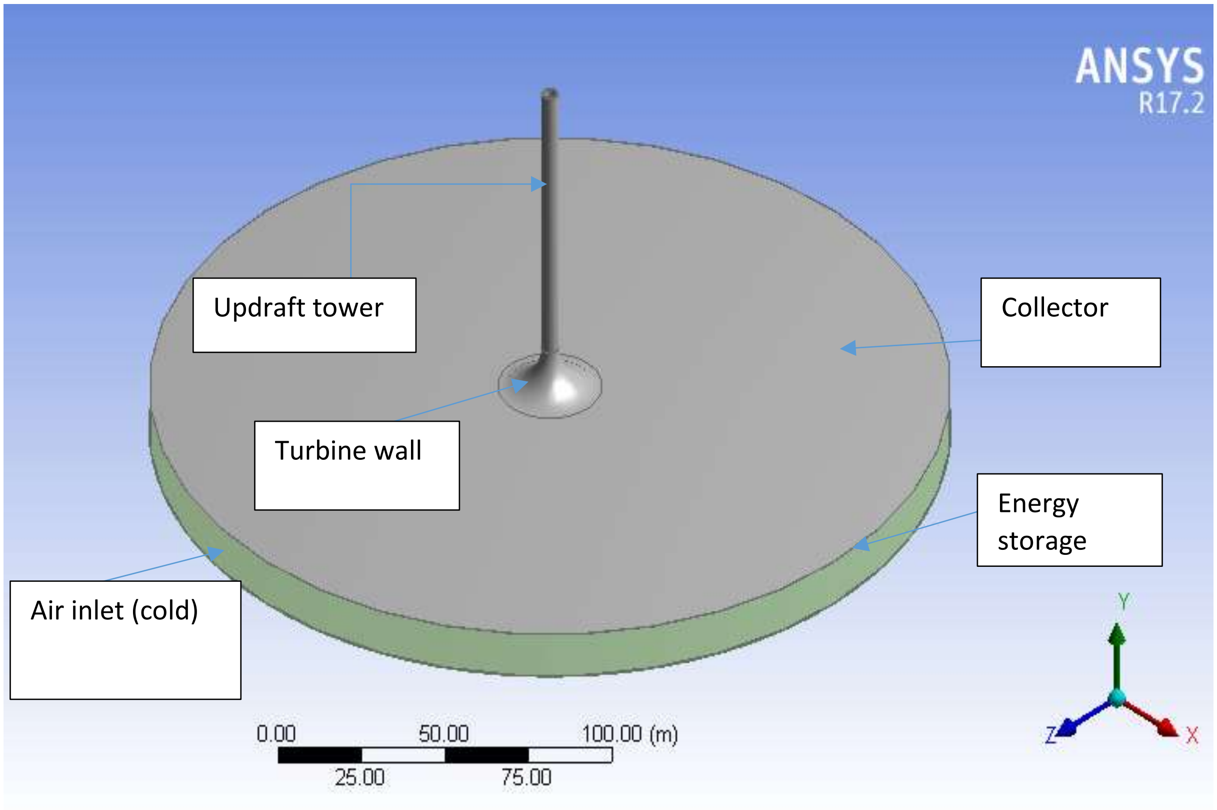

Figure 3.12 full- geometry solar updraft power plant modeled using Ansys fluent R17.2

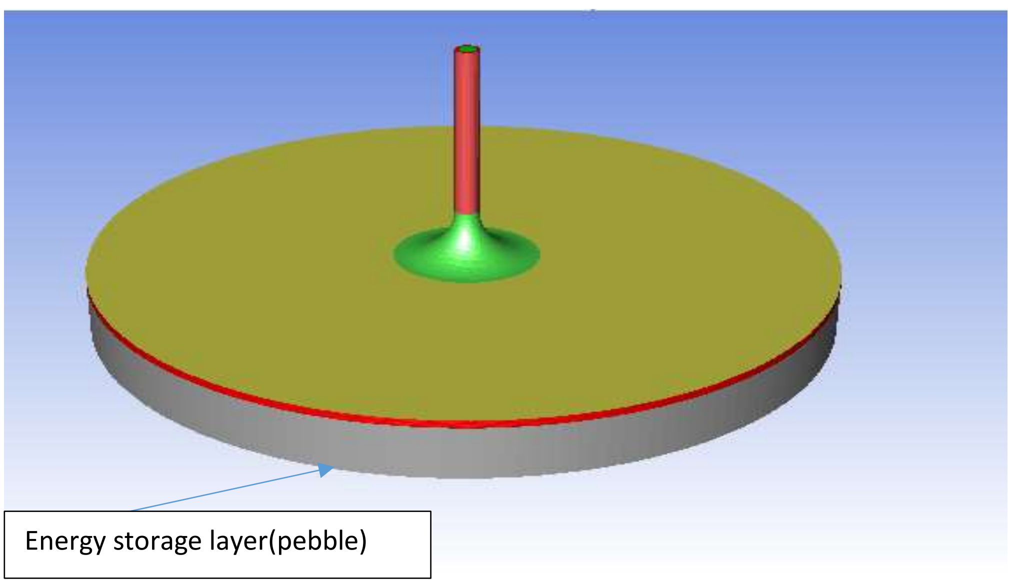

Figure 3.13 SUPP modeled using Ansys fluent R17.2 with the energy storage layer

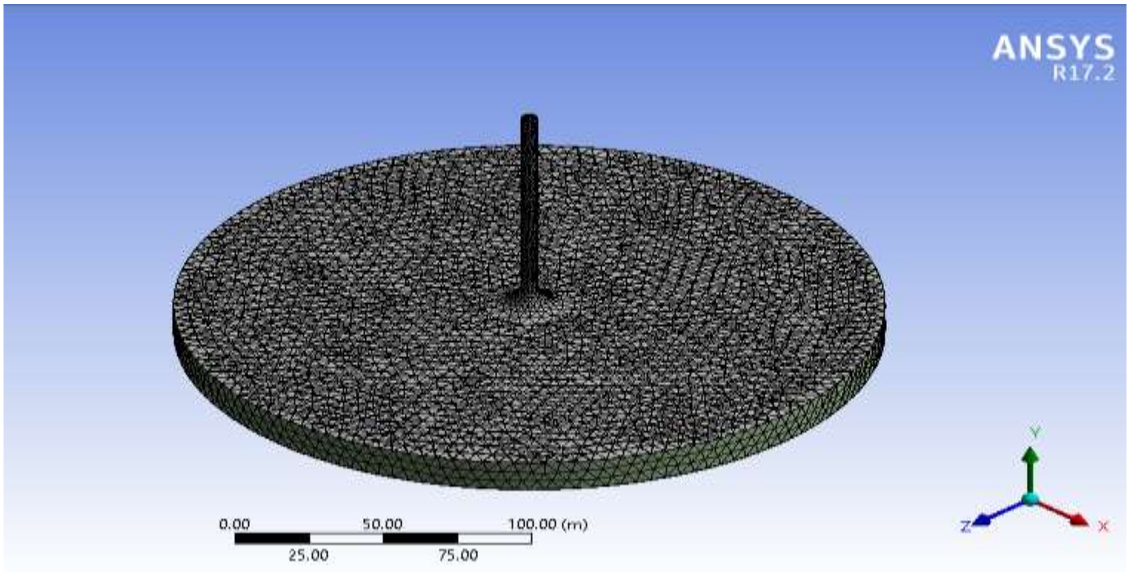

Figure 3.14 full- geometry solar updraft power plant meshing on Ansys fluent R17.2

Two-dimensional axisymmetric is easier and can be analyzed with less computer resources. But, the majority of flows encountered in engineering are turbulent. Most turbulent flows can be regarded as time-dependent, **three-dimensional fluctuations** superimposed on a mean flow. This is the reason behind why not axisymmetric geometry is not used in this designation.

3.10.4. Boundary Conditions and Solution Procedures

At the inlet of the solar collector, the pressure inlet boundary condition is specified and equated as the atmospheric gauge pressure $pa = o\ pa$

The same boundary condition is used for the chimney's outlet. No-slip boundary condition is used for the chimney's wall, the ground, and the transparent cover. The heat flux to these walls adjacent to the fluid elements is:

$$q_{total} = q_{heat-gen} + q_{rad} \text{ ------------------------------ } (131)$$

$$q_{heat-gen} = \frac{ks}{\Delta n}(T_w - T_s) \text{ ------------------------------ } (132)$$

For all the boundaries in the Solar updraft Power Plant (SUPP) system, the optical radiation properties have to be specified. The complete boundary conditions used to model the SUPP for simulation are explained in detail by the Table 3.5. The simulated results were validated against the experimental results of pilot plant. The boundary conditions employed in the simulation were derived from the operating conditions and the weather data at Adama meteorological center. In this study, the heat flux was equated to zero at the wall surface of radiation model in relation to the boundary condition. Considering the solar radiation-induced model, under ambient conditions where there was no thermal interference from other external heat sources, the surface temperature and the surrounding air temperature were at equilibrium, and thus, the change in temperature equated to zero. Therefore, the local heat flux at the surface equals to zero which showed that there was no internal heat generation from the medium. With the introduction of radiation heat transfer model, the energy gained by the surface drives the system which caused influences on temperature of the various components of the system including the operating fluid. Moreover, the greenhouse effect was considered in the CFD model of the SUPP.

3.10.5 Boundary Conditions for SUPP Simulation Model

Boundary conditions specify the flow and thermal variables on the boundaries of the physical model. They are; therefore, a critical component of the FLUENT simulations and it is important that they are specified appropriately. The boundary conditions applied are those shown in Table 3.4 and No additional thermal boundary conditions are required for coupled wall boundary conditions because the solver will calculate heat transfer directly from the solution in the adjacent cells.

Table 3.4 Boundary Conditions for SUPP Simulation Model

Boundaries	Boundary types	Values
Inlet	pressure	✓ Gauge pressure = 0 pa ✓ Temperature = 300 ✓ Turbulence intensity = 0.1 (Pastohr et al., 2004) ✓ Turbulence viscosity ratio = 10
collector	Convection	✓ With h =10 $\frac{w}{m^2}$, $Tfilm = 319\ K$ ℃
Turbine wall	wall	✓ Wall, no slip
Chimney wall	wall	✓ Wall, no-slip, adiabatic
Outlet	Pressure	✓ Gauge pressure = 0 pa ✓ Temperature = 300 ✓ Turbulence intensity = 0.1 (Pastohr et al., 2004) ✓ Turbulence viscosity ratio = 10

3.10.6. The general brief steps followed in the simulation are described below:

- ✓ Creating geometry on design modeler
- ✓ Meshing the model (refining, smoothing, applying methods, sizing, nomenclature)
- ✓ Setting boundary conditions and operating condition
- ✓ Preprocessing on FLUENT
- ✓ Displaying the grids
- ✓ Checking the grids
- ✓ Setting models (solver, viscous, energy and radiation)
- ✓ Setting materials (air, solid, glass)
- ✓ Defining boundary conditions
- ✓ Solution control (selecting coupling methods, initializing, residuals, surfaces, iterating)
- ✓ checking for convergence
- ✓ post-processing on fluent
- ✓ Displaying results (contours, XY plots, etc.)

After boundary conditions are settled, materials are selected appropriately and the model is checked the next step is solution manipulation step.

3.10.7 Solution control and checking for convergence:

The following are used in the solution control handled before initializations.

- Pressure interpolation scheme: **standard**
- Pressure-velocity coupling: **Simple**
- Up winding schemes for Momentum, Turbulence Kinetic Energy, Turbulence Dissipation Rate, and Energy: **Second-Order Upwind**
- Default under-relaxation factors.

Plotting of residuals during the calculation was enabled by letting all the residuals to be 10^{-6} for energy and for DO intensity the residuals were set to be 10^{-6} and below that value is possible.

To check for convergence of the solution, monitoring the residuals is one method. Convergence will occur when the Convergence Criterion for each variable has been reached. If the residuals set above 10^{-6} and 10^{-9} are satisfied, the solution is said to be converged. Figure 3.16 shows that all the scaled residuals are below 10^{-6} and variation between each value are constant on further iteration.

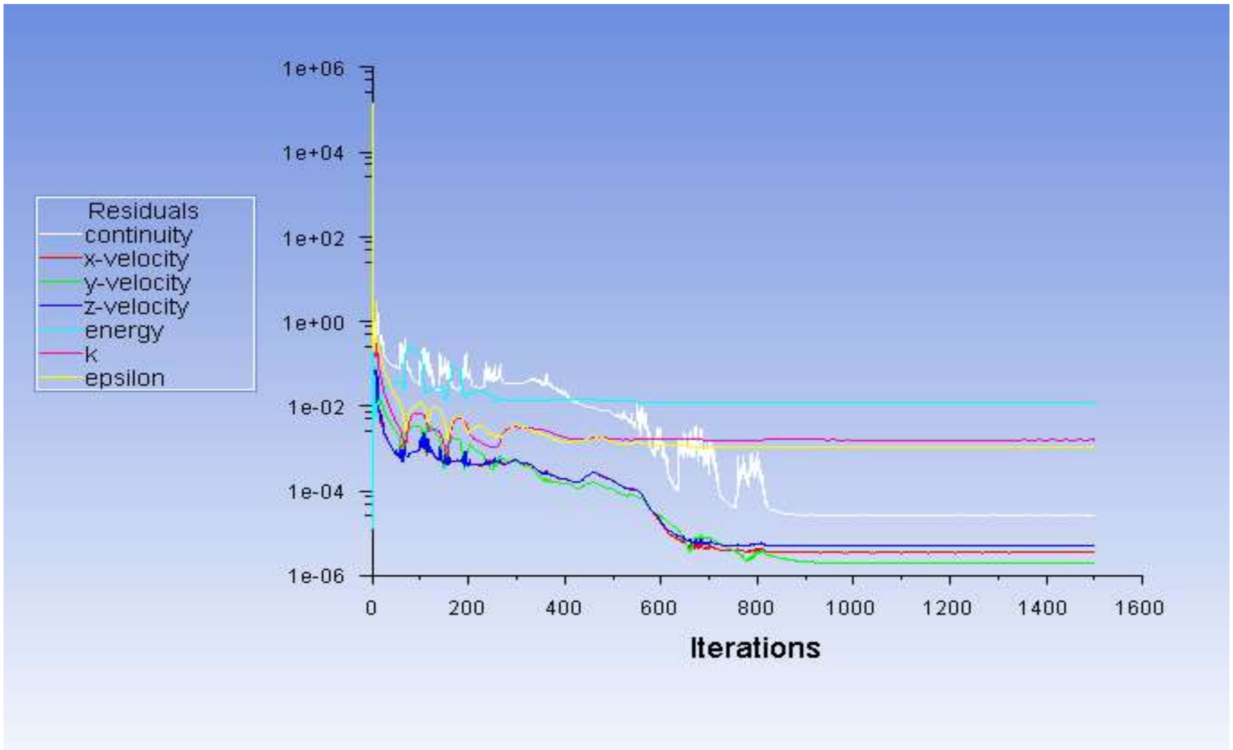

Figure 3.15 Scaled residuals showing convergence

Grid independency study

Simulations have been carried out using different grid sizes. The total numbers of elements are 526500, 628366, 727485 and 897744. The HTF air properties are observed to be in similar nature and the variation in average air properties between 928754 and 897744 nodes is very negligible. Due to minimizing the computational expenses, reducing iteration duration 897744 elements were used for remaining simulations rather than studying very discrete mesh sizes and relevance.

Table 3.5 Mesh independency study for Solar updraft tower

Trials	Relevance center	smoothing	Min. size	Max. size	nodes	Elements	Temperature outlet Results (K)
1	coarse	Medium	4.98	997	7452	526500	335
2	medium	Medium	2.49	498	17905	628366	337.25
3	Fine	Medium	2.46	292	81866	727485	340.2
4	Finer	High	1	80	461738	897744	341.2
5	Finest	High	1	50	1104072	928754	341.8

CHAPTER FOUR

RESULTS AND DISCUSSIONS

4.1 Post-Processing on Fluent

Once the iteration is completed and converged solutions are obtained, different types of results can be analyzed.

4.2 Displaying graphical results

Graphics tools available in FLUENT allow to process the information contained in the CFD solution and to easily view the results. Some of these methods are described below.

1). Displaying contours

FLUENT allows the plotting of contour lines superimposed on the physical domain. Contour lines are lines of constant magnitude for a selected variable (like velocity, temperature, pressure, etc.)

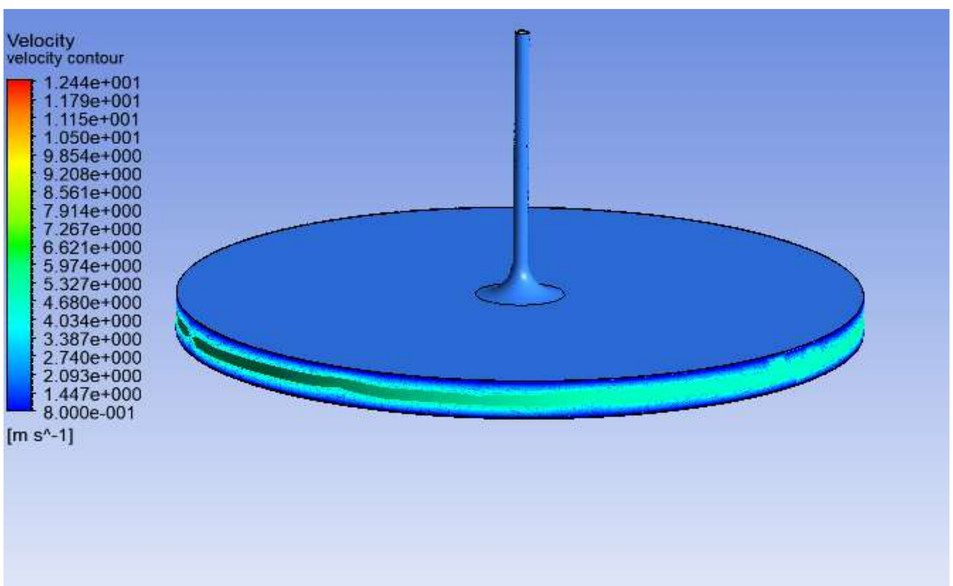

Figure 4.1 inlet velocity contours to chimney through collector

The flow velocity is important parameter in fluid dynamics and particularly in this solar thermal power plant. This is due to velocity of air movement the kinetic energy is generated. Kinetic energy turns the blades of a turbine and generates mechanical energy at the turbine. Therefore, the fluent describes the contour for this movement of air which is the heat transfer fluid in the system. This graphical display indicates that velocity increases from collector inlet to the chimney draft tube.

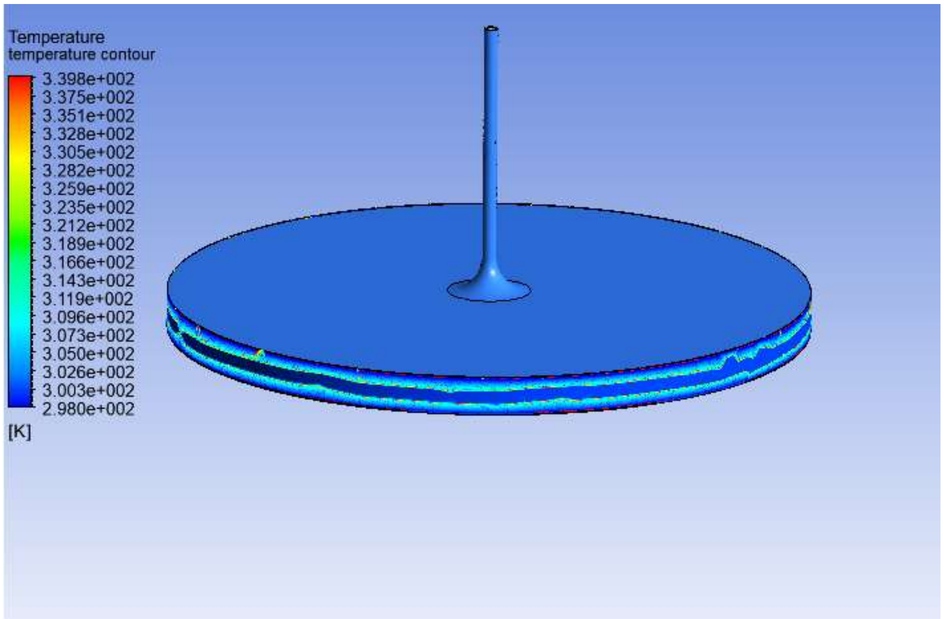

Figure 4.2 Temperature contour at the collector inlet

Validation:

In the Manzanares prototype, the air velocity at the chimney inlet V_c = 8.8 (m/s) and the air temperature rise through the collector ΔT=20 K were reported [19]. In numerical simulations, the mean air velocity at the chimney inlet V_c = 9.1 m/s and the air temperature rise through the collector ΔT= 21 K are predicted and therefore, there are good agreements between the predicted values and the experimental data.

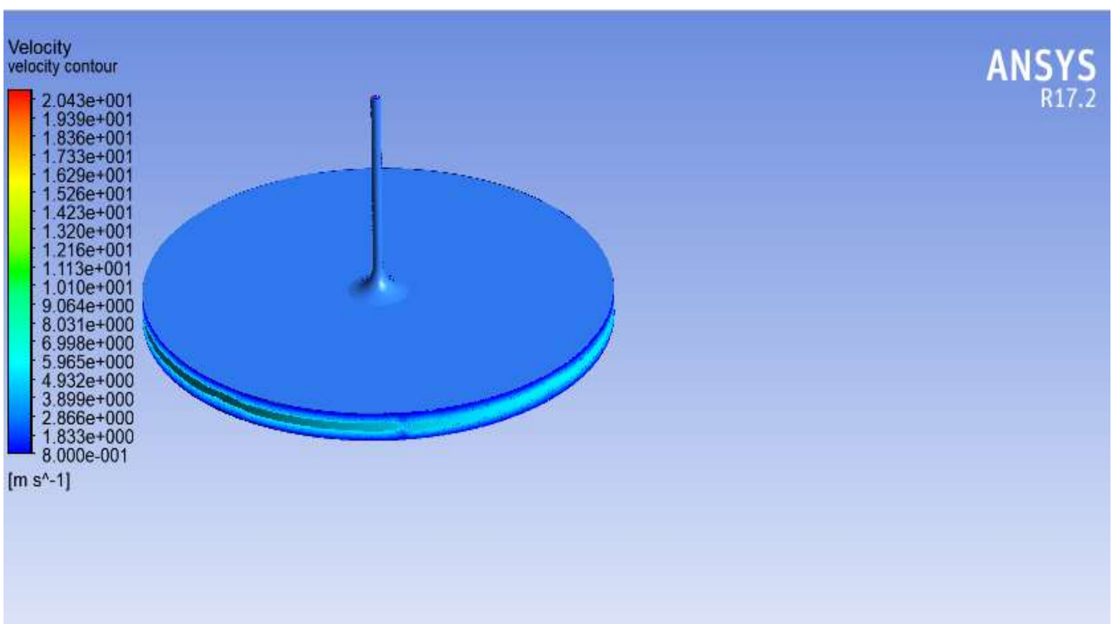

Figure 4.3 Velocity variation through the solar updraft power plant

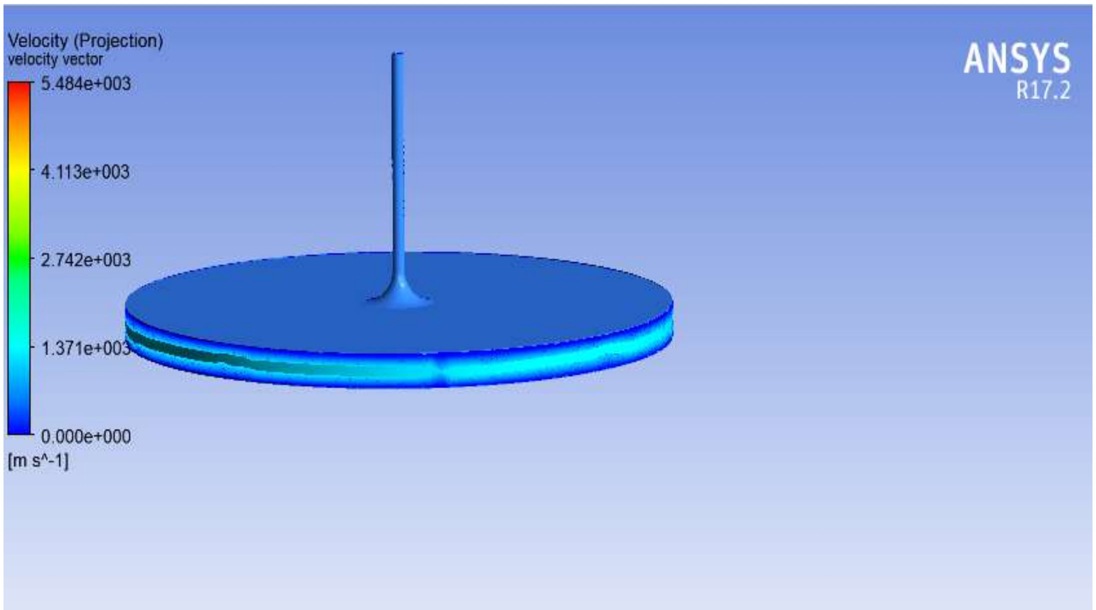

Figure 4.4 Velocity vector through the plant

Figure 4.1 and Figure 4.4 show that the velocity gradually increases from collector inlet to the chimney inlet. The velocity gradually increases in the chimney as shown in Figure 4.4. It can also be seen from Figure 4.2 that the temperature at the ground becomes very high in the depth of few units. This indicates that the ground together with packed-bed thermal storage stores energy, which will be used to heat the air when there is no radiation.

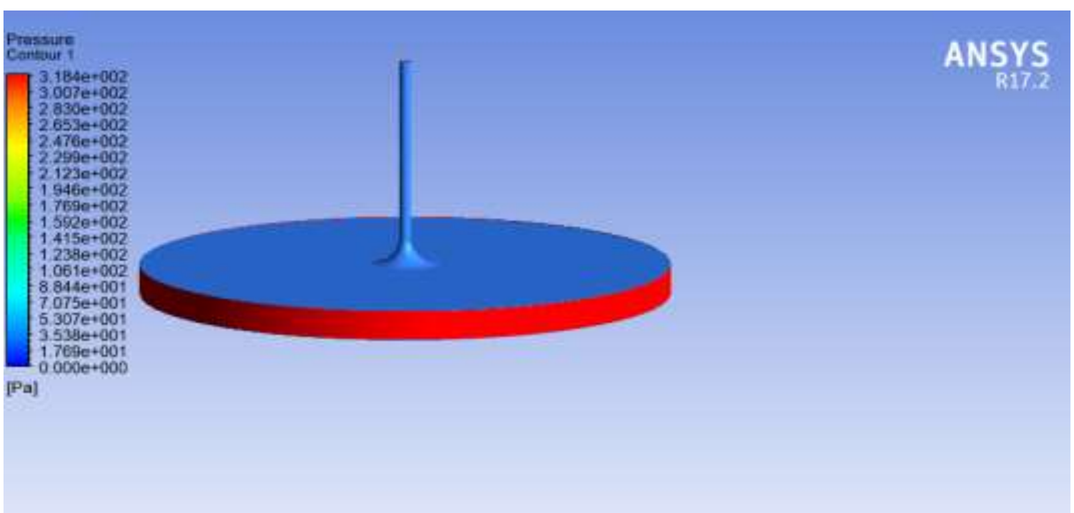

Figure 4.5 High pressure at the entry section

From the above figure the pressure at inlet is very high compared to another boundary condition. Because this pressure is a driving potential in the solar updraft power plant.

2) Displaying stream lines

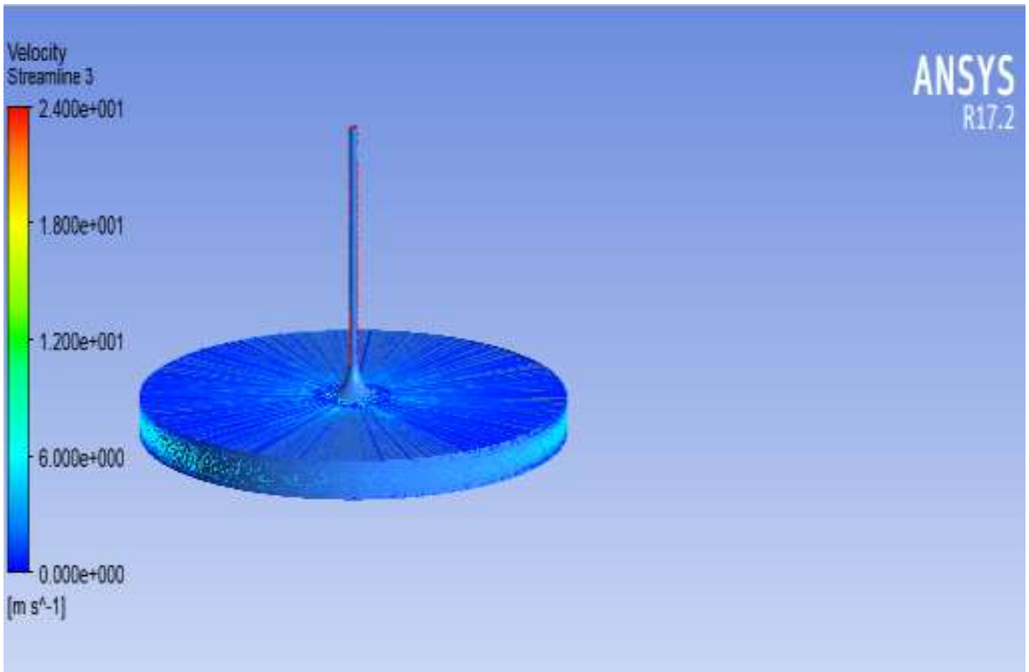

Figure 4.6 Velocity stream line through the system for high scale geometry

Grid independency is achieved by starting with the coarse mesh, which is the default selection of the mesh generation code (mesh code of ANSYS-Fluent), then using the medium and fine meshes. Afterwards, the grid size was further reduced until no change in the output parameters is observed. A comparative analysis is made to check the present simulation results with existing results from previous researchers. The geographic location, environment conditions and geometric configuration have greater impact on the outcomes of SUT power plant. In my work geometry is large and it takes a long duration to generate stream lines. In addition to that high computer memory is required when grid generation become finer and finer. For instance, using a coarse relevance may save time and memory but the variation between parameters are large. Fine grid gives minimum variation between various parameters and needs a long duration. Therefore, geographic location, geometric configuration and environmental condition are requirements in this determination.

3) XY Plots

An XY (abscissa/ordinate) plot is a line and/or symbol chart of data. Virtually any defined variable or function is accessible for this type of plot. Furthermore, one may read in an externally-generated data file in order to compare results with experimental data. If plotting of results on some surfaces is of interest, FLUENT allows creating such surfaces in the grid. Then, the XY-plot facility is used to plot the results.

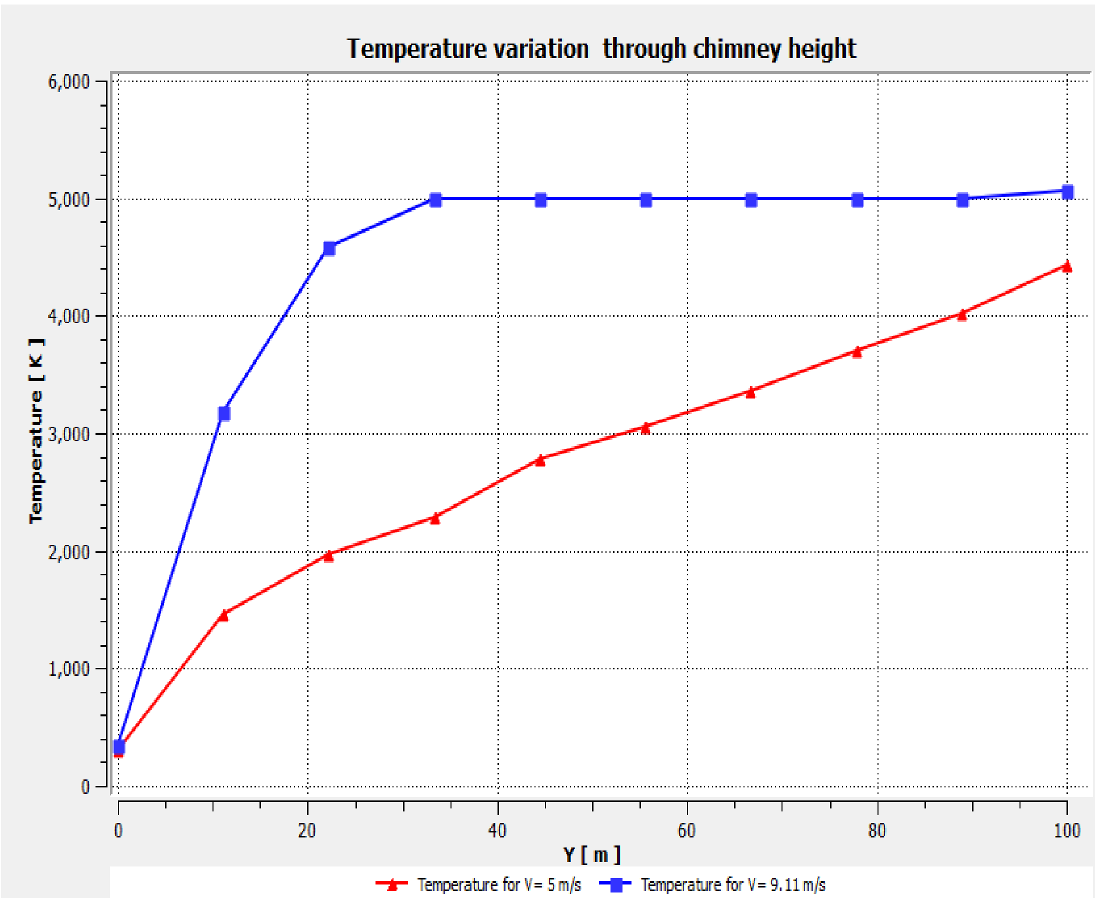

Figure:4.7 a) temperature variation through chimney height for large scale power

In general, the temperature increases when the solar radiation intensity increases. The variation for the chimney outlet temperature is therefore dependent on sun radiation intensity. For the large-scale power generation, the chimney height can be very large and turbine location should be at the base of the chimney as in the smaller scales. This due to the fact that maintenance and operation at the higher location is very difficult. In increasing the chimney height to a very large value, the efficiency of the plant increases intensely. Generally, temperature determines the effectiveness of collector depending how the heat transfer fluid is energized and outlet results of temperature used in various operating range for the required activities.

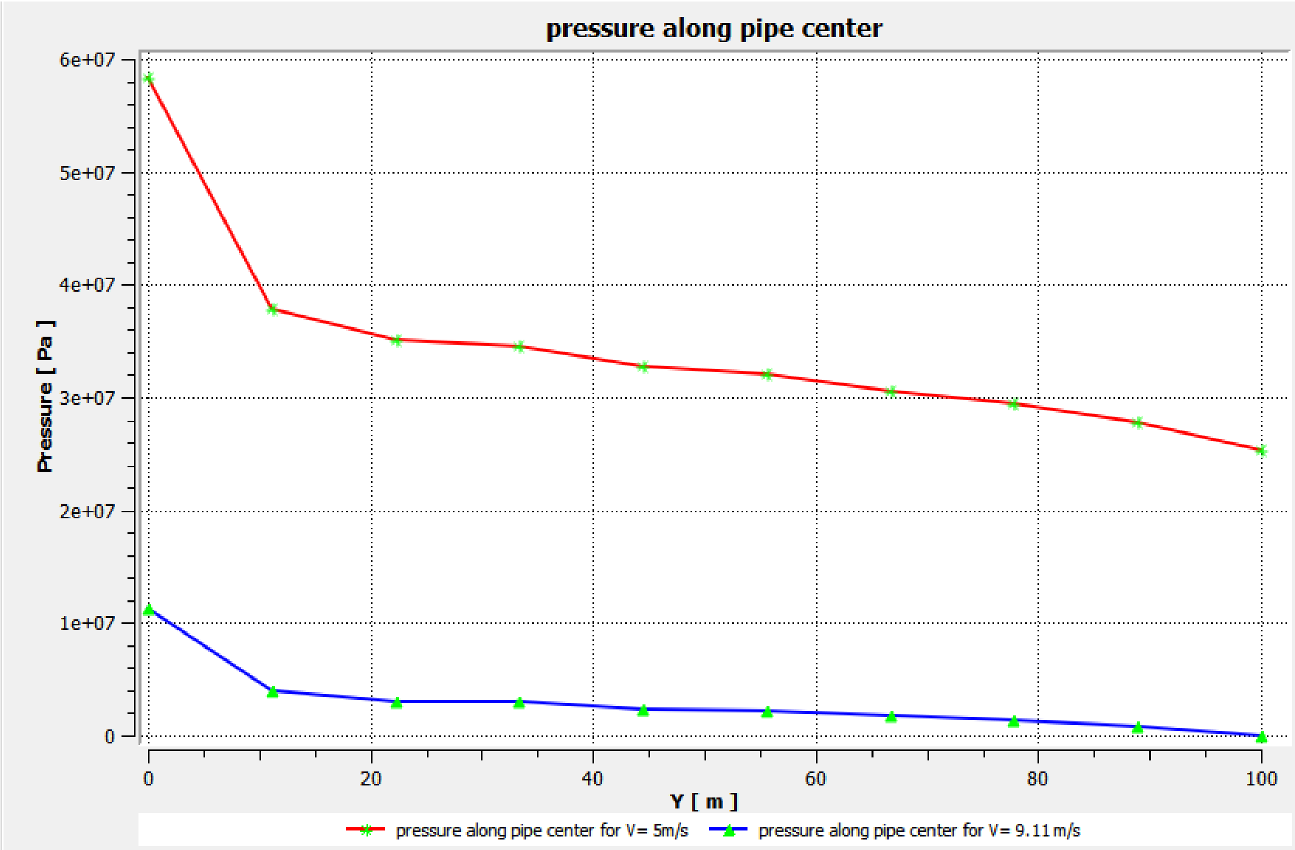

Figure 4.7 b) Pressure drop through the chimney

It can be found that when the turbine pressure drops increase, the inside–outside pressure difference of the system increases, velocity of the air flow decreases while the temperature of the air flow increases, for which the main reason is that the turbine pressure drop has an inversely effect on the air velocity. Thus, the heating up period is prolonged, and the temperature at chimney outlet increases with the pressure drop across the turbine. This pressure difference which is drive potential in solar thermal updraft tower plant is crucial parameter in turbine modeling in the power plant. Due to the fact that turbine extracts work from the heat transfer fluid, turbine blades impediment the air flow and drops pressure at that location. This pressure drop is used in intensifying the work done by the turbine. The requirement here is the increments in the work produced. This work is important in driving the generator which converts the obtained potential in to electrical energy which is the final requirement in in solar thermal power plant, particularly solar updraft tower power generator.

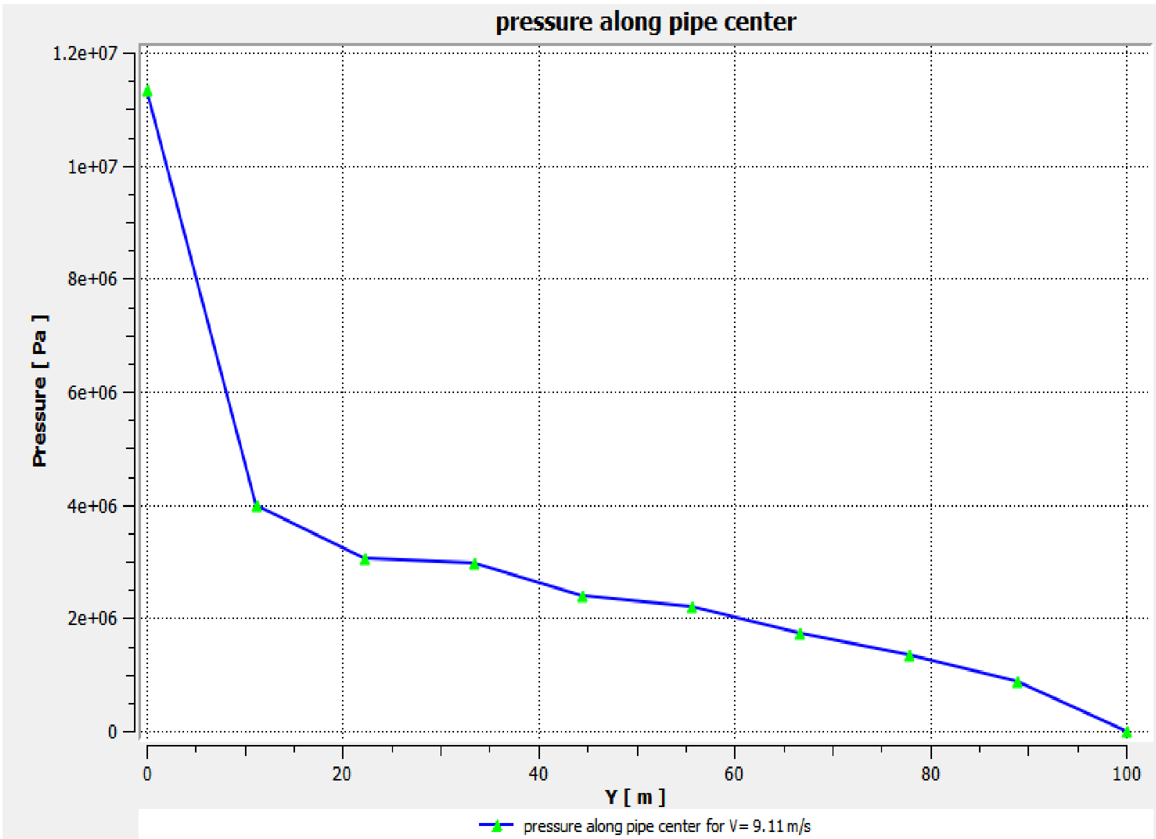

Figure 4.8 pressure drop through the Updraft Tower

This shows high pressure value before the Turbine and pressure drop occur at the turbine. Here there is extraction of energy from the working fluid. At the height of 10m pressure decreases from high value to the lower due to the turbine location at this position.

The expressions developed for the plant performance indicators were computed using some parameters that are given in Table 4.1. Figure 4.9 shows the effect of solar radiation on power out-put. Figure 4.10 shows the effect of collector radius on the generated power at a constant insolation of (100- 1000) w/m^2 and the effect of chimney height on plant performance. It can be noted that the power production increases with the increase in the chimney height and solar radiation. The relationship of both chimney height and solar radiation with power produced is linear.

Table 4.1: Technical data used in the analysis of solar updraft power plant performance.

Parameters	Value	parameters	Value
Chimney Height	200 m	Collector efficiency	0.65
Chimney diameter	10 m	Solar radiation	5200 kwh/m^2 day.
Collector diameter	244 m	Ambient temperature	21 ℃
Turbine efficiency	0.85	Collector Height	2 m

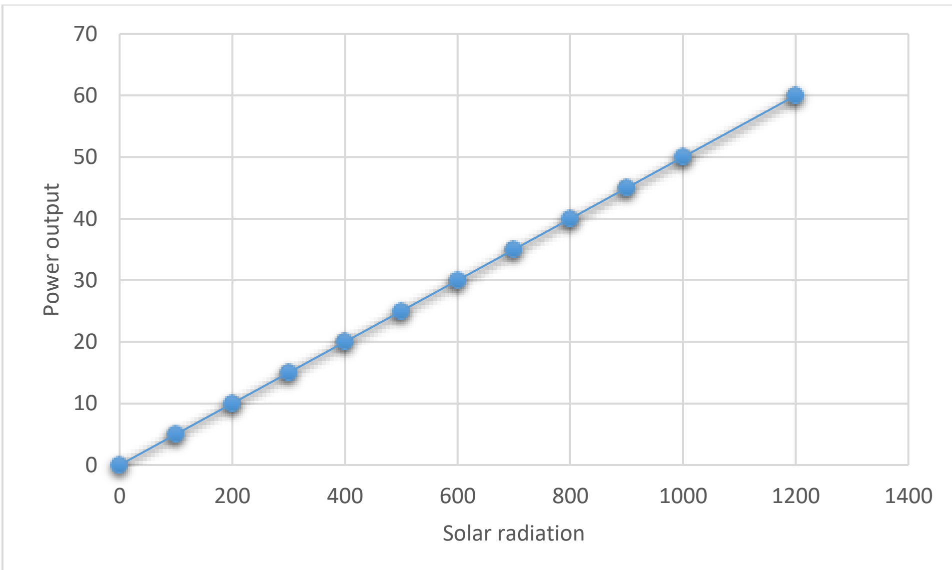

Figure 4.9: Effect of solar radiation on solar updraft power plant power output

When the incident radiation intensity increased, the temperature change between chimney and ambient increased and resulted in the increase of pressure. This pressure is crucial and driving potential in the solar updraft tower power plant. The chimney stacking effect is another important parameter which should be considered in this power plant.

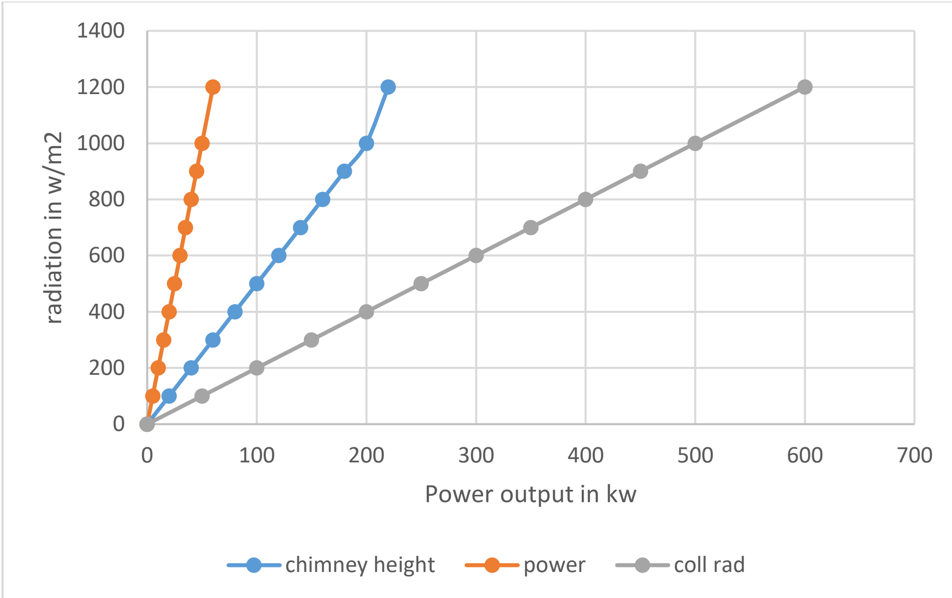

Figure 4.10: Effect of collector radius and chimney height on power output

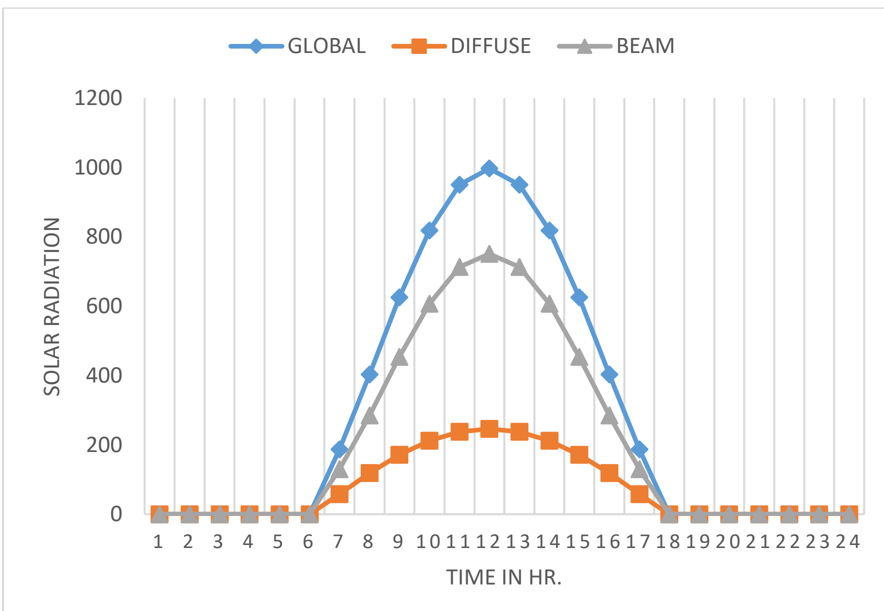

Figure 4.11 Hourly global, beam and diffused radiation on inclined surface

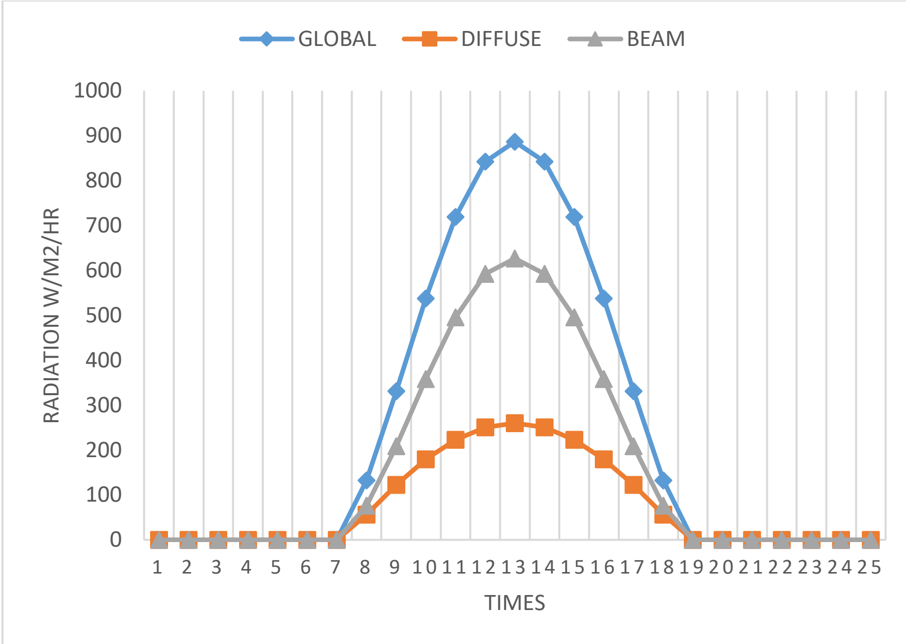

Figure 4.12: Incident Solar radiation for Jan 17, 2018 in Adama

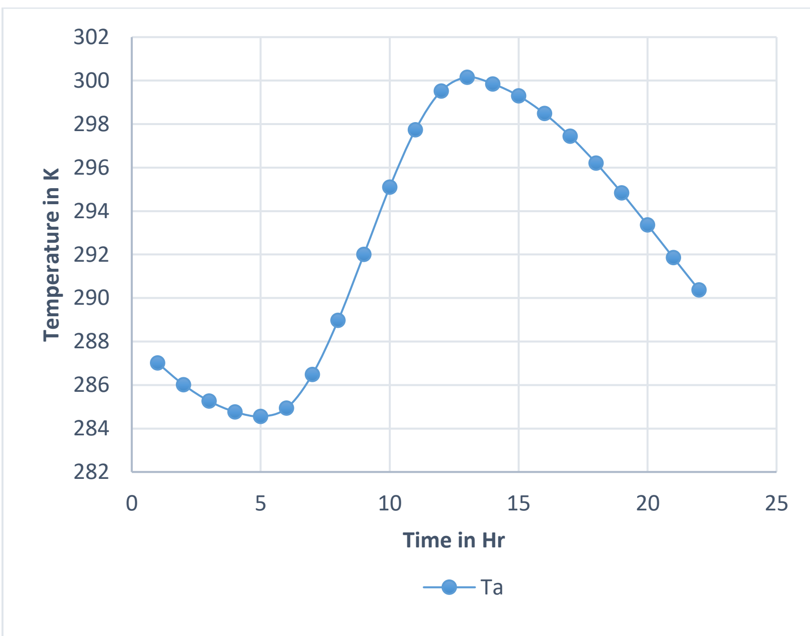

Figure 4.13 Temperature profile for Jan 17

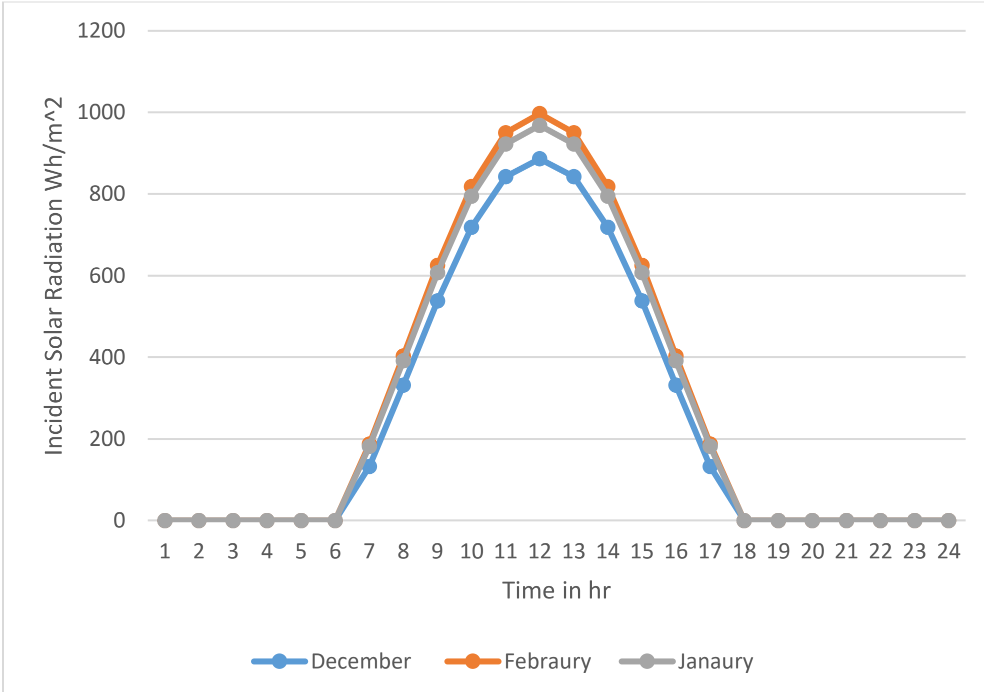

Figure 4.14 Hourly incidence radiation on collector for Adama winter season 2018

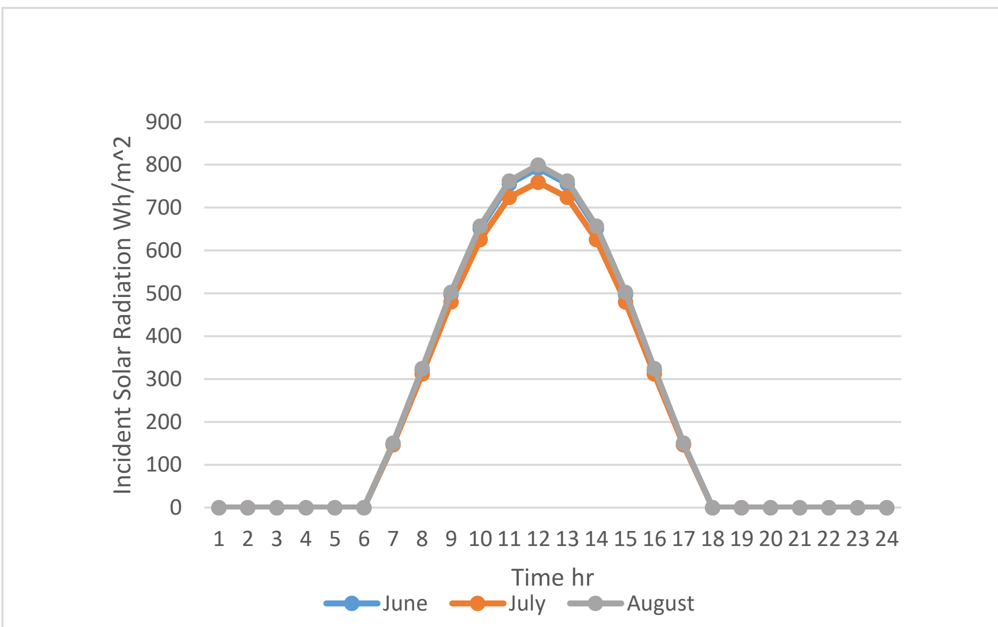

Figure 4.15 Hourly incidence radiation on collector for Adama Summer season 2018

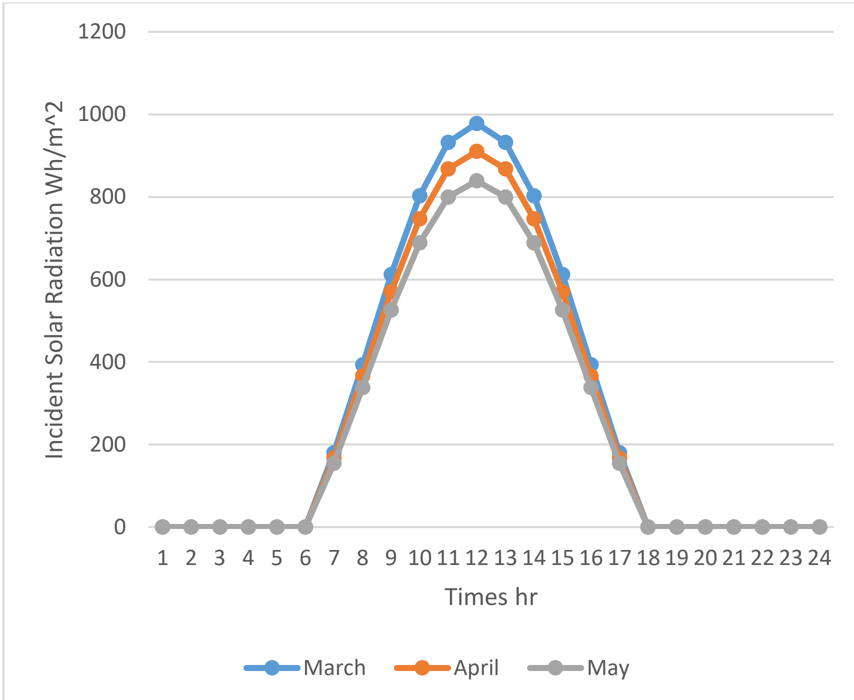

Figure 4.16 Hourly incidence radiation on collector for Adama Spring season 2018

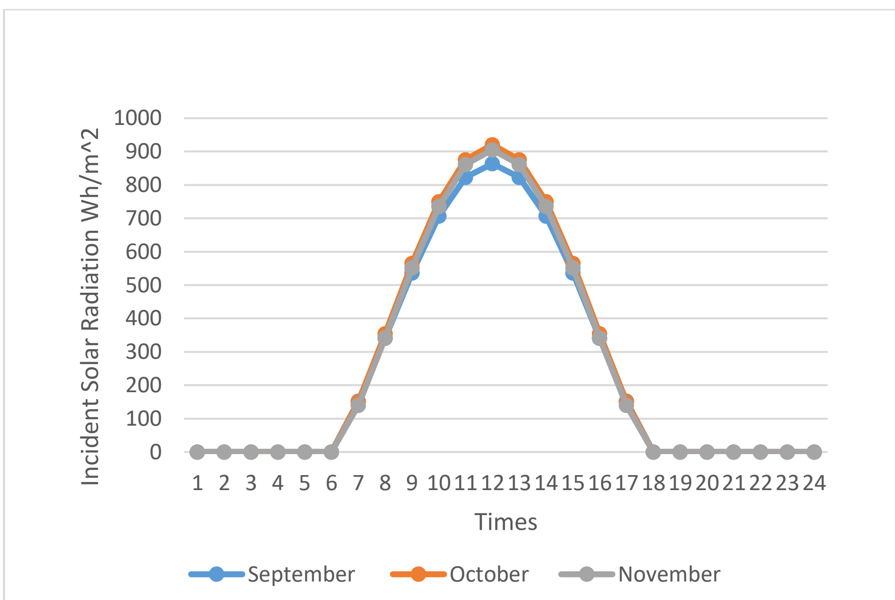

Figure 4.17 Hourly incidence radiation on collector for Adama Autumn season 2018

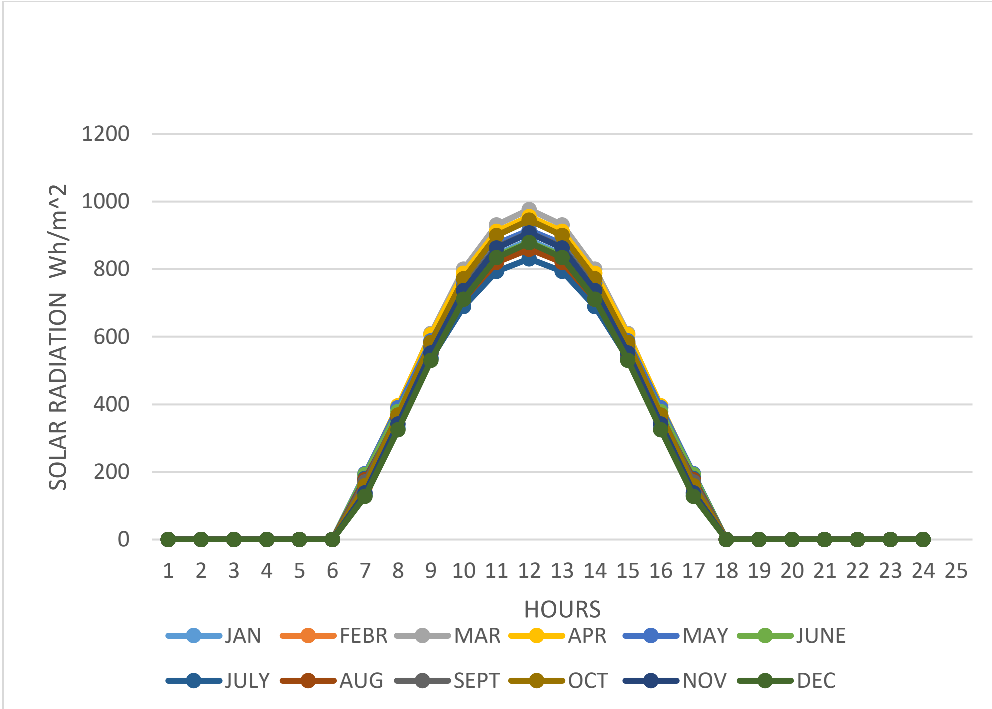

Figure 4.18 Average monthly mean hourly beam radiation for Adama 2018

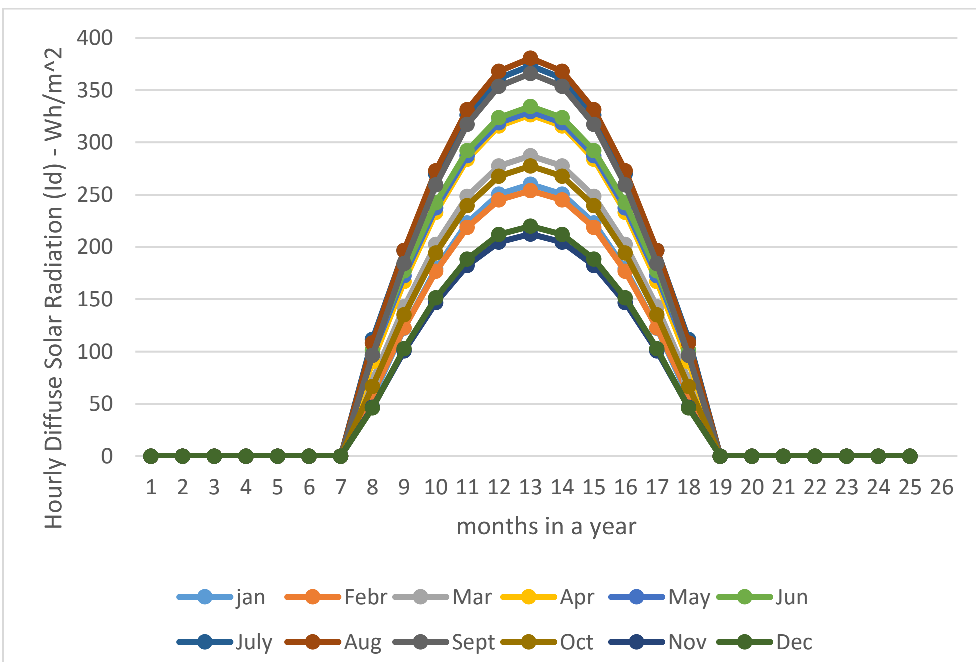

Figure 4.19 Average monthly mean hourly diffused solar radiation on horizontal surface.

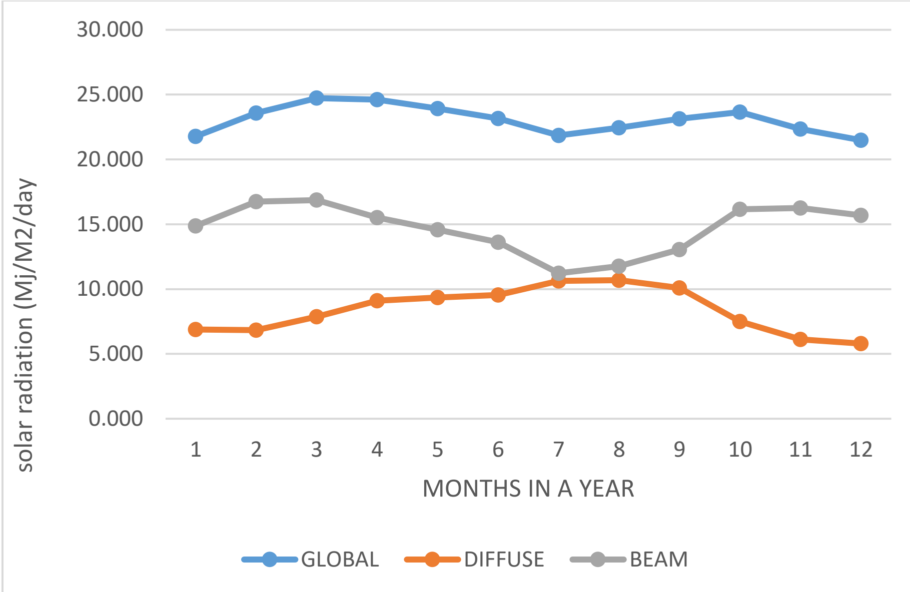

Figure 4.20 Solar radiation on a horizontal surface Mj/m2/day

A useful energy gained by a unit flat plate collector for each hour interval from sunrise to sunset is calculated from the result found from outlet fluid temperature variation of flat plate collector throughout the day, by multiplying temperature rise of the heat transfer fluid to its mass flow rate and specific heat capacity of the fluid.

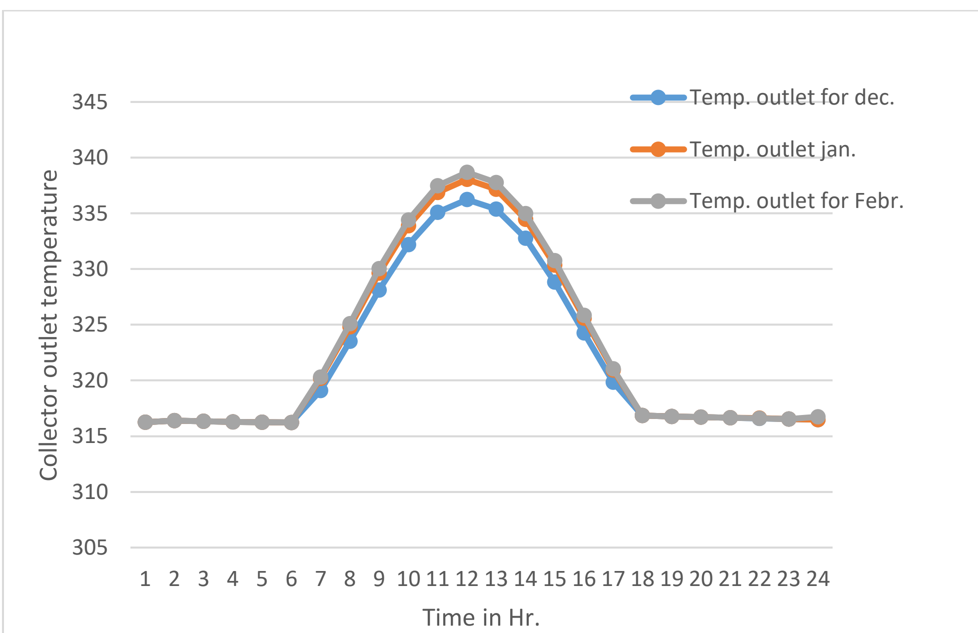

Figure 4.21 Heat transfer fluid outlet temperature variation for collector in winter

The amount of energy collected by a flat plate collector continuously increases from sunrise hour up to noon time and reach a maximum amount at noon time, then decreases continuously up to sunset hour. Thermal energy storage is used in up-grading the energy decreased during this situation.

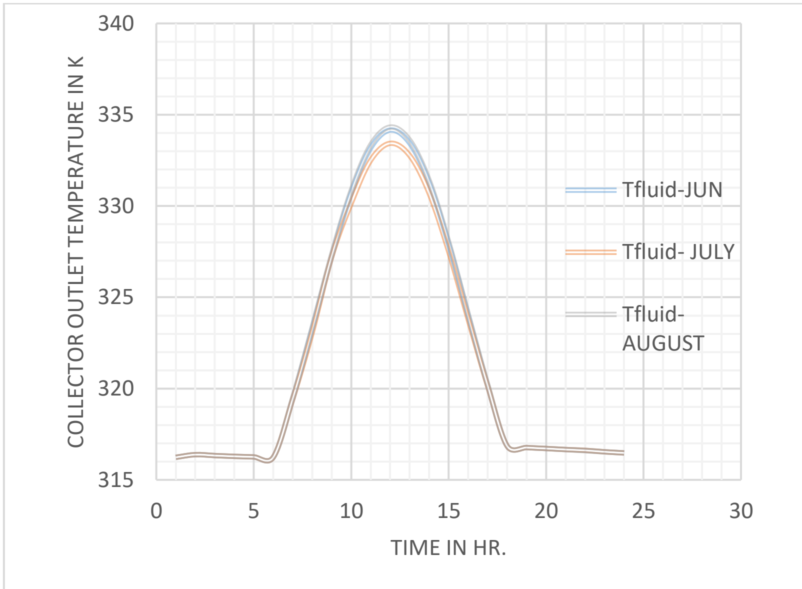

Figure 4.22 Heat transfer fluid outlet temperature variation for collector in summer.

4.4 Economic Analysis of Solar Updraft Tower Power Plant

4.4.1 Introduction

Solar processes are generally characterized by high initial cost and low operating costs. Thus, the basic economic problem is one of comparing an initial known investment with estimated future operating costs. Investments in buying solar energy equipment are important factors in solar process economics. Costs of installing this equipment must also be considered as these can match or exceed the purchase price. Also, to be included are costs of structures to support collectors and other alterations made necessary by the solar equipment. Companies considering solar power generation have to look very carefully at economics to ensure that such a project will be profitable to them. This guide was developed to help illustrate the process involved in completing a Life Cycle Cost (LCC) economic analysis of competing energy solutions. It also introduces the concept of accounting for subsidies and/or externalities in an economic analysis, an increasingly important issue to many policy and other decision makers. To help illustrate the number of variables that can influence an economic analysis of SUPP, the list below has been considered.

a) Performance Variables

- ✓ Solar energy available.
- ✓ Ambient air temperature & hot inner wall temperature.
- ✓ Collector tilt and orientation.
- ✓ Collector shading.
- ✓ Solar energy system size and orientation.

b) Economic Variables

- ✓ Current and future fuel costs.
- ✓ Current and future inflation rate.
- ✓ Discount rate generally known as interest rate and is also referred to as "time
- ✓ value of money".
- ✓ System replacement and maintenance costs over time

4.4.2 Economic Indicators

a) Life Cycle Cost of Solar Energy

The life cycle cost includes investment capital and present worth of operating cost during the useful life of the plant. The operating cost of SUPP system is mainly the maintenance and PCU cost. The life cycle cost of SUPP system is determined from the investment cost and the present value of maintenance and PCU cost distributed over the life as follows [88].

$$\text{LCC} = \text{CI} + C_m \frac{1}{i}\left(1 - \frac{1}{(1+i)^n}\right) \text{-----------------------------} (133)$$

Where: CI is the investment cost of SUPP system, and Cm is annual maintenance and PCU cost.

To determine the unit price of solar energy cost, Pe the life cycle cost has to be equal to the life cycle savings of the SUPP during its life time [88]

The annual energy saving is, ES = $f_a\ Q_a$ -------------------------(134)

The life cycle saving of SUPP is the energy cost saved due to replacement of Fuel and water by solar system.

$$\text{LCS} = p_e f_a Q_a \frac{1+i_e}{i-i_e}(1 - \left(\frac{1+i_e}{1+i}\right)^n \text{----------------------------} (135)$$

To determine the unit price, LCC = LCS

$$\text{CI} + C_m \frac{1}{i}\left(1 - \frac{1}{(1+i)^n}\right) = p_e f_a Q_a \frac{1+i_e}{i-i_e}(1 - (\frac{1+i_e}{1+i})^n$$

The unit price of solar energy for SUPP is therefore, obtained from the relation.

$$p_e = \frac{\text{CI} + C_m \frac{1}{i}\left(1 - \frac{1}{(1+i)^n}\right)}{f_a Q_a \frac{1+i_e}{i-i_e}(1 - (\frac{1+i_e}{1+i})^n} \text{-------------------------} (136)$$

For solar energy to be economically viable, the unit cost of SUPP system must be less than that of other alternatives.

b) Payback Period

To determine the pay-back period, the maintenance cost is neglected. Hence the investment of the SUPP has to be pay-backed by the life cycle saving of fuel cost.

$$\text{LCCS} = C_f f_a Q_a \frac{1+i_e}{1-i_e}(1 - \left(\frac{1+i_e}{1-i_e})^n\right) \text{-------------------------} (137)$$

$$\text{LCCS} = \text{CI at n} = N_p \text{-----------------------------} (138)$$

$$C_f f_a Q_a \frac{1+i_e}{1-i_e}(1 - \left(\frac{1+i_e}{1-i_e})^{N_p}\right) = CI$$

$$N_p = \frac{ln\left[1 + \frac{CI \frac{i_{e-i}}{1+i_e}}{C_f f_a Q_a}\right]}{ln\left[\frac{1+i_e}{1+i}\right]} \text{----------------------------} (139)$$

- ✓ Where: LCS is the life cycle saving of a solar water heating system [kWh]
- ✓ LCCS is the life cycle saving of fuel cost [Birr].
- ✓ C_f is the unit cost of fuel for the first year of analysis [Birr /kwh]
- ✓ f_a is annual fraction of load supplied by solar energy.
- ✓ Q_a the annual heating load [kWh].
- ✓ CI is the initial investment cost, [Birr]
- ✓ i is the annual market discount rate.
- ✓ i_e is the annual market rate of fuel escalation and

- ✓ n is the years of economic analysis.

c) Maintenance & Replacement Costs

Repair and replacement costs are so central to the success of solar water heating. On the other hand, they are difficult to obtain. It has to be mentioned that the replacement and repair cost depends on the manufacturer and the type of the system used. The reason for this is the best approximation of the life cycle costing.

Collectors

In terms of life-time and replacement this is the most difficult section solar water heating system component to evaluate. From the various companies manufacturing solar collectors just a few of them were notable to give an exact average replacement age. Most of them certified that the solar collectors would last for at least 20-25 years. The total cost of a solar updraft power plant is the sum of the costs of its main components: the chimney, the collector and the power converting units (PCU). These components have sub-components to which costs are associated (Table 4.3).

Table 4.2: Components of the SUPP system

Components	Sub-components
Chimney	▪ Chimney shell ▪ Ring stiffeners and ▪ Chimney foundation
Collector	▪ Glass ▪ Column system ▪ Support matrix
Thermal Storage Media	▪ Pvc pipes of 20cm diameter filled with water ▪ Pebble bed (ceramic structure)
Power Conversion Unit	▪ Balance of station ▪ Controls ▪ Power electronics ▪ Generators ▪ Supports ▪ Central structures and Turbines

The costs associated with these components include material, construction, hoisting and transport costs. The economic analysis of the power plant, therefore, requires the knowledge of these specific costs. To make the cost analysis simple, different detailed investigations have been made to get unit costs that are independent of the plant size. One of these investigations is that done by Haaf et al., According to this work the chimney cost is proportional to its skin area ($228 per square meter), the collector cost is proportional to its area ($53 per square meter) and power conversion unit cost is proportional to peak power output ($715 per kilowatt peak). Based on the above assumptions components and total costs were calculated as shown in Table 4.3. The annual operation and maintenance costs were assumed to be about 0.3% of the total investment.

Table 4.3: Components and total costs for solar updraft with thermal storage system

Height of Chimney - 200m Radius of Chimney -5m Skin Area of Chimney - 2xΠx5x200= 6280m^2	228 x 6280 = $1431840	Total Investment Cost 1431840+2476997.4 + 35750+51,094.08 = $3995681.48
Outer Radius of Collector 122m Area of Collector Π x (122)^2 = 46735.8m^2	Cost of Collector 53x46735.8 = $2476997.4	
Machinery for 715 days(2year)	Cost of Machinery 715x50= $35750	
Thermal storage media (Total pipe length) Total pipe length = 51,094.08m	Cost of thermal storage Tank = 51094.08x$1 = $51,094.08	
Operation and Maintenance Cost (0.3%)	0.003x 3995681.48 = $ 3 944 740.682	

Generally, the electricity cost obtained is very high when compared to the hydroelectric energy and other conventional energy costs in Ethiopia. The cost analysis was based on European context. The cost is expected to decrease in developing countries like Ethiopia because the labor cost and the materials necessary to construct the chimney are cheap.

CHAPTER FIVE

CONCLUSIONS AND RECOMMENDATIONS

5.1 Conclusions

In this study, a comprehensive literature review is conducted based on over 80 studies over the past 30 years on solar updraft systems. It was found that providing energy to rural semi-arid Ethiopia with solar tower would greatly improve the lives of its inhabitants, especially in the evenings when villagers only have candle-light to illuminate their homes. The study has investigated the airflow and power output from the solar updraft system by developing a simplified numerical model with ANSYS Fluent. Intentionally this study evaluated the performance of solar updraft power plants in semi-arid regions of Ethiopia theoretically to estimate the quantity of the electric Power produced. The models based on the energy balance were used to estimate the power output of solar updraft s as well as examine the effect of various ambient conditions and structural dimensions on the power output. A solar updraft power plant with 200 m chimney height and 244 m collector diameter is capable of producing monthly average 51 kw. The capacity of power generation is dependent on ambient conditions and structural dimensions such as solar irradiation, ambient temperature, chimney height and collector diameter. The power generation capacity increased with the increase in solar updraft height and solar collector radius. Also, the higher the solar radiation is, the greater the power generation. From the fact that our country Ethiopia is located under tropical zone with high solar insolation intensity and availability of construction materials, implementing the solar updraft power plant can minimizes the problem of energy in the rural community.

5.2 Recommendations for The Future Work

Computational fluid dynamics is a vital numerical tool in the research of solar updraft power plants due to the extensive construction costs to build such large structures. A major goal of the current study was to replicate the prototype built in Manzanares, Spain with a simplified numerical model in ANSYS Fluent. Therefore, encouragement should be given to this software. The following recommendations are made out of this research; some of them are directed to the researchers while the others are directed to decision-makers. Ethiopia has a huge potential of renewable energy resources which can be used for rural electrification through the off-grid system. There are, however, many challenges like low purchasing power of the rural community, unfavorable conditions towards the utilization of renewable energies, absence of awareness how to use these resources, etc. Thus, the government, non-governmental organizations and the private sectors should make combined efforts to overcome these challenges by using more flexible approaches to improve the current poor status of rural electrification in Ethiopia. As far as the environmental aspects are concerned, different kinds of hybrid systems have to be widespread in order to cover the energy demands of rural communities and in that way to help in reducing the greenhouse gases and the pollution of the environment. This is an important point to be taken into consideration. As a conclusion the following suggestions and recommendations might be found useful in future work.

- Increasing the height of the chimney and the diameter of the collector to improve the power output and efficiency.
- As part of government strategy in promoting renewable power development, the Energy Commission of Ethiopia could conduct a comprehensive economic analysis on the commercial viability of the power produced by the SUPP.
- The Thermal Engineering Department and the Energy Center could as well provide technical support and financial assistance to PG students to mount a pilot plant to promote further studies and research into this area.
- Finally, another area that calls for further investigation is the usage of thermal storage media to improve efficiency. Packed-bed thermal energy storage is used in this document. however, different types of thermal storage media have to be studied in detail further.

References

[1a]. Agust´ın Pérez - Barahona1: Economic growth and the use of non-renewable energy resources, 2007

[1b]. Stefan Heimann, 2007, Renewable Energy in Ethiopia, 13 Months of Sunshine for sustainable Development.

[2]. J. Null, "Harnessing the Sun: The Promises of Solar Energy," Weather-wise, July 2009.

[3]. R. Wengenmayr and T. Bührke, *Renewable Energy*. John Wiley & Sons, 2011.

[4]. C. Ngo and J. Natowitz, *Our Energy Future: Resources, Alternatives, and the Environment*. John Wiley & Sons, pp.184-186, 2009.

[5]. C. M. Meyer ''Towers of power-the solar updraft tower,'' Docstoc.com. [online]. Available: http://www.docstoc.com/docs/73010840/Towers-of-power-the-solar-updraft-tower. [Accessed: 25-Nov-2012].

[6]. T. Hamilton, *Mad Like Tesla: Underdog Inventors and Their Relentless Pursuit of Clean Energy*. ECW Press, pp.93-103, 2011.

[7]. W. Ley, Engineers, dreams. Viking Press, 1954.

[8]. T. W. Von Backstrom, R. Harte, R. Hoffer, W. B. Kratzig, D. G. Kroger, H.-J. Niemann, and G. P. a. G. Van Zijl, ―State and Recent Advances in Research and Design of Solar updraft Power Plant Technology, VGB Powertech, vol. 88, no 7, 2008, pp.64-71.

[9]. I. S. F. Jones, *Engineering Strategies for Greenhouse Gas Mitigation*. Cambridge University Press, 2011.

[10]. W. Haaf, K. Friedrich, G. Mayr, and J. Schlaich, "Solar updraft Principle and Construction of the Pilot Plant in Manzanares," International Journal of Solar Energy, vol. 2, no. 1, pp. 3-20, 1983.

[11]. T. K. Grose, "Solar updraft s Can Convert Hot Air to Energy National Geographic, 16 April 2014.

[12]. A. Dhahri and A. Omri, "A Review of Solar updraft Power Generation Technology," International Journal of Engineering and Advanced Technology, vol. 2, no. 3, 2013.

[13]. M. Humphries, "Solar Tower in Arizona to power 150,000 homes for 80 years," GEEK, 21 July 2001.

[14a]. "Power Africa", United States Agency for International Development, May 2014.

" http://www.usaid.gov/powerafrica".

[14b]. 2015, "Solar GIS," Online, http://solargis.info/doc/free-solar-radiation-maps-GHI.

[15]. http://solargis.info/doc/free-solar-radiation-maps-GHI. [Accessed June 2014].

[16]. http://educypedia.karadimov.info/library/Solar%20Updraft%20Towers.pdf. [Accessed 21 April 2014].

[17]. A. Holgate, the Art of Structural Engineering: The Work of Jorg Schlaich and His Team. Edition Axel Menges, 1997-2000.

[18] http://data.solar-tower.org.uk/pdf/AufwindkraftwerkDemonstration sanlage.pdf. [Accessed February 2014].

[19] W. Haaf, "Solar updraft s Part II: Preliminary Test Results from the Manzanares Pilot Plant," International Journal of Solar Energy, vol. 2, no. 2, pp. 141-161, 1984.

[20] A brief history of solar updraft. Retrieved 10.11.2004 from; http://www.vision engineer.com/env/solar flue.shtml

[21] http://www.eere.energy.gov/solar/pdfs/solar_timeline.pdf. [Accessed 22 April 2014].

[22] Enviro Mission Limited -Technology: Technology Overview, http://www.enviro mission.com.au. 2006.

[23] Al-Haroun, 2012, performance evaluation of solar updraft power plant in Egypt.

[24] Hamdan MO. Analysis of a solar updraft power plant in the Arabian Gulf region. Renewable Energy. 2011; 36:2593-8.

[25] Kasaeian, A., Ghalamchi, M., Ghalamchi, M. Simulation and optimization of geometric parameters of a solar updraft in Tehran. Energy Conversion and Management. 2014

[26] Kirstein C.F, von Backstrom T.W. Flow-through a solar updraft power plant collector-to chimney transition section. Journal of solar energy engineering. 2006; 128:312-7.

[27] Koonsrisuk A, Chitsomboon T. Accuracy of theoretical models in the prediction of solar chimney performance. Solar Energy. 2009; 83:1764-71.

[28] Koonsrisuk A. Comparison of conventional solar updraft power plants and sloped solar chimney power plants using second law analysis. Solar Energy. 2013; 98:78-84.

[29] Larbi S, Bouhdjar A, Chergui T. Performance analysis of a solar updraft power plant in the southwestern region of Algeria. Renewable and Sustainable Energy Reviews. 2010;

[30] Jiakuan Y, Jin L, Po X. A novel technology of solar updraft for power generation. ACTA Energie Solaris Sinica. 2003; 24:570-3.

[31] Maia CB, Castro Silva JO, Cabezas-Gómez L, Hanriot SM, Ferreira AG. Energy and

exergy analysis of the airflow inside a solar updraft. Renewable and Sustainable Energy Reviews. 2013; 27:350-61.

[32] Kulunk H. A prototype solar convection chimney operated under Izmit conditions. Proceedings of the seventh MICAS. 1985;162.

[33] Pasumarthi N, Sherif S. Experimental and theoretical performance of a demonstration solar chimney model Part II: experimental and theoretical results and economic analysis. International Journal of Energy Research. 1998; 22:443-61.

[34] Lodhi, M.A.K., 1999. Application of helio-aero-gravity concept in producing energy and suppressing pollution. Energy Conversion and Management 40:407–421.

[35] Gannon AJ, von Backstrom TW. Solar updraft cycle analysis with system loss and solar collector performance. Journal of Solar Energy Engineering-Transactions of the ASME. 2000; 122:133-7.

[36] Pastohr, H., Kornadt, O. and Gürlebeck, K. (2004). Numerical and analytical calculations of the temperature and flow field in the upwind power plant. International Journal of Energy Research, vol. 28, pp. 495–510.

[37] Liu, W., Ming T.Z, Yang K., Pan Y., 2005. Simulation of the characteristic of heat transfer and flow for MW-graded solar updraft power plant system. Journal of Huazhong University of Science and Technology 33(8):5–7.

[38] Schlaich J., Weinrebe G., 2005. Design of commercial solar updraft tower systems-utilization of solar-induced convective flows for power generation. Journal of Solar Energy Engineering 127:117–124. DOI:10.1115/1.1823493.

[39] Pretorius, J.P., Kroger, D.G., 2006a. Critical evaluation of solar updraft power plant performance. Solar Energy 80, 535–544.

[40] Ninic, N., 2006. Available energy of the air in solar updraft s and the possibility of its ground-level concentration. Solar Energy 80 (7), 804–811.

[41] Bilgen, E. and Rheault, J. (2006). Solar updraft power plants for high latitudes. Solar Energy, vol. 79 (5), 449–458.

[42] Pretorius, Kroger., 2006b. Solar updraft power plant performance. Transactions of the ASME 128, 302–311.

[43] Koonsrisuk, A., Chitsomboon, T., 2007. The dynamic similarity in solar updraft modeling. Solar Energy 81 (12), 1439–1446.

[44] Bernardes, von Backstrom TW. Evaluation of operational control strategies applicable to solar updraft power plants. Solar Energy. 2010; 84:277-88.

[45] Cao, *et al.*, "Simulation of a sloped solar updraft power plant in Lanzhou", *Energy Conversion and Management*, vol. 52, pp. 2360-2366,2011.

[46] Chen, W., Qu, M. Analysis of the heat transfer and airflow in the solar updraft drying system with porous absorber. Renewable Energy. 2014; 63, 511-518.

[47] Dai Y, Huang H, Wang R. Case study of solar updraft power plants in Northwestern regions of China. Renewable energy. 2003; 28:1295-304

[48] Dehghani S., Mohammadi A. H. The optimum dimension of geometric parameters of solar updraft power plants–A multi-objective optimization approach. Solar Energy2014; 105, 603-612.

[49] Al-Kayiem, Hussain H., Sing, Chin Yee, and Jia Lin, 'Performance Influence of the Solar updraft Power Plant by Variation of the Canopy and Tower Heights'

[50] H. F. Fasel, F. L. Meng, E. Shams, and A. Gross, "CFD analysis for solar updraft power plant systems," *Solar Energy,* pp. 12-22, 2013.

[51] Xu H., Karimi F., Yang M. Numerical investigation of thermal characteristics in a solar updraft project. Journal of Solar Energy Engineering, Transactions of the ASME. 2014; 136(1), Article number 011008.

[52] T. Ming, W. Liu, Y. Pan and G. Xu, "Numerical analysis of flow and heat transfer characteristics in solar updraft power plants with energy storage layer," *Energy Conversion and Management*, no. 49, pp. 2872-2879, 2008.

[53] Ming T et al., Numerical analysis on the influence of ambient crosswind on the performance of the solar updraft power plant system. Renewable and Sustainable Energy Reviews.2012; 16:5567-83.

[54] Guo, Li J-y, Wang Y. Numerical simulations of solar updraft power plant with radiation model. Renewable Energy. 2014; 62:24-30.

[55] Guo, J.-y. Li, and Y. Wang, "Numerical simulations of solar updraft power plant with radiation model," *Renewable Energy,* no. 62, pp. 24-30, 2014.

[56] E. Gholamalizadeh and M. Kim, "Three-dimensional CFD analysis for simulating the greenhouse effect in solar updraft power plants using a two-band radiation model," *Renewable Energy,* no. 63, pp. 498-506, 2014.

[57] Zhou, J. Yang, B. Xiao, G. Hou, and F. Xing, "Analysis of chimney height for the solar updraft power plant," *Applied Thermal Engineering,* vol. 29, pp. 178-185, 2009.

[58] Sangi R, Amidpour M, Hosseinizadeh B. Modeling and numerical simulation of solar chimney power plants. Solar Energy. 2011; 85:829-38.

[59] Von Backstrom TW et al., State and recent advances in research and design of solar updraft power plant technology. VGB Powertech. 2008;88.

[60] Zhou, F. Wang, and R. M. Ochieng, "A review of solar updraft power technology," *Renewable and Sustainable Energy Reviews,* vol. 14, pp. 2315- 2338, 2010.

[61] Zhou, Xinping, Jiakuan Yang, Bo Xiao, and Guoxiang Hou. "Simulation of a pilot solar updraft thermal power generating equipment." Renewable Energy 32, no. 10 (2007):1637-1644.

[62] Chergui, S. Larbi and A. Bouhdjar, "Thermo-hydrodynamic aspect analysis of flows in solar updraft power plants-A case study," *Renewable and Sustainable Energy Reviews,* no. 14, pp. 1410-1418, 2010.

[63] Tahar and Mahfoud, "Numerical Analysis of Flows in a Solar updraft Power Plant with a Curved Junction," *International Journal of Energy Science*, vol. 3, no. 4, pp. 280-286, 2013.

[64] Hedderwick RA. Performance evaluation of a solar updraft power plant: Stellenbosch: University of Stellenbosch; 2000.

[65] Beyers, J. H. M., T. M. Harms, and D. G. Kroger. "A finite volume analysis of turbulent convective heat transfer for accelerating radial flows." Numerical Heat Transfer: Part A: Applications 40, no. 2 (2001): 117-138.

[66] Pretorius and D. G. Kroger, "Critical evaluation of solar updraft power plant performance," *Solar Energy,* vol. 80, pp. 535-544, 2006.

[67] Bernardes, Weinrebe G. Thermal and technical analyses of solar updraft s, Solar Energy, 2003 75:511-24.

[68] Huang H, Zhang H, Huang Y, Lu F. Simulation Calculation on Solar updraft Power Plant System. Challenges of Power Engineering and Environment: Springer; 2007. p. 1158

[69] Koonsrisuk. A single dimensionless variable for solar updraft power plant modeling. Solar Energy. 2009; 83:2136-43.

[70] http://www.cfd-online.com/Wiki/Turbulence_modeling, March 2007

[71] Fluent user's guide, January 2005

[72] Okoye CO, Atikol U. A parametric study on the feasibility of solar updraft power plants in North Cyprus conditions. Energy Convers Manag 2014; 80: 178-87

[73] Dai Y, Huang H, Wang R. Case study of solar updraft power plants in Northwestern regions of China. Renew Energy 2003; 28:1295–304. DOI:10.1016/S0960-1481(02)002276.

[74] Ong KS. A mathematical model of a solar updraft. Renew Energy 2003; 28:1047 60. doi:10.1016/S0960-1481(02)00057-5.

[75] Duffie JA, Beckman WA. Solar engineering of thermal processes. Third Edit. John Wiley & Sons, INC; 2006.

[76] Stigka EK, Paravantis JA, Mihalakakou GK. Social acceptance of renewable energy sources: A review of contingent valuation applications. Renew Sustain Energy Rev 2014; 32:100–6. doi: 10.1016/j.rser.2013.12.026.

[77] Xu, Ming, Pan, Y., Meng, F., and Zhou, C., 2010, "Numerical Analysis of the Performance of solar updraft Power Plant System," Energy Conservation and Management

[78] Doerte Laing *Solar Thermal Energy Storage Technologies* German Aerospace Center (DLR), 2008; http://213.133.109.5/video/energy1tv/Jan%20NEU/ Konferenz/ Wirtschaft/10,000S GW/23 MS/23 04 MS 05 Solar Thermal Energy Storage Technologies Hannover

[79] Prof. Dr.-Ing. B. Hoff Schmidt Lecture notes on Thermal Heat Storage Systems Aachen University of Applied Sciences, 10.11.2008 Newly revised lecture notes at http://www.fhaachen. de/uploads/media/RE Thermische Speicher 2010 11 22 cb. pdf

or http://www.fh-aachen.de/hoffschmidt.html

[80] Thermocline test at Sandia National Laboratories http://www.nrel.gov/csp/troughnet/thermal energy storage.html Last Updated: 28 January 2010

[81] Disadvantages of a 2-tank storage system http://social.csptoday.com/industry insight/carving-costs-single-tank-thermal storage Published on 11 December 2009

[82] Aerial views of Andasol I http://news.soliclima.com/noticias/energia-solar/se-inagura planta de-energia termoelectrica- en-Granada

[83] The Thermal Insulation Association of Southern Africa, 2001. "Thermal Insulation Handbook"

[84] Nikolai V. Khartchenko Thermische Solaranlagen Grundlagen, Planung and Auslegung

Published by: Pringer-Verlag Berlin Heidelberg 1995 ISBN 3-540-58300-9

[85] Fried, J.R., 1973. "Heat Transfer Agents for High-Temperature Systems" 1980, 1989.

[86] American Thermal Insulation Manufacturers Association (ATIMA), 2005. “Energy Saving Guide,”

[87] Yunus Cengel, A., 2003. “Heat transfer: A practical Approach” 2nd Ed; Tata McGraw-Hill

[88] Collares-Pereira, Gordan, J. M., Rabi and Zarmi, Y. “Design and Optimization of Solar Industrial Hot Water System’’, Solar Energy, Vol. 32, 1984.

Appendix

Annex A: Properties of Various Materials

Table A.1 Thermal Conductivities of Absorber Materials

Material	Thermal Conductivity (W$m^{-1}K^{-1}$)
Copper	385
Aluminum	205
Mild steel	54
Stainless Steel	24
Acrylic	0.20
Polyethylene	0.30- 0.44
polypropylene	0.20
PVC	0.16

Table A. 2 R-values of different insulating materials

Material	R-value [m2k/watt]
Hardwood siding (1 in. thick)	0.91
Wood shingles (lapped)	0.87
Brick (4 in. thick)	4.00
Concrete block (filled cores)	1.93
Fiberglass batting (3.5 in. thick)	10.90
Fiberglass batting (6 in. thick	18.80
Fiberglass board (1 in. thick)	4.35
Cellulose fiber (1 in. thick)	3.70
Flat glass (0.125 in thick)	0.89
Insulating glass (0.25 in space)	1.54
Air space (3.5 in. thick)	1.01
Drywall (0.5 in. thick)	0.45

There are different types of insulation materials among those; fiberglass, cellular glass, foamed plastic, and calcium silicate are the most commonly used materials.

Annex B: Adama meteorological data sun -shine hours

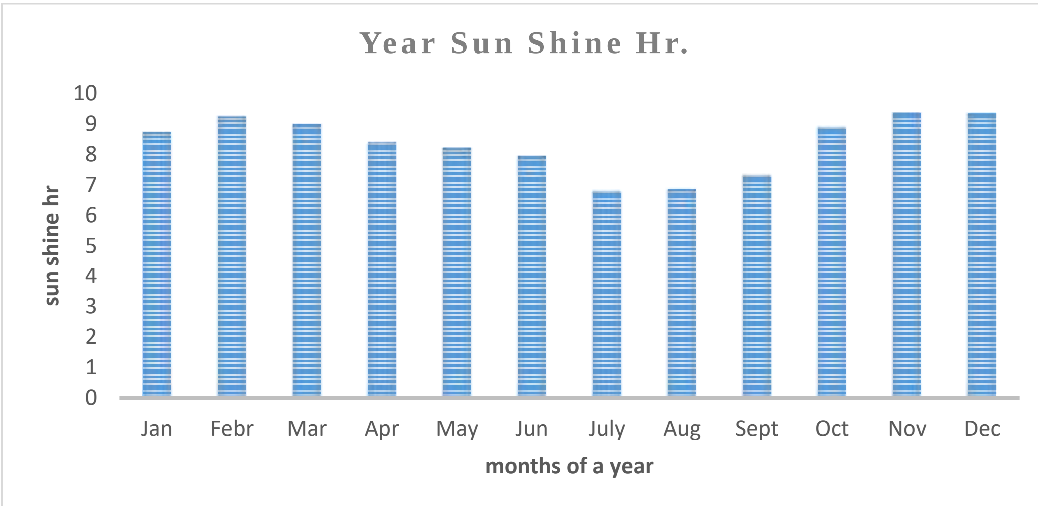

Annex C

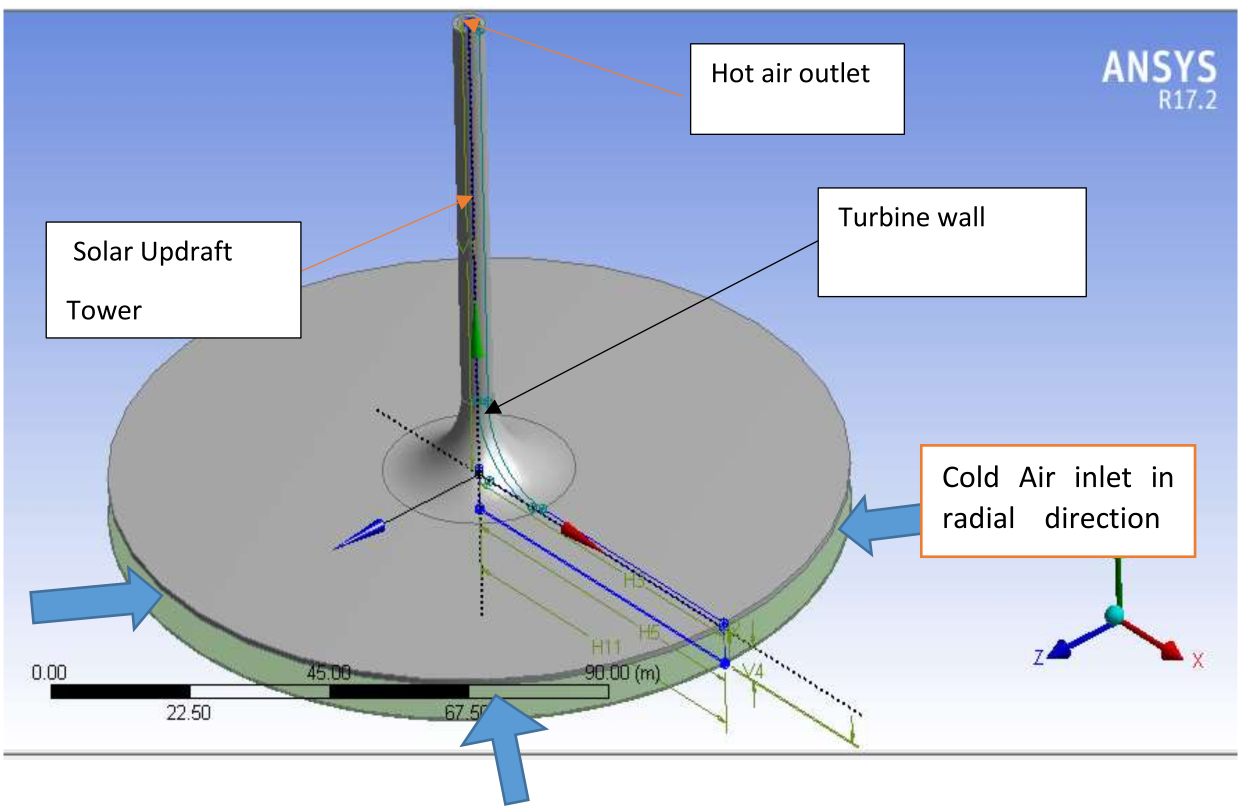

Figure C.1 Three-dimensional geometry of solar updraft power plant model on Ansys modeler

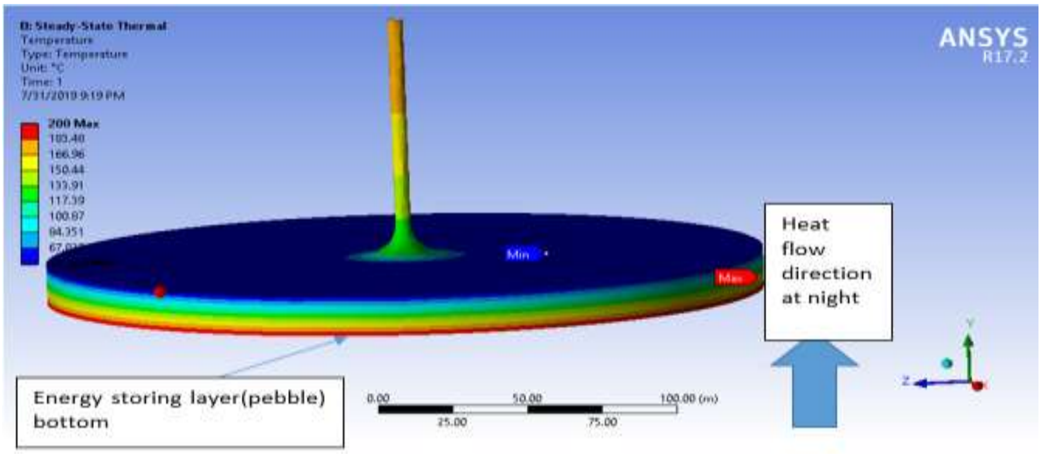

Figure C.2 steady-state heat regenerator heat flow direction at night

Annex D

Climatic Condition of Adama

Adama region is characterized by a climatic condition of tropical; it has high intensity of solar radiation. The monthly average temperature of Adama ranges between 18.2 ℃ (December) and 22.5 ℃ (April). Above Twenty-year average monthly average temperatures and wind speed in Adama are presented in Table D.1

Table D.1: Monthly average annual climatic condition of Adama (Ethio- national meteorology agency)

	MONTHS											
Temperature(℃)	Jan	Feb	Mar	Apr	May	Jun	July	Aug	Sept	Nov	Oct	Dec
Average	19.5	20.5	21.5	22.5	22.4	22.3	18.4	20.6	21	20.1	18.6	18.2
Min	11.4	12.9	14.2	15.1	14.5	15.2	12.4	15.1	14.7	12.3	10.7	10.7
Max.	27	28.1	29.5	30	30.4	29.5	24.4	26.1	27.4	27.9	26.6	25.7
Wind speed(m/s)	3.5	2.7	3.5	3.5	3.5	2.8	2.8	2.7	2.8	3.4	4.3	3.4

Meteorological data are required for evaluating heat transfer between the SUPP and its surrounding.